Master Thesis
Arie-Jan van Renswoude

An evaluation and improvement of the limit- and design values stated in CUR 236 – Micropiles

September, 2017

TU Delft

Heijmans

An evaluation and improvement of the limit- and design values stated in CUR 236 - Micropiles

By

A. J. van Renswoude

in partial fulfilment of the requirements for the degree of

Master of Science
in Applied Physics

at the Delft University of Technology,
to be defended publicly on Tuesday September 1, 2017 at 10:00 AM.

Supervisor:	Ing. H. J. Everts	TU Delft
Thesis committee:	Prof. dr. K. G. Gavin	TU Delft
	Ir. K. J. Reinders	TU Delft
	Ing. L. Tiggelman	Heijmans
	Ir. A. C. M. Kimenai	Heijmans

TU Delft

Preface

This thesis has been written in collaboration with Heijmans to conclude the MSc Geo-Engineering program at the Civil Engineering and Geosciences faculty of The TU Delft. Heijmans was in the possession of an interesting database which they wanted to be analysed. This thesis aimed to do so and then in the direction of the effects of installation on the final capacity of a pile.

The data study proved to be very time consuming and did not result in the sought relations between installation aspects and pile capacity. However, one of the outcomes of the data study questioned the use of limit values, which was interesting to further investigate. The aim was therefore changed to an evaluation of the limit values stated in CUR 236. An interesting topic which lies close to the practice.

During the whole process I received much assistance people working at the university and Heijmans. I would like to thank them all. Furthermore I would like to thank Ir. A. C. M. Kimenai from Heijmans who introduced me to the micropile topic and helped me with obtaining lots of information. Special thanks to the other assessment committee members, Prof. dr. K. G. Gavin, Ing. H. J. Everts, Ir. K. J. Reinders and Ing. L. Tiggelman, for guiding me with guidance, support and feedback.

A. J. van Renswoude
Delft, September 2017

Contents

List of Figures

List of Tables

Abstract

In this thesis an evaluation of the limit values which are stated in CUR 236 – Micropiles is presented. This evaluation has been done by means of a dataset. The dataset contained information on failure tests performed on four different types of micropiles, and was initially used for research on relations between logged installation aspects and the final capacity of the piles; such relations were however not found. This was mainly caused by the shape in which the data was logged, and the lack of details in the data. During this research, significant differences between raw data and data adapted according the limit values stated in CUR 236, were found. This led to a change in research direction towards the evaluation of the limit values.

Limit values are values that are used to build in additional safety in a design, and thus, to prevent unsafe situations. The values are based on the shape of data in which in general a linear relation between maximum mobilized shear stresses ($\tau_{mob;max}$) and cone resistance (q_c). This relation continues up to a certain cone resistance level, after which $\tau_{mob;max}$ does not increase significantly anymore. The point where no significant increase in $\tau_{mob;max}$ over q_c was seen, was used as the limit value for the cone resistance. The limit for α_t was chosen to be 2.5% and the limit for $\tau_{mob;max}$ 2.5% of the cone resistance limit. Data with values above these limits, has to be reduced to the limit values. (CUR236, 2011)

Differences were thus found between raw data, the same data but then adapted according the limit value method stated in CUR 236, and values stated in CUR 236 Table 6.1. For further investigation on how these differences were caused, the available dataset was combined with data from the appendix '*Bijlage A. Proefbelastingen*' of CUR 236. This showed that the current limit values did not suit the shape of the data very well. Investigation on the usefulness of the limit values showed that they are useful for the design process by preventing under- and overestimations of the capacity. Limit values are thus useful, but not in their current form. New limit values were therefore proposed based on a statistical analysis of the available data points. Next to limit values, also design values (expectancy and lower bound) are added.

Because no detailed data for all micropile types was available, it is advised to re-elaborate the limit- and design values for the types that were left out of the proposal given in this thesis, in a similar, statistical way. Furthermore is it advised to investigate a different method to estimate the shear stresses that can be mobilized along the anchor body of a micropile, based on a more fundamental approach. Currently are those stresses often based on full-scale tests from which $\tau_{mob;max}$ is derived, but bounded by the limit values. A different approach to this might be more time- and cost-effective.

1 Introduction

1.1 Background

In 2014, Heijmans started a project at the Drachtsterweg to improve the transit of traffic in and around the city of Leeuwarden, Friesland (NL). The plan was to deepen the biggest part of the Drachtsterweg, and to build an aqueduct to replace the old bridge. During the project, Heijmans used several different micropile types for the foundation of the aqueduct.

For all pile types, test piles were installed and tested on tension according to the first version of the Dutch design guide regarding micropiles (CUR 236), resulting in a database of different piles and pile types installed in similar soil conditions.

The data obtained by Heijmans is according to the guidelines for failure tests presented in CUR 236. Four different types of piles were installed and at least 3 piles were tested for each different pile diameter within a type. The considered pile types are: (Pile numbers based on CUR 236)

- B – single tube with an outside spoil
- C – Self drilling
- D – Screwed
- E – High frequently vibrated

No data was available for type A – double tube with an inside spoil, it was therefore left out of consideration.

It is quite rare that four different micropile types were installed and tested during a single project, especially in a similar soil type. This makes it possible to mutually compare the pile types quite well.

1.2 Problem description

Currently there are still lots of uncertainties around the capacity and use of different types of micropiles. This is mainly because the piles are formed in the soil with different techniques and it is generally assumed that the installation of the pile, has a significant influence on its final capacity.

There are guidelines to design micropiles present in the form of CUR 236, but they do not directly take the installation mechanism or the pile differences into account, except for different shaft friction coefficients (α_t), maximum allowed shear stresses and cone resistances for different pile types are used. It is also stimulated to test piles and base the design on values derived from the test data in order to come to a more customized design.

A quick review of the previously mentioned data base showed differences in shaft friction coefficient α_t within the dataset itself and between the data and CUR 236 Table 6.1. Further investigation on these differences and the effects of installation which probably cause them is therefore required. This was planned to be done by means of a dataset consisting out of installation logs and failure test data.

Investigation of the logs did however not result in interesting findings or relations. This was mostly due to the quality of the installation logs, but also the shape of the information in it, which made it impossible to couple it to a final capacity. During comparison between the data and data from CUR 236, significant differences between the average and limit values stated in Table 6.1 from CUR 236 and the data from the Drachtsterweg were found.

This led to a change in scope towards evaluation of the values in Table 6.1 in CUR 236. In C193 – '*Verborgen Veiligheden*' (Deltares, 2012), it was also stated that changing the limit values for micropiles seemed to be a reasonable option.

1.3 Research question

In the previous paragraph it was mentioned that evaluation of the currently applied limit values stated in CUR 236 might be useful. Together with the analysis of the test data from several pile types this resulted in the following goal:

"To evaluate the limit- and design values for tensionally loaded micropiles, as currently applied in CUR 236 - Micropiles."

In order to reach this goal, a main research question has been formulated: **"Is optimization of the current limit values in CUR 236 possible?"**. This question is split up in three parts: a data study, an evaluation and a conclusion.

The first part is a data study on the database received from failure tests performed at the Drachtsterweg project. In this data study answers to the three following questions will be sought:

1. How do different pile types relate to each other?
2. How does raw data relate to data adapted according limit values stated in CUR 236?
3. How does the data (raw and adapted) relate to values presented in CUR 236 Table 6.1?

Based on the answers of those questions, a next step where the limit values are compared to the shape of the data. For this step, the dataset from the Drachtsterweg is combined with data from CUR 236 '*Bijlage A. Proefbelastingen*', on which the current values in CUR 236 are based. Evaluation of the data shape compared to the limit values will then result in the conclusion in which the current values are confirmed, or a proposal for new values will be given. Evaluation of the limit value gives then basically answer to the main research question.

The thesis will then be concluded with, final conclusions, a discussion and recommendations for further research.

Prior to the data study, literature needed for better understanding of the data is gathered. If during the data study more unclarities arise, as much literature as needed will be added.

1.4 Reading guide

Chapter 2 *Literature review* presents the literature needed for understanding and explaining the available data. Then in the next chapter (chapter 3) a summary of the data study is presented. The full data study can be found in Appendix A: *Data study*, this Appendix is split up into seven parts, the first on the general geological layering as present at the project location, four on each considered pile type, one on the comparison of the different pile types and a conclusion of the data study as a whole.

In Chapter 4, the limit values that are used are evaluated in order to see their usefulness or not. In chapter 5 a proposal for new limit values is given based on a statistical analysis of the data that was available. Then in chapter 6, also design values are added for completeness of the proposal.

Chapter 7 deals with the consequences that a new proposal has for the design strategy. Finally in chapter 8, final conclusions are drawn, a discussion on the results and limitations, and recommendations on further research are given.

2 Literature review

In this chapter the literature needed to interpret the data is presented.

2.1 Considered pile types

CUR 236 distinguishes five different sorts of micropile types, based on their mechanism. In CUR 236, the piles are given letters A to E for easy reference:

A. Micropile bored with a double tube/casing and inside spoil
B. Micropile bored with a single tube/casing and an outside spoil
C. Self-boring micropile
D. Screwed micropile
E. Micropile installed with high frequent vibrations

In this data study, pile type A is left out of consideration due to the lack of data on this pile. The other piles were all installed and tested at the project location. Installation of these types is explained in more detail in the next paragraphs.

2.1.1 Type B: Piles bored with a single casing, outside spoil

Pile type B can be installed as a tube with an open drill head, or with a sacrificial drill bit which will be lost after installation (Figure 2-1). During drilling, a bore fluid or water is used to flush out the excavated soil via the outer side of the tube. After design depth is reached, the GEWI-bar is placed and the bore fluid is replaced with a 0.45—0.5 w/c-ratio grout mixture. To ensure a better attachment to the soil layers, an overpressure is applied to the grout mixture. Then the casing is pulled for half a meter, water is squeezed out of the mixture due to the pressure applied to the grout, and the mixture hardens. The casing is again pulled for half a meter and the same procedure repeats itself until maximum four meters below surface. The overpressure is there changed to hydrostatic pressure to prevent from blow out, and the casing is pulled out entirely.

Figure 2-1: Sacrificial drill bits of Type B micropiles as applied at the Drachtsterweg (Picture B. Niezen)

The theoretical diameter of the pile is the diameter of the drill bit, plus twice 10 millimetres of 'grout penetration depth'. Grout does not really penetrate into the soil, therefore the grout particles are too big. The extra 10 millimetres that has to be taken into account on each side of the drill bit is due to the outside spoil. Because this spoil returns to the surface between the tube and the soil, it removes additional soil particles and flushes them away. Applied grout fills the space that is created due to this.

Local compression of the soil due to the applied grout pressure is nearly impossible regarding the depth at which the anchor body is normally created. If, for some reason the soil is not strong enough to bear the applied grout pressure, a blow-out can occur. A soil layer is then partly lifted and grout fills the gap.

At the Drachtsterweg, micropiles with sacrificial drill bits were used. According CUR 236, the behaviour of type B piles is neutral to soil displacing.

2.1.2 Type C: Self-boring piles

The self-drilling pile is a thick-walled tube with a drill bit which is several centimetres bigger than the tube itself (Figure 2-2). Through the hollow tube, a bore fluid is injected which keeps the borehole stable and helps the drill bit to cut loose the soil. When anchor depth is reached, the bore fluid is changed to a mixture with a w/c-ratio around 0.45—0.5, which is applied under high pressure. The grout flushes the soil away and forms the anchor body of the pile. The bore tube is used as the anchor steel.

Following CUR 236 a 10 millimetre 'grout penetration depth' has to be taken into account. It is however the question if this pile is able to form a smooth cylindrical anchor body. Due to the applied grout pressures which flush away the soil in front of the pile, the anchor body will more logically have a 'plug' or 'chunk' like shape. The different anchor body shape will have effect on how shear stresses are mobilized, and might lead to a more brittle failure behaviour. Installation of self-boring micropiles is assumed to have a neutral to soil-removing character in CUR 236.

Figure 2-2: Drill bit of a Type C micropile as applied at the Drachtsterweg (Pictures Ir. J. Kimenai)

2.1.3 Type D: Screw injection piles

A screwed anchor pile is an anchor pile with screw blades at the pile tip as can be seen in Figure 2-3. The pile is screwed into the soil while a bore fluid is injected at the blades. The soil that was cut loose is mixed with this bore fluid and keeps the borehole stable. When anchor depth is reached, the bore fluid is changed to grout. This grout is also mixed with the loose soil and forms the anchor body of the pile while the pile continues its way to end depth. For these types of micropile, no 'grout penetration depth' has to be taken into account. It is however possible that the grout applied under high pressure flushes more soil out than needed. These piles might also have a non-perfect cylindrical anchor body.

It is possible that the pile is partly raised and lowered during installation to obtain a better mixture between the soil and grout. A negative downside to this is the chance of relaxation in the soil around the pile due to the local removal of soil. According to CUR 236, screwed micropiles have a neutral to soil-removing character.

Figure 2-3: Screw blade of a Type D micropile as applied at the Drachtsterweg (Pictures Ir. J. Kimenai)

2.1.4 Type E: Vibro-fluidization piles

This pile type is a relative new micropile that is installed by means of vibrations and fluidization. First a steel casing which is closed at the top and with a sacrificial plate or 'drill bit' as tip (see Figure 2-4), is brought to depth with a vibrator. Meanwhile also water is applied which has a fluidizing effect on the soil at the tip of the casing. Together with the vibrations which cause local liquefaction and densification of the soil, the weight of the casing and vibrator bring the pile down. When the desired depth is reached, a GEWI-bar is placed and the casing is filled with water. Then the casing is pulled while at the bottom of the casing, grout is applied under high pressure.

The diameter of the anchor body is equal to the diameter of the casing. Applied grout pressures are expected to not compress the soil or penetrate into it. This due to the depth at which the anchor body is formed and the grout particles that are bigger than the pores. Installation of type E piles will have a neutral to soil-displacing character according to CUR 236.

Figure 2-4: Casing of a vibro-fluidization pile with the 'drill bit' next to it (joostdevree.nl)

2.2 Pile design

All previously mentioned pile types are designed based on CUR 236. The general formula that is used to determine the capacity in tension is defined based on a combination of formulas from NEN 9997-1:

$$R_{t,d} = \int_0^{L_a} \frac{O_{p;gem} \cdot f_1 \cdot f_2 \cdot f_3 \cdot \alpha_t \cdot q_{c;z;exc}}{\xi \cdot \gamma_{s;t} \cdot \gamma_{m;var;qc}} dz \qquad 2\text{-}1$$

With:

$R_{t,d}$	Design value for tensional resistance $[kN]$
$O_{p;gem}$	Average circumference of the pile $[m]$
L_a	Length over which shaft friction can develop $[m]$
z	Designation of depth $[m]$
α_t	Tensional shaft friction coefficient $[-]$
$q_{c;z;exc}$	Due to excavation reduced cone resistance $[MPa]$
	$q_{c;z;exc} = q_{c;z} \cdot \frac{\sigma_{v;z;exc}}{\sigma_{v;z;0}}$ for pile type E
	$q_{c;z;exc} = q_{c;z} \cdot \sqrt{\frac{\sigma_{v;z;exc}}{\sigma_{v;z;0}}}$ for pile types other than E
	$q_{c;z;NC} = q_{c;z;OC} \cdot \sqrt{\frac{1}{OCR}}$ for pile type E in a geologically overconsolidated situation
OCR	Overconsolidation ratio $[-]$
ξ	Correlation factor for the number of CPT's and the redistributive capacity of a construction $[-]$
$\gamma_{s;t}$	Partial resistance factor for piles in tension $[-]$
$\gamma_{m;var;qc}$	Factor which indicates the change in loads. $[-]$
f_1	Factor for compaction effect ($f_1 = 1.0$ for micropiles) $[-]$
f_2	Factor for soil relaxation due to tensional loads on a pile group ($f_2 \leq 1.0$) $[-]$
f_3	Factor for pile length effect $[-]$

The bearing capacity of a pile is thus basically expressed as a relation between the frictional area which the pile has with the soil: $\int_0^{L_a} O_{p;gem} dz \rightarrow O_{p;gem} \cdot L_a$ [1], the cone resistance received from CPT-data: $q_{c;z}$, a relation between the CPT data and the friction causing shear stresses, and several coefficients. Failure between grout and soil is thus assumed to be decisive in CUR 236, in which α_t is the coupling between CPT data and the shear stresses.

Following CUR 236 there are two options to come to a micropile design, both options are based on the tensional shaft friction coefficient α_t.

The first option is to use the lower bound values ('ondergrens waarden') presented in Table 6.1 in CUR 236 (Figure 2-5) and base a design on them. The expected values for α_t are normally about 50% higher than the lower bound values, resulting in a tensional capacity which is also 50% higher (following equation 2-1). If the lower bound values are used, it will most likely result in an over-dimensioned design which might be cost-effective for smaller projects where testing costs are relatively high, but not for bigger projects in which a large amounts of piles (100+) need to be installed. Testing costs are in such case insignificant compared to the cost that installation of all piles cost.

It is therefore allowed to install test piles, test them, derive a value for α_t from them and use that as design parameter (second option). Extra condition to this option is that at least 3% with a minimum of 3 piles of all installed piles, have to be checked by means of a validation test. Next to that is it also required to do additional checks on at least 3% with again a minimum of 3 piles, on the other piles. The way to determine α_t from the failure tests will be explained in one of the next sections.

In Appendix D, a flowchart is presented which gives an overview of how the determination of α_t goes.

[1] For a constant cone resistance q_c over the depth

Anker-paal type	Wijze van installatie	Afsnuiten	Rekendiameter paalschacht	Paalklasse factor α_t		
				range van paalschacht diameter waar van toepassing	ondergrens waarden geen in-situ testen (1), (2)	verwachtings waarden wel in-situ testen (1), (2), (3)
		q_c [MPa]	D_{reken} [mm]	D_{min} - D_{max} [mm]	$\alpha_{t;min}$ [-]	$\alpha_{t;verw}$ [-]
A	gespoelboorde ankerpalen, verbuisd ingeboord	20	$D_{boorbuis}$ + 20	180 - 200	0,011 (0,008)	0,017 (0,012)
B	gespoelboorde ankerpalen, met enkele buis ingeboord	20	$D_{boorkroon}$ + 20	180 - 200	0,011 (0,008)	0,017 (0,012)
C	zelfborende ankerpalen	20	$D_{boorpunt}$ + 20	180 - 380	0,008	0,012
D	schroefinjectiepalen	15	$D_{schroefblad}$	180 - 350	0,008	0,012
E (4)	ingetrilde ankerpalen	15	D_{buis}	ca. 200	0,006	-

Figure 2-5: Table 6.1 in CUR 236 (CUR236, 2011)

2.3 Pile testing

When the second design is chosen, test piles have to be installed and tested. Testing of the piles has to be done according to CUR 236. A summary of the most important aspects related to testing up to failure, loading procedure and test setup are presented in this section.

For the complete procedure, but also for rules regarding validation tests and checks, see CUR 236. This due to the fact that α_t is determined based on the failure test, which is relevant for the data study. The other test are less relevant and therefore left out of this literature review.

2.3.1 Failure testing in general

Failure tests are used to determine the maximum capacity of a pile. With this capacity, friction relations can be made between the pile shaft and the bearing soil layers. Besides finding values for the shaft friction coefficient, it can also be used to find out if a pile type is suitable to use under site specific soil conditions.

Values found for the tensional shaft friction coefficient α_t based on failure tests are, following CUR 236, specific for the test location and supplier of the piles. It is not allowed to base a design for a different project location on.

Furthermore states CUR 236 that data received from failure tests is not suitable for predictions on the expected axial stiffness of production piles. This because test pile conditions differ too much from conditions of production piles.

2.3.2 Soil investigation

Before installation, CPT's have to be performed in order to know the cone resistance (q_c). To determine α_t, according to NEN 6745-2:2005, at least three 'class 2' CPT has to be performed close to where the

pile is planned to be installed. Definition of a 'class 2' CPT can be found in (NEN-EN-ISO 22476-12, 2009). Besides that the CPT has to be performed 'close to' the pile, no quantified distances were stated.

2.3.3 Loading procedure

Before actual testing of the piles is started, the expected failure load ($F_{test,max,gross}$ or F_p) is determined. This is defined as:

$$F_{test;max;gross} = R_{s;max} + R_{s;fr} + R_{s,head} \qquad 2\text{-}2$$

With:

$R_{s;max}$	The net bearing capacity at which soil mechanical failure is expected [kN]
$R_{s;fr}$	Value of friction losses which still occur along the free length, although measures applied to prevent this [kN]
$R_{s,head}$	Pile head resistance [kN]

Based on this value for F_p, the load is applied step wise as can be seen in Figure 2-6.

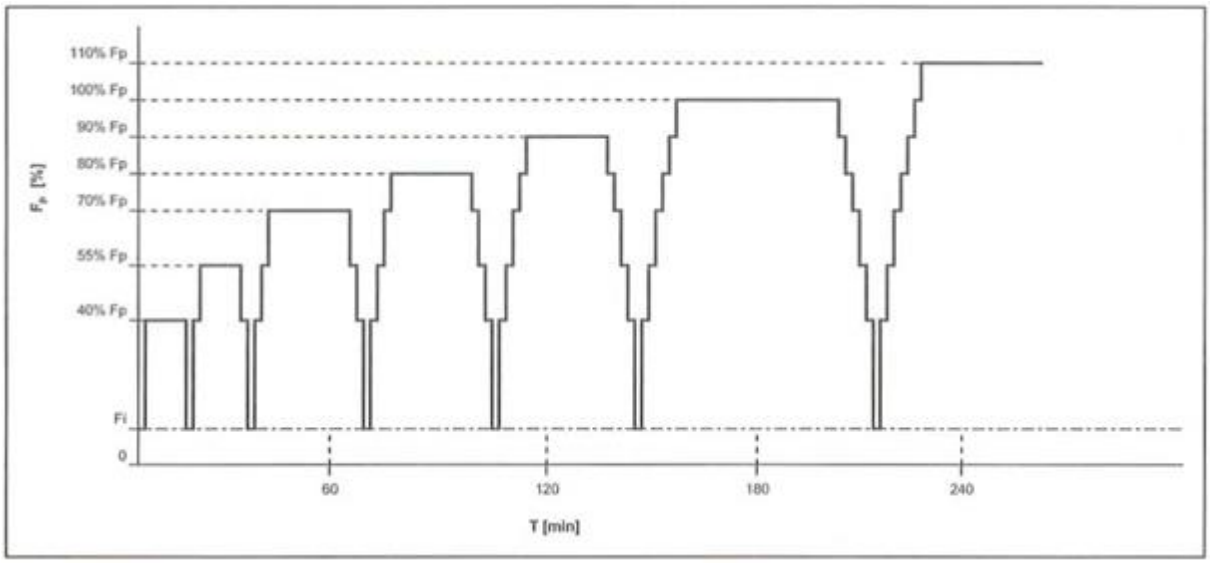

Figure 2-6: Loading steps of a failure test (CUR236, 2011)

The load is thus increased from an initial load between 50 and $100\ kN$, towards the applied loading step. An overview of the height of these steps, the time span over which this load is held constant and the moments at which a measurement has to be noted, can be found in Table 2-1. When the pile did not show failure when 110% of F_p is reached, the load steps are increased with 10% each time until failure occurs.

During testing, at certain points in time, displacements of the pile head are measured. These measurements are used as an indication if soil mechanical failure has been reached. The definition of failure will be explained in the next section.

Table 2-1: Time periods and points for creep measurements during failure testing (CUR236, 2011)

Load (% of F_p)	Time span creep measurements [min]	Measurement points [min]
F_i	5	t = 0, 1, 2, 3, 5
40%	15*	t = 0, 1, 2, 3, 5, 7, 10, 15
55%	15*	t = 0, 1, 2, 3, 5, 7, 10, 15
70%	30**	t = 0, 1, 2, 3, 5, 7, 10, 15, 20, 30

80%	30**	t = 0, 1, 2, 3, 5, 7, 10, 15, 20, 30
90%	30**	t = 0, 1, 2, 3, 5, 7, 10, 15, 20, 30
100%	60***	t = 0, 1, 2, 3, 5, 7, 10, 15, 20, 30, 45, 60
110%	60***	t = 0, 1, 2, 3, 5, 7, 10, 15, 20, 30, 45, 60
* If between t = 7 to 15 min, the displacement $> 0.66\ mm$, continue for 15 more minutes		
** If between t = 15 to 30 min, the displacement $> 0.60\ mm$, continue for 30 more minutes		
*** If between t = 30 to 60 min, the displacement $> 0.60\ mm$, continue for 60 more minutes		

When the maximum capacity of the test equipment has been reached or failure occurred in the anchor steel, the highest applied load has to be used to determine the friction coefficient. Extrapolation of the results is not allowed.

2.3.4 Failure criterion

In the previous section it was said that the pile is loaded until soil mechanical failure occurred, and based on the load at soil mechanical failure, the friction characteristics are determined. In CUR 236, soil mechanical failure is defined to occur when the creep rate (k_s) becomes bigger than $2.0\ mm$. The creep rate can be determined with the formula presented in equation 2-3:

$$k_s = \frac{u_2 - u_1}{\log(t_2/t_1)} \qquad 2\text{-}3$$

With:

k_s	Creep size [mm]
t_1	Start time of a loading step [$mins$]
t_2	final measured time of a loading step [$mins$]
u_1	Pile head displacement at t_1 [mm]
u_2	Pile head displacement at t_2 [mm]

This formula shows basically how much the pile head moves over time, under a constant load. If these displacements over time are too big, the pile has failed and cannot function as a reliable foundation element anymore.

2.3.5 Test setup

The three main components needed for testing of piles are a construction to redistribute the forces due to testing to the soil, a jack to put the load on the pile and sensors to measure the displacement.

The first component, a construction to redistribute the forced due to loading of the pile, is generally made up out of dragline mats on which steel girders are placed (Figure 2-7). It is important that the structure is robust and safe, because the load can sometimes increase to $200\text{-}300\ t$. Between the construction and the test pile, at least 1 meter has to be present to make sure that during testing, interaction between construction and pile is solely through the jack.

The jack that is used for testing has to be calibrated beforehand in order to know the relation between the jack pressure and actual applied force on the pile. The jack is then placed on top of the dragline construction, where the pile and jack are coupled to each other (Figure 2-8)

The final part is placing the sensors which measure the displacements of the pile head. The setup of the sensors must be independent from the dragline construction and the jack, because those two can move or settle due to the applied load. In Figure 2-9 an example of a test construction can be seen. The girder to which measurement equipment is attached, stays apart from the test construction to prevent possible influences on the measurements.

Figure 2-7: Construction to redistribute the test load towards the soil (Pictures Ir. J. Kimenai)

Figure 2-8: Installation of the jack (Pictures Ir. J. Kimenai)

Figure 2-9: Example of test setup in which the measurement equipment is separated from the test construction (CUR236, 2011)

For more details about the setup of failure test and rules and remarks on it, see chapter 10 in CUR 236.

2.4 Test data interpretation

In the previous chapter, testing and aspects related to tested were briefly shown. In this chapter, the way to go from the failure load in the test to the shaft friction coefficient α_t is explained.

The way to determine α_t from the failure test data following CUR 236 consists out of the following eight steps:

Step 1:

A pile is tested according to CUR 236. From that test, the maximum load that has been applied while the creep rate (k_s) stays below or equal to 2.0 mm, is used.

$$F_{test;max;gross} = F_{test;max} \text{ with } k_s \leq 2.0\ mm \qquad 2\text{-}4$$

Step 2:
From this gross test load, the net test load is determined with equation 2-5. This net test load is the load that is actually working on the grout body which connects the pile to the soil.

$$R_{s;max} = F_{test;max;gross} - R_{s;fr} - R_{s;head} \qquad 2\text{-}5$$

With:

$R_{s;fr}$ Loss due to friction along the free length of the pile (Figure 2-10). To be determined with strain gauges along the free length. Compare the theoretical shortening due to removal of the test load with the measured shortening. [kN]

$R_{s;head}$ Head resistance due to a not fully bored or flushed free length. [kN]

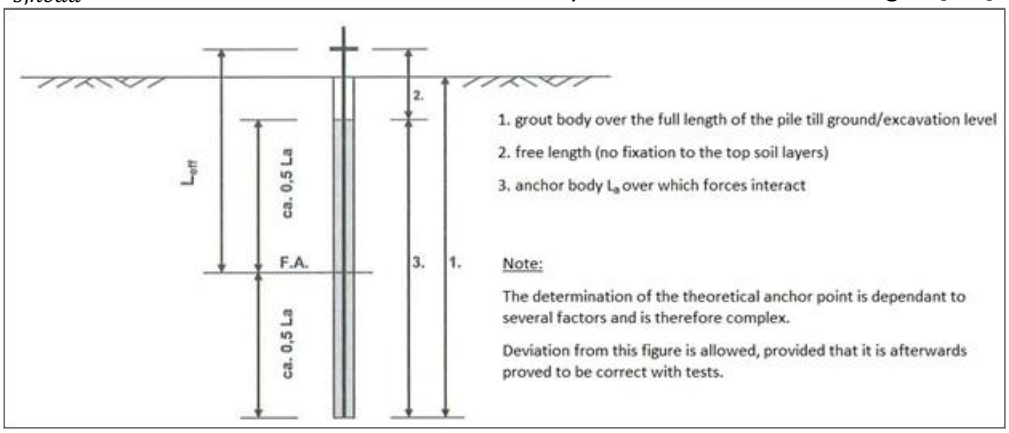

Figure 2-10: Free length of the pile (translated Figure 8.1 from CUR 236)

During installation of the test piles and the setup of the test itself, measures to prevent losses due to friction or resistance along the free length of the pile are taken. Based on the elastic deformation, the amount of eventual 'lost' load due to friction losses can be estimated and reduced for.

Step 3:
With the net maximum test load, the mobilized shear resistance along the anchor body can be determined by dividing it by the area over which friction can develop:

$$\tau_{mob;max} = \frac{R_{s;max}}{\pi \cdot \emptyset \cdot \mathrm{L_a}} \qquad 2\text{-}6$$

With:

$\tau_{mob;max}$ The maximum mobilized shear resistance [kN/m^2]

$\emptyset$ Outer diameter of the anchor body [m]

L_a Effective length of the anchor body (Figure 2-10) [m]

Step 4:
Determine per test pile $q_{c,avg}$ over the length of the anchor body, based on the CPT's.

Step 5:
Determine the friction coefficient. This coefficient is not allowed to be higher than 2.5%.

$$\alpha_{t;i} = \frac{\tau_{mob;max}}{q_{c;avg}} \leq 2.5\% \qquad 2\text{-}7$$

With:

$\alpha_{t;i}$ Friction coefficient along the surface of the anchor length. [$-$]

$\tau_{mob;max}$ The maximum mobilized shear resistance along the anchor body. [kN/m^2]
Following CUR 236, maximum values for $\tau_{mob;max}$ that are allowed in designs are:
500 kN/m^2 ($= 0.025 \cdot 20\ MPa$) for pile types A, B and C*
375 kN/m^2 ($= 0.025 \cdot 15\ MPa$) for pile types D and E*
* values for C and E not proven in reality

$q_{c,avg}$ Average measured cone resistance over the length of the grout body. [MPa]
Maximum values that are allowed for $q_{c,avg}$ in designs are:
$20\ MPa$ (pile types A, B and C)
$15\ MPa$ (pile types D and E)

Step 6:
Determine the average value for the friction coefficient α_t based on the amount of piles tested:

$$\alpha_{t;avg} = \frac{\sum \alpha_{t;i}}{N} \quad \text{2-8}$$

With:

$\alpha_{t;i}$ Friction coefficient along the surface of the anchor length for test pile i [−]
N Number of tested piles [−]

Note that the coefficient of variation of all independent values of the maximum test load, has to be maximal 0.12.

$$CV = \frac{\sigma_{test;max;avg}}{\mu_{test;max;avg}} \quad \text{2-9}$$

With:

$\mu_{N;test;max}$ The average value of the maximum gross test loads:
$\mu_{N;test;max} = \frac{\sum F_{test;max;gross}}{N}\ [kN]$

$\sigma_{N;test;max}$ The standard deviation of the maximum gross test loads:
$\sigma_{N;test;max} = \sqrt{\frac{\sum_{i=1}^{N}\left(F_{test;max;gross,i} - \mu_{N;test;max}\right)^2}{N}}\ [kN]$

If the coefficient of variation is equal to or lower than 0.12, go to *Step 7*, if CV is higher than 0.12, go to *Step 8*.

Step 7:
Determine the design value based on:

$$\alpha_t = \beta_t \cdot \alpha_{t;avg} \quad \text{2-10}$$

With:

α_t The design value for the friction coefficient along the surface of the anchor body for construction piles
$\alpha_{t;avg}$ Average friction coefficient of the test piles [−]
β_t Coefficient for the number of successfully tested test piles following Table 2-2

Table 2-2: β_t values, dependent on the number of test piles N. (CUR236, 2011)

N	**1**	**2**	**≥3**
$\boldsymbol{\beta_t}$	0.8	0.9	1.0

Step 8:
If the coefficient of variation is higher than 0.12, the friction coefficient has to be equal to the lowest α_t value that resulted from the tests:

$$\alpha_t = \alpha_{t;min} \qquad 2\text{-}11$$

α_t values found based on this scheme are used to optimize the micropile design to a more economic form within a project. In the data study however, only the basic ideas behind this scheme are used to determine the mobilized shear stresses and values for the shaft friction coefficient based on raw CPT data.

2.5 Relation shear strength and cone resistance

It was seen that α_t is made up out of a division of the mobilized shear strength or stresses, by the average cone resistance. These two values have to be related in some way, otherwise α_t would be a random value. In this section, the relation between the shear strength and the cone resistance is presented. Note that the presented relation only yields for sand. The relation with other soil types is less interesting because micropiles are preferably installed in sand layers in order to reach a proper bearing capacity.

The relation between the cone resistance and the shear stresses consist out of two steps. The first step is the link between the cone resistance (q_c) and the drained friction angle (ϕ'). In 1983 research on this relation was presented by Robertson and Campanella. They suggested a correlation between the drained friction angle and the corrected cone resistance based on calibration chamber test results (Figure 2-11). The empirical relation they found was:

$$\phi' = \tan^{-1}[0.1 + 0.38 \cdot \log\left(\frac{q_t}{\sigma'_v}\right)] \qquad 2\text{-}12$$

With:

ϕ'	Drained friction angle [°]
q_t	Corrected cone resistance [kPa]
σ'_v	Effective overburden pressure [kPa]

The corrected cone resistance is defined as (VertrekCPT, 2015):

$$q_t = q_c + u_2(1 - a) \qquad 2\text{-}13$$

With:

q_c	Measured cone resistance [kPa]
u_2	Pore pressure behind the head of the cone [kPa]
a	Cone area ratio, often between 0.6 and 0.8 [−]

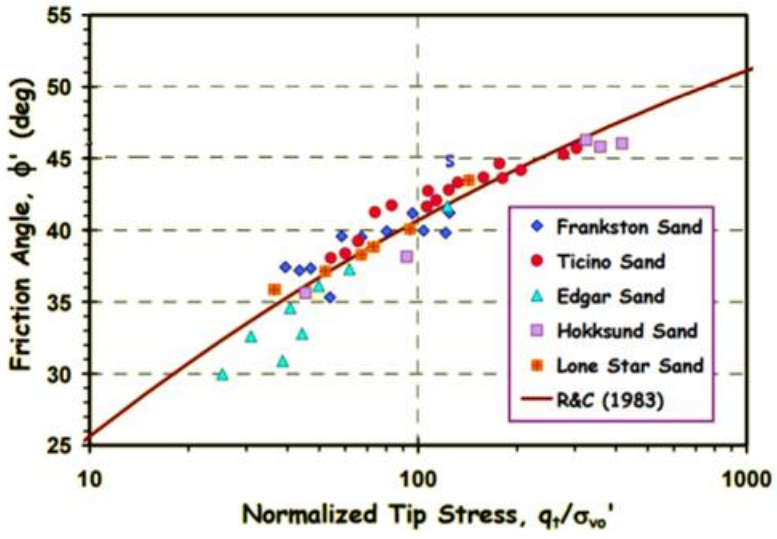

Figure 2-11: Friction angle of Sands from CPT, based on (Robertson & Campanella, 1983)

In the second step the drained friction angle is substituted in the formula that describes the Mohr-Coulomb failure envelope (equation 2-14), in order to determine the shear strength of the soil (Mayne, 2014).

$$\tau_f = c' + \sigma_v' \tan(\phi') \quad \text{2-14}$$

With:

τ_f	Shear strength of the sand $[kN/m^2]$
c'	Cohesion $[kPa]$
ϕ'	Drained friction angle [°]
σ_v'	Effective overburden pressure $[kPa]$

Because the cohesion of sand is negligibly small and the piles considered in this data study are installed in sand layers, the cohesion can be left out of this equation.

To estimate the shear strength of the soil along the anchor body of a micropile, the horizontal component of the effective overburden pressure must be determined. This because the component of the overburden pressure that acts on the pile in the normal direction is needed. In the case of a vertical pile, this is the horizontal effective stress σ'_h. This can be done with the coefficient of lateral earth pressure K, which is defined as the ratio between the horizontal and vertical effective stress (Verruijt, 1999). This can be expressed as:

$$\sigma'_n = K \cdot \sigma'_v \quad \text{2-15}$$

With:

σ_v'	Effective overburden pressure $[kPa]$
σ_n'	Normal effective stress (basically σ_h') $[kPa]$
K	Lateral earth pressure coefficient $[-]$

The height of K is dependent on the material type (ϕ') and how the material is loaded. There are basically three pressure states, each with a different value for K: active (K_a), passive (K_p) and neutral (K_0). The active and passive lateral earth pressure coefficients can be determined following the Rankine theory (Bartlett, 2011):

$$K_a = \frac{1-sin(\phi')}{1+sin(\phi')} \quad \text{2-16}$$

$$K_p = \frac{1+sin(\phi')}{1-sin(\phi')} \quad \text{2-17}$$

The coefficient for normally consolidated soils at rest, can be estimated by the correlation suggested by Jaky (Bartlett, 2011):

$$K_0 \approx 1 - sin(\phi') \quad \text{2-18}$$

Equations 2-12, 2-14 and 2-15 combined gives the relation between the cone resistance and the shear strength of the soil, with K dependent on the pressure state:

$$\tau_f = K \cdot \sigma_v' \cdot \tan\left(\tan^{-1}[0.1 + 0.38 \cdot \log\left(\frac{q_t}{\sigma_v'}\right)]\right) \quad \text{2-19}$$

$$= K \cdot \sigma_v' \cdot \left(0.1 + 0.38 \cdot \log\left(\frac{q_t}{\sigma_v'}\right)\right) \quad \text{2-20}$$

It can be seen that the shear stresses are highly dependent on the cone resistance. The overburden pressure also plays a significant role.

2.5.1 Theoretical bearing capacity

In the previous section a formula was presented that describes the relation between the cone resistance and the shear strength of the soil, in order to prove that α_t is a legit parameter with physical meaning. This formula can slightly be adapted to estimate the theoretical bearing capacity of the pile.

To do so, equation 2-14 is replaced by a formula from the American Petroleum Institute (API) that can be used for estimating the shaft shear for axially loaded piles (U.S. Department of Transportation, 2006). This formula yields:

$$f_s = \sigma_v' \cdot K \cdot \tan(\delta) \qquad 2\text{-}21$$

With:

f_s	Unit side shear stress $[kPa]$
σ_v'	Effective overburden pressure $[kPa]$
K	Lateral earth pressure coefficient $[-]$
δ	Interface friction angle between pile and soil [°]

The interface friction angle δ is assumed to be 1 due to the roughness of the grout, and the cementation between grout and the surrounding soil particles. This leads, together with equation 2-12 to:

$$f_s = \sigma_v' \cdot K \cdot (0.1 + 0.38 \cdot \log\left(\frac{q_t}{\sigma_v'}\right)) \qquad 2\text{-}22$$

It can again be seen that the shear stress on the pile-soil interface is dependent on the cone resistance and the overburden pressure. Also the load state of the soil expressed in K, plays an important role.

2.5.2 Formula application for micropiles

The way how this formula can be applied for micropiles lies mostly in the parameter K for the load state of the soil. For micropiles it is assumed that the load state of the soil, lies between a fully passive load state and the neutral load state. This due to the application of grout under higher pressure which applies a lateral pressure on the surrounding soil, and thus a more passive load state.

In Figure 2-12 and Figure 2-13 the unit side shear stress can be seen for respectively the passive– and the neutral load state. Note that for the neutral load state instead of K_0 according equation 2-18, $K_0 = 1$ was used. This based on the advice of the API (Pelletier, et al, 1993). For The passive load state K_p, the formula described in equation 2-17 was used.

Note that the graph is based on theoretical values which are not always likely to occur in reality, i.e. a cone resistance of 40 MPa at an overburden pressure of 100 kPa ($\pm$ 10-15 m depth). Note furthermore that the lateral earth pressure coefficients used, are for problems that can be modelled in 2D. Piles however, are more towards a 3D problem due to the radial aspect of a pile

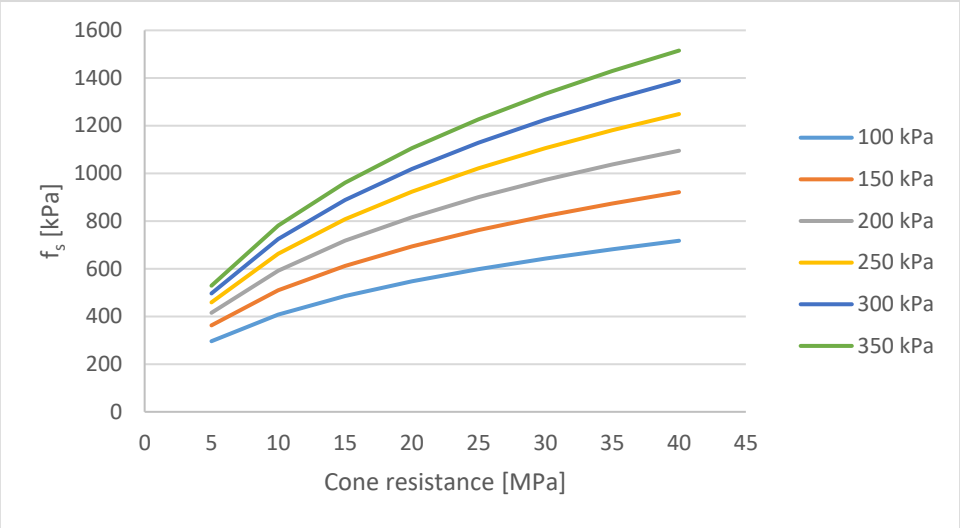

Figure 2-12: Unit side shear stress as function of cone resistance and overburden pressure, for passive load state of the soil

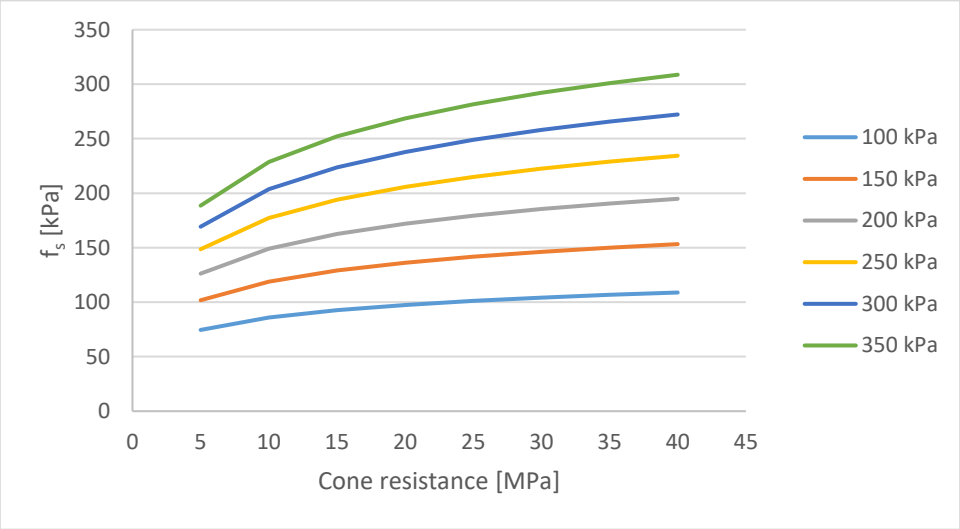

Figure 2-13: Unit side shear stress as function of cone resistance and overburden pressure, for neutral load state of the soil

It can be seen that the shear stresses increase with an increasing cone resistance and overburden pressure. It can furthermore be seen that the increase slows down over the increasing cone resistance.

2.6 Friction losses along free length

In section 2.3.3 friction losses along the free length were mentioned. The way to determine the height of the friction losses is presented here.

The friction losses along the free length can be determined based on the difference in force needed elastically deform the anchor steel, and the actual force needed for this elastic deformation. The elastic deformation is determined on the back spring of the pile when it is unloaded.

First the elastic spring stiffness anchor steel needed. This can be determined by using a combination of the following formula's:

$$\epsilon = F/EA \qquad 2\text{-}23$$

$$\Delta L = \epsilon \cdot L_{eff} \qquad 2\text{-}24$$

With:

ϵ	The strain $[-]$
F	Force acting on the anchor steel $[N]$
E	Elastic modulus of the steel $[N/mm^2]$
A	Area of the steel $[mm^2]$
L_{eff}	Effective length of the steel $[mm]$
ΔL	The elastic elongation of the steel $[mm]$

Combining and rewriting of 2-23 and 2-24 leads to:

$$\frac{\Delta L}{F} = \frac{EA}{L_{eff}} \qquad 2\text{-}25$$

Because during testing the load is not brought back to zero but to an initial value, the difference between the total load and the initial load must be taken. Together with the load difference, also the corresponding displacement difference must be taken. This gives the elastic spring stiffness:

$$k_{el} = \frac{\Delta u}{\Delta F} = \frac{EA}{L_{eff}} \qquad 2\text{-}26$$

With:

ΔF	Difference between total and initial loading force on the anchor steel $[N]$
Δu	Difference in displacement between a certain test load step and the displacement after the load is brought back to the initial load $[mm]$

The next part is then determining how much force was actually needed for an elastic elongation of 1 mm. The actual spring stiffness of the pile thus, which includes the spring stiffness of the steel but also the extra force needed due to friction along the free length. This can be determined by dividing the difference in load of a certain loading−unloading step i, by the back spring of the same step. Due to the elastic characteristics of the system, it should not matter which loading−unloading step is taken. Often the last step before failure occurred is used. The spring stiffness of the pile is then:

$$k_{pile} = \frac{\Delta u_i}{\Delta F_i} \qquad 2\text{-}27$$

The difference between the spring stiffness of the actual installed pile (k_{pile}) and the theoretical value based on the characteristics of the steel (k_{el}) gives then the amount of force which is due to friction losses. That difference multiplied by the elastic deformation of the step closest to failure, indicated by subscript n. Gives the amount of friction losses along the free length of the pile for $i = n$:

$$R_{s,fr} = (k_{pile} - k_{el}) \cdot \Delta u_n \qquad 2\text{-}28$$

With:

$R_{s,fr}$	Friction losses along the free length of the pile $[N]$

The final load step is used because the load, and thus elastic deformations, are the closest to the load and deformations during the step where failure occurred. The friction losses can be deducted from the total failure load to get a representative value for the load which is applied to the anchor body.

2.7 Statistics

For evaluation of the data and proposal of new, or confirmation of the current limit values, some basic statistics are applied.

2.7.1 Population and sample

The data set that is used for this research is a collection of failure tests, applied on different micropiles. The failure tests are performed in order to estimate the capacity of piles that will be installed at a project.

All piles that will be- or were installed can be seen as the population (set of similar items which is of interest for statistical investigation). Parameters of the population can then be estimated based on a small part of the population (a sample), in this case the available dataset. The relation between sample and population can be seen in Figure 2-14.

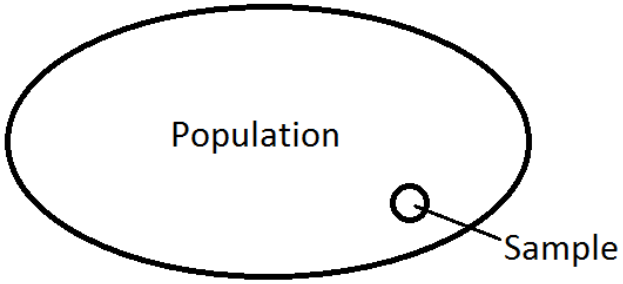

Figure 2-14: Population and sample

2.7.2 Mean and standard deviation

From the sample, the sample mean, variance and standard deviation can be determined as a first step in estimating a population parameter.

$$\bar{X} = \frac{1}{n}\sum_{i=1}^{n} X_i \qquad 2\text{-}29$$

$$S^2 = \sqrt{\frac{\sum_{i=1}^{n}(X_i - \bar{X})^2}{n-1}} \qquad 2\text{-}30$$

$$S = \sqrt{\frac{\sum_{i=1}^{n}(X_i - \bar{X})^2}{n-1}} \qquad 2\text{-}31$$

With:

$\bar{X}$	Sample mean [$*$]
S	Sample standard deviation [*]
S^2	Sample variance [*]
X_i	A certain data point i [*]
n	The number of data points in the sample [$-$]

* dependent on the unit of the data

In statistics, the mean, variance and standard deviation of the population are denoted by respectively μ, σ^2 and σ. There is a slight difference in determination of the sample variance an standard deviation, and the population variance and standard deviation. While determining the sample parameters the sum is divided by $n-1$, instead of just n for the population parameters, to make it unbiased. If a biased estimator would be used, it would systematically produce too small estimates. (Dekking, Kraaikamp, Lopuhaä, & Meester, 2005).

2.7.3 Characteristic values determination

Based on the sample parameters, the characteristic values with a 5 and 95% chance of exceedance for respectively the upper and lower bound, can be found following: (CUR Bouw & Infra, 2008)

$$\bar{X}_{frac;5\%} = \bar{X} + t_{0.05;n-1} \cdot \frac{s}{\sqrt{1+\frac{1}{n}}} \qquad 2\text{-}32$$

$$\bar{X}_{frac;95\%} = \bar{X} - t_{0.05;n-1} \cdot \frac{s}{\sqrt{1+\frac{1}{n}}} \qquad 2\text{-}33$$

With:

$\bar{X}_{frac;5\%}$	Upper bound which has a 5% chance on exceedance [$*$]
$\bar{X}_{frac;95\%}$	Lower bound which has a 95% chance on exceedance [*]
$t_{0.05;n-1}$	Value of t-distribution [$-$]

* dependent on the unit of the data

The value for the t-distribution ($t_{0.05;n-1}$) is dependent on the degree of freedom ($n-1$) of the sample, and can be found in the Table for the t-distribution in Appendix E. The t-distribution is basically a 'weighted on the number of data points' normal distribution. This distribution can be used to estimate the population probability values based on sample parameters and the number of data points n.

Dependent on the number of data points in the sample shifts the t-distribution towards a normal distribution as can be seen in Figure 2-15. More data points result thus in an higher certainty of the estimated population parameters.

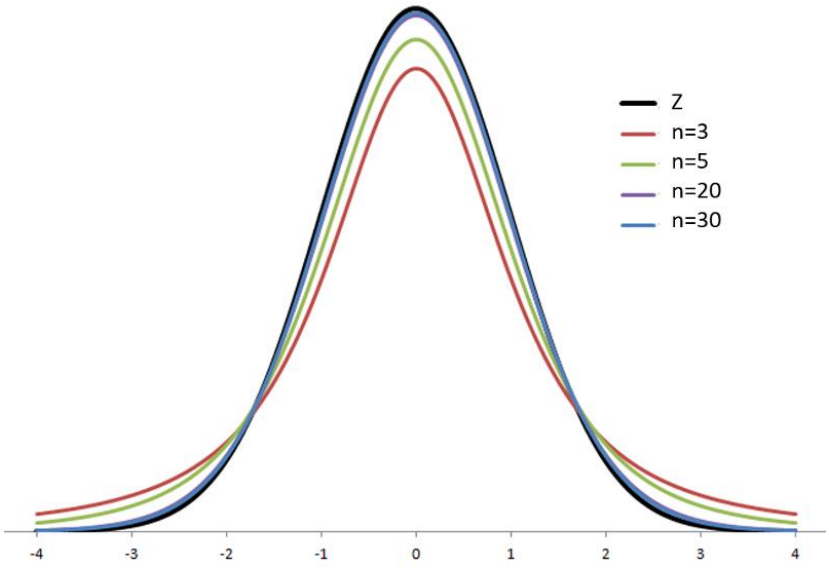

Figure 2-15: t-distribution development as function of the degree of freedom n (Boston University)

3 Data study

In this chapter a concise summary of the data study is presented. For the full data study, see Appendix A. The data study was used to validate the integrity of the piles by investigation of the installation logs. After validation of the individual piles, the α_t value for different pile types were compared. This was done for micropile types B, C and D (numbering according CUR 236). Furthermore a comparison between the data and CUR 236 was done.

3.1 Methodology and Limitations

Before the findings of the data study are presented, first the methodology and limitations to the study are discussed. This in order to be able to see the results in their context.

3.1.1 Methodology

Following CUR 236, the values received for the cone resistance (q_c) and the maximum mobilized shear stress ($\tau_{mob;max}$), are not allowed to be higher than a certain, pile type-bound, value. In the data study however, only raw values were used. Adapted values might remove possible relations or trends from the data, or might give a distorted view on it. The raw values are thus needed to make realistic comparisons.

At the end of the data study, a comparison between the raw values and values based on CUR 236 are compared. This was done by comparing the α_t values. α_t was defined as the ration between $\tau_{mob;max}$ and q_c (see equation 2-7).

3.1.2 Limitations and uncertainties

During the data study several uncertainties or limitations arose. It is important for the results to them. This also helps evaluating the results and they can furthermore act through in the recommendations that will be given at the end of this report.

3.1.2.1 Diameter

The first uncertainty is the diameter of the piles. This uncertainty affects the frictional area of the pile, and thus the maximum mobilized shear stress, $\tau_{mob;max}$. The reason that the diameter of the applied piles is unsure, lies in the fact that the piles are formed in the soil and that after testing, they were not completely pulled out in order to verify the diameter. In the data study, diameters are based on the ones presented in the reports on the failure tests, and thus on CUR 236. Dependent on the smaller or bigger actual diameter, this leads to respectively and over- and underestimation of $\tau_{mob;max}$.

3.1.2.2 Shape of the grout body

The second uncertainty is the shape of the anchor- or grout body. This is somewhat connected to the uncertainties in diameter of the pile, but it also affects the net failure load. This uncertainty yields mostly for micropiles of type C, which are self-boring piles. When these piles are installed and grout is ejected through the tip, the applied grout might flush away significant volumes of soil. The void left by the soil is filled with grout, the diameter and shape of the body are then unknown.

The diameter was already mentioned in the previous section, but the shape of the body is also important. The described grout-applying mechanism results in a more plug-like grout body which has a bigger diameter than the borehole. When this pile is then tested, not only friction along the shaft is realized, but also soil resistance on the top of the grout body. This resistance is defined as the head resistance ($R_{s;head}$) of the pile, and is deducted from the gross failure load as was seen in equation 2-5. An anchor body with a plug-like shape will lead to and overestimation of the net failure load, and following equation 2-6, thus $\tau_{mob;max}$.

3.1.2.3 Length of the grout body

The length of the grout body is also an uncertainty. Because the pile is created in the soil, it is unknown what its exact length is. It is possible that during installation, grout leaks away, or grout ends up higher than the planned level. This might result in a shorter or longer grout body length which affects the frictional area of the pile. Because the theoretical length is used when determining the mobilized shear stresses, a longer or shorter anchor body can result in respectively an over- and underestimation of $\tau_{mob;max}$.

3.1.2.4 Gross failure load

The next uncertainty is the exact value of the gross failure load. The reason for this is the way how testing is done with the load increment steps of 10%. When a certain load step is successfully reached, the next step is that load step plus 10% of the expected failure load (except for the first three steps which are respectively 40, 55 and 70% of the expected failure load). When for example the load step of 100% is successfully reached, but the load step of 110% not; the load step of 100% is taken are decisive. Although failure only occurred at for example 106% of the expected failure load. This way of testing results thus often in an underestimation of the actual load at which failure occurred.

3.1.2.5 Soil conditions

Another uncertainty lies in the soil investigation. CPT's are performed close to the location of the pile, but not exactly at the location. Due to the highly variable character of soil, there will always be a slight difference between the soil conditions measured by the CPT and the conditions which actually apply to the pile. It cannot be said that this leads to an over- or underestimation. Furthermore are the results based on CPT's performed before installation. The influence of installation on the soil conditions is unknown.

3.1.2.6 Capacity of the steel

While testing, several piles reached the capacity of the steel, no soil mechanical failure occurred. For these piles, the load at failure for the steel was taken to be decisive, an underestimation of the actual failure load thus. When certain comparisons were made in the data, these piles were left out or a note about this was made.

3.1.2.7 Pile installation

Several piles of type D were not installed correctly in the shallow sand layer. Piles had their grout body in both the sand, and the clay above it. It is important to know this when those piles are compared to other pile types.

3.1.2.8 Specific location

Results found based on the data study, are specific for the soil at the Drachtsterweg project site. It is possible that at a different location, different values or behaviour is found.

3.2 Results

In the data study first the different pile types were compared. Then the data was compared to data adapted according the limit values from CUR 236, and the values stated in CUR 236 Table 6.1.

Micropiles of type E are left out of the comparisons because their integrity could not be verified. CPT's were taken after installation, which gives an incorrect image of the initial soil conditions due to the vibrations caused by installation. Furthermore was the data in the installation logs sparse and equal for all piles in a layer. It is almost impossible to create identical in-situ piles. The logs were therefore assumed to be filled in not correctly, which was the reason why the piles could not be verified.

3.2.1 Pile types

The first step was to compare the pile types mutually (visualisation in Figure 3-1). This showed that pile type B, has a significantly higher α_t value and thus a larger capacity than types C and D. The higher α_t value is due to the higher value for the maximum mobilized shear stresses. Possible causes for the observation might be in the height of the grout pressures, the way how grout is applied, the method of installation and the load-state of the soil.

For type B, significantly higher grout pressures are applied: 10 to 25 Bar against 0 to 6 Bar for types C and D. Furthermore the way how grout is applied. For type B, the pressure is put directly on the soil around the pile while the casing is pulled upwards. For types C and D, grout is ejected from the pile tip and flushes away the soil, or is mixed with it.

Installation of the piles differs mostly in the way of boring. Types C and D are bored and screwed in respectively. Together with boring or screwing, grout is ejected from the tip which flushes away the soil. For type D, the soil is then mixed with the grout to form an anchor body.

Piles that press the soil away due to the grout pressures, are more in a passive loading state, which results in higher horizontal soil stresses, and thus a higher maximum mobilized shear stress. This yields mostly for type B where higher grout pressures are applied directly to the soil. Installation of types C and D might quicker result in relaxation due to the removal and mixing of the soil. It is therefore more likely that the soil around those piles is in a more neutral to slightly active state. This might also explain the differences in maximum mobilized shear stress.

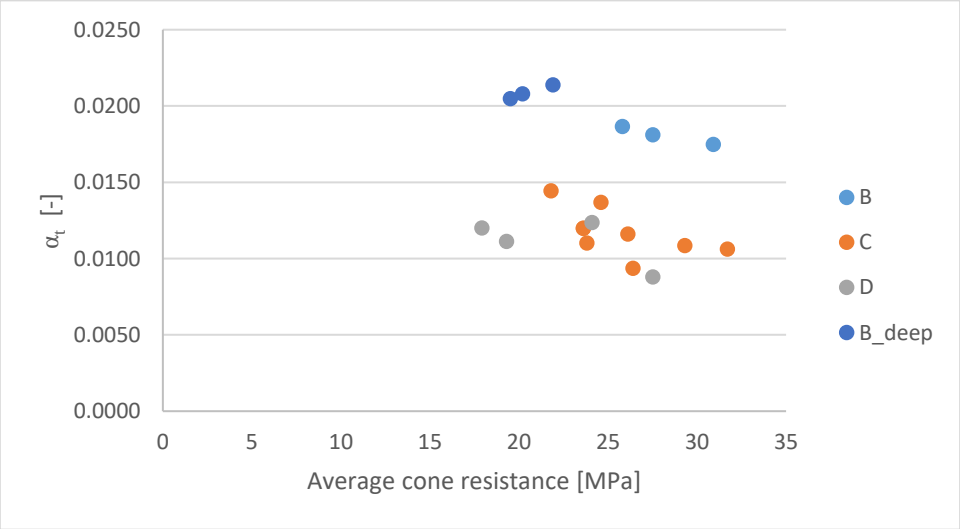

Figure 3-1: α_t as function of the average cone resistance for all piles (based on raw data)

3.2.2 Design based on CUR 236 (limit values)

Next to a mutually comparison between the pile types, are the α_t values of the piles compared to the values that would have been received if the design scheme of CUR 236 was followed. CUR 236 states that limit values for the cone resistance have to be used. Values above the stated limit, have to be reduced to the limit value. These values are 20 MPa (Types A, B and C) and 15 MPa (Type D). The maximum mobilized shear stress has a limit of 2.5% of the maximum cone resistance; 500 kN/m^2 and 375 kN/m^2 thus. A design based on CUR 236 is thus a design in which limit values are applied; also referred to as the 'design scheme'.

From the comparison it was observed that the values for α_t based on the design scheme, are significantly higher than values based on raw data (Table 3-1). Investigation on what this meant for the final

capacity showed that there were no significant differences between them. A design based on raw values resulted thus in a nearly equal capacity as when the design scheme from CUR 236 is applied.

Table 3-1: Average values for α_t and the corresponding standard deviation

		Raw data		Limit values (CUR 236)	
	Type	μ [−]	σ [−]	μ [−]	σ [−]
Shallow	B	0.0181	0.00058	0.0250	0
	C	0.0117	0.00156	0.0178	0.00150
	D	0.0111	0.00161	0.0175	0.00223
Deep	B	0.0209	0.00046	0.0246	0.00059

The capacity based on raw values was for only a single pile of type B higher than based on the design scheme of CUR 236 where limit values have to be applied.

3.2.3 CUR 236 Table 6.1

Finally comparisons between the average α_t values and expected values presented in Table 6.1 from the CUR were made (Table 3-2). In the average α_t values, both the values based on raw data, and values based on the design scheme from CUR 236, are included.

It was observed that the values based on raw data, are more in line with the expected values presented in Table 6.1 from CUR 236, than the values based on the design scheme of the same CUR. It must however be said that the 'expected' values in Table 6.1, are more the lower-average values than the actual average values. Furthermore are the values in Table 6.1 based on failure test executed in soil conditions below the maximum allowed cone resistance. Due to this, it gives the same image as results based on raw data. Because no limit values have to be applied, the outcome is the roughly same as when based on raw data.

When expected values from Table 6.1 are used in the design scheme following CUR 236, this will lead, based on the results of the data study, to a significant underestimation of the actual capacity. At least, when the soil has higher cone resistances than the limit values.

Table 3-2: α_t values based on raw data, the design scheme from CUR 236 and values presented in CUR 236

		Raw data	Limit values	CUR 236, Table 6.1 values	
	Type	μ [−]	μ [−]	Lower bound	Expected
Shallow	B	0.0181	0.0250	0.011	0.017
	C	0.0117	0.0178	0.008	0.012
	D	0.0111	0.0175	0.008	0.012
	E	0.0185	0.0250	-	-
Deep	B	0.0209	0.0246	0.011	0.017
	E	0.0250	0.0231	-	-

3.3 Conclusion

The first thing that can be concluded is that pile type B has a higher capacity in the soil conditions at the project site, than types C and D. The most probable cause for this is the height of the grout pressure, and the way how the grout is applied.

The next thing that can be concluded from the data study is that for the data from the Drachtsterweg, Leeuwarden, a design based on limit values does not lead to a significantly different pile capacity than when based on raw values. This might question the usefulness of the limit values for the cone re-

sistance and mobilized shear stresses. Besides that, does reducing those limit values also result in significantly higher α_t values, which gives the idea that the pile capacity is much higher than it actually is. α_t values based on data adapted according limit values, give thus a misleading view on the capacity.

The final aspect that can be concluded is again that the α_t values based on the CUR 236 design scheme are relatively high. The expected values in CUR 236 Table 6.1 are more in line with values based on raw data than on the CUR 236 based values. The results of the data study question thus the usefulness of limit values, or at least the height of the current limit values.

4 Limit value evaluation

In the previous chapter, the usefulness of limit values was questioned based on a data study. It showed that by using limit values during failure test interpretation, values for the tensional shaft friction coefficient α_t were artificially heightened. When again limit values were applied to q_c in a possible design, this led to no significant differences in capacity if no limit values were used at all.

The question then is, if it is better to change the limits to values that suit the data better, or to use none at all. In this chapter the use and effects of the limit values are investigated. Based on this a conclusion will be drawn whether to use and propose new limit values, or to remove the limit values completely form the design method.

4.1 Limit values

In CUR 236, limit values are stated. The values are used to prevent unrealistic designing based on failure testing. Failure tests are basically full-scale test on which the design is based. Those tests are preformed due to the high uncertainty about the micropile capacity. The limit values say basically that based on experience (data from previous tests at different locations), values higher than the limits are not realistic. The limit values that have to be applied according CUR 236 are presented in Table 4-1.

Table 4-1: Limit values presented in CUR 236

Pile type:	**A**	**B**	**C**	**D**	**E**
$q_{c;lim}$ **[MPa]**	20	20	20	15	15
$\tau_{mob;lim}$ **[kN/m²]**	500	500	500	375	375
$\alpha_{t;lim}$ **[−]**	0.025	0.025	0.025	0.025	0.025
$\alpha_{t;expected}$ **[−]**	0.017 (0.012)	0.017 (0.012)	0.012	0.012	-
$\alpha_{t;lower\ bound}$ **[−]**	0.011 (0.008)	0.011 (0.008)	0.008	0.008	0.006

* values in brackets have to be applied when the grout body was not pressurized over the whole length

There are thus three types of limit values as could be seen in Table 4-1. One for the cone resistance, one for the maximum mobilized shear stress and one for the tensional shaft friction coefficient α_t. The other 2 values for α_t, are respectively the expected and lower bound values. The three limit values are related to each other's following:

$$\alpha_t = \frac{\tau_{mob;max}}{q_c} \qquad 4\text{-}1$$

Which can also be seen in Figure 4-1 for point A. α_t is thus basically the slope of the assumed linear relation indicated by α_a in Figure 4-1. In the next sections, each limit value will be explained in more detail, and how the limit value affects a possible design.

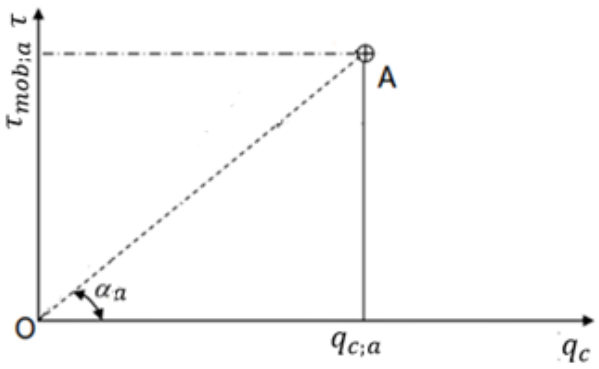

Figure 4-1: relations between α_t, q_c and $\tau_{mob;max}$

4.1.1 Cone resistance

The first limit value is the one for the cone resistance ($q_{c;lim}$). Within the guidelines and norms, these values differ much. In NEN 9997-1 is for example stated that values higher than 12 MPa have to be reduced to 12, except when they are present in a layer which is at least one meter thick. In that case, the peaks have to be reduced to 15 MPa. In CUR 236, the limit values are higher than the values stated in NEN 9997-1 as was seen in Table 4-1. There is thus no uniform rule for all geotechnical applications.

4.1.1.1 Reason for the limit value

There are two main reasons to make use of limit values for the cone resistance. The first on is that there is no proven relation between the cone resistance and the mobilized shear stresses above the limit value. When higher values are applied, this is basically an extrapolation of the relation which might lead to safety issues.

The second reason has to do with overconsolidation of sands. Over consolidated sands carried a high overburden pressure (due to i.e. glaciers) in the past, due to which it consolidated. Particles got packed together more tightly, and higher horizontal and vertical stresses were present in it. After a while, the overburden was removed and the vertical stresses returned to normal. The horizontal stresses however, stayed the same because there was no horizontal option for them reach a new stress state. Installation however, might create the possibility for the overconsolidated sand to lose its higher horizontal stress state. And because a higher cone resistance basically tells something about the stress state of the soil, might it be dangerous to make use of the higher cone resistance values in a design. Installation might thus bring the stress state to a lower level, which can have problematic effects on a designed capacity.

4.1.1.2 Application of the limit value

Limit values for the cone resistance have to be applied by reducing the measures peaks to the limit value. In Figure 4-2 this can be seen as applied for the limit values stated in NEN 9997-1. Peaks higher than 15 MPa are reduced to 15 when they are present in a layer thicker than one meter; and to 12 MPa when the layer is thinner than one meter. The limit values stated in CUR 236 have to be applied in the same way as presented in Figure 4-2.

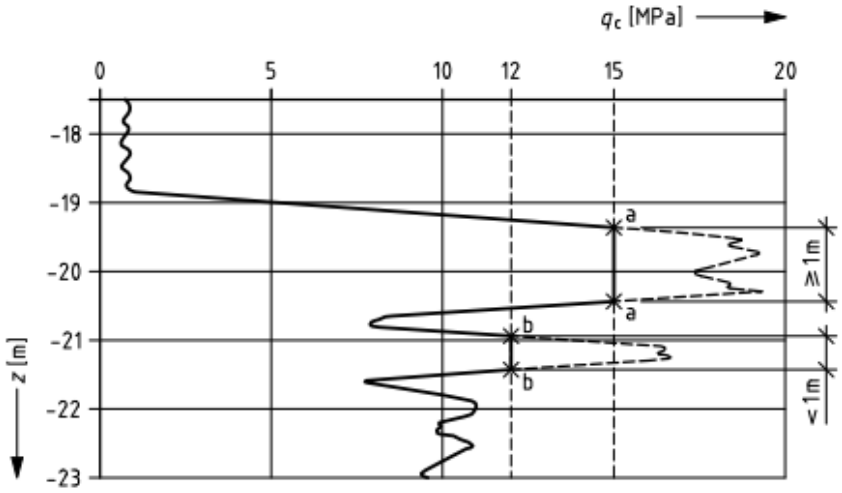

Figure 4-2: Application of limit values on a CPT (NEN 9997-1)

4.1.1.3 Effect of the limit value

Limit values for the cone resistance only affect a possible design, when there are values present which are above the limit value. Values below the limit, do not have to be adapted, and stay thus the same.

Measured values above the limit value have to be reduced to the limit value. The result of this can be seen in Figure 4-3.

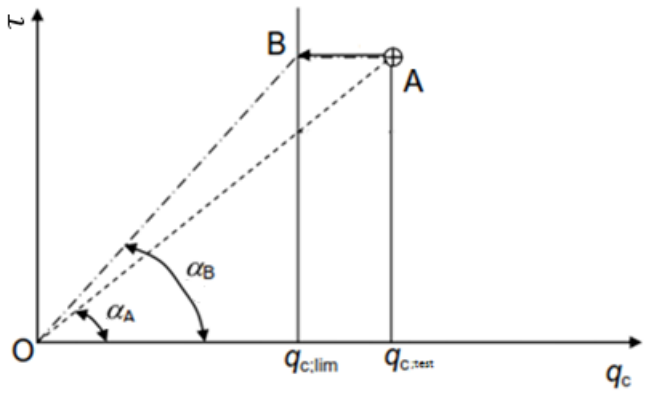

Figure 4-3: Effect of applying the limit value for the cone resistance

Figure 4-3 shows a point A, with an average cone resistance above the limit value and a maximum mobilized shear stress within the limit boundaries. It can be seen that this point has a slope of α_A. Then the limit values are applied and point A shifts left, to position B. The slope α_B becomes now steeper due to the appliance of the limit value.

For a design with cone resistance values above the limit value, this does not matter much as was also seen in section A.6.3. Only the average cone resistance is lower due to the applied limit, and α_t is higher. When back-calculated to the mobilized shear stresses, this results in the same value. A minor problem with this is that α_t loses its physical meaning.

A bigger problem might occur when in the same geological layer, cone resistances above and below the limit are present. If for example the tested piles were present in an area with higher cone resistance values and the limit is applied, the specific α_t for that layer becomes higher. When this value is then applied in a design where lower (than the limit) cone resistance values are present, this results in an overestimation of the actual maximum shear stresses that can be mobilized; and thus of the capacity of the pile.

The opposite occurs when no limit value is used. Piles tested at a location with a high cone resistance result in a lower α_t. When this value is applied in a design where the cone resistances are lower, the capacity is underestimated.

4.1.2 Maximum mobilized shear stress

The second limit value is the one for the maximum mobilized shear stress $\tau_{mob;max}$. From the test load and the theoretical frictional area which the pile has with the soil, $\tau_{mob;max}$ is determined. In CUR 236, the limit for the maximum mobilized shear stress ($\tau_{mob;lim}$) is defined to be 2.5% of $q_{c;lim}$. For pile types A, B and C 500 kN/m^2; and for types D and E, 375 kN/m^2 thus.

4.1.2.1 Reason for limit value use

An upper limit for the mobilized shear stresses is basically a safety valve which is used to prevent un-realistically high values. As mentioned before, the theoretical area over which friction can develop is used to determine $\tau_{mob;max}$. In reality however, it is possible that the anchor body has a bigger area than the theoretical one due to extra length or diameter. This might then result in mobilized shear stress which cannot be reached with the theoretical frictional area. The use of a limit value prevents then an overestimation of the actual capacity of the pile.

4.1.2.2 Application of the limit value

Application of the limit value for the maximum mobilized shear stress is done by reducing the value, to the limit value. If for example the $\tau_{mob;max}$ from a failure test is 530 kN/m^2, and the limit $\tau_{mob;lim}$ is 500 kN/m^2; $\tau_{mob;max}$ becomes 500 kN/m^2 when the limit value is applied.

4.1.2.3 Effect of the limit value

Applying the limit value results in a downward shift of a point as can be seen for point A in Figure 4-4. This figure shows point A received from a failure test. Based on the mobilized shear stress of this point and the corresponding average cone resistance, the slope α_A can be determined. If the limit value is applied, point A shifts to the location of B and the slope decreases to α_B.

Application of the limit value results thus in a decrease of the slope, and might therefore result in a more conservative design if the height of the limit value is too low.

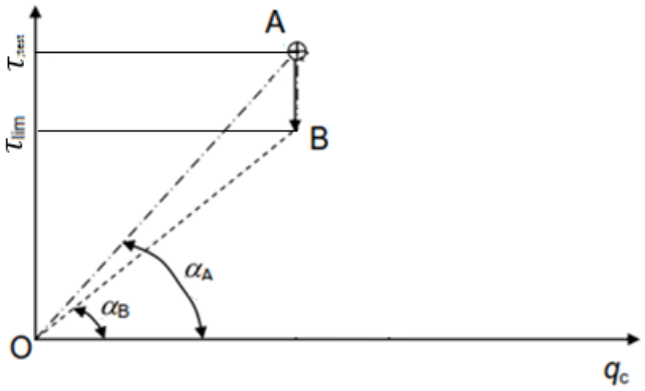

Figure 4-4: Effect of applying the limit value for the maximum mobilized shear stress

4.1.3 Slope or α_t

The final limit value is the slope or α_t value. This is basically the coupling between the cone resistance and the maximum mobilized shear stress. α_t values based on failure tests are following CUR 236 specific for a geological layer at a project site. Values are not allowed to be used for a design at another location or soil layer. The limit value for α_t is 2.5% or 0.025 and links the limit values for the mobilized shear stresses and the cone resistance.

4.1.3.1 Reasons for the limit value

The reason to use the limit value for α_t, is basically the same as for the maximum mobilized shear stress. It is some sort of safety lock, which prevents unrealistically values, and with that, pile capacities.

4.1.3.2 Application of the limit value

Application of the limit value is done by reducing the values that are above the limit, to the limit value. If for example an α_t value of 3% is found from a failure test, this value has to be reduced to the limit of 2.5%.

4.1.3.3 Effect of the limit value

When the limit value for α_t has to be applied, this leads to a reduction of the expected maximum mobilized shear stress. This can be seen in Figure 4-5, where α_A is reduced to $\alpha_{B;lim}$. Due to this reduction of the slope, point A shifts downward to the location of B.

For a design this means that for a similar cone resistance, less shear stresses can be mobilized. This results thus in a lower pile capacity.

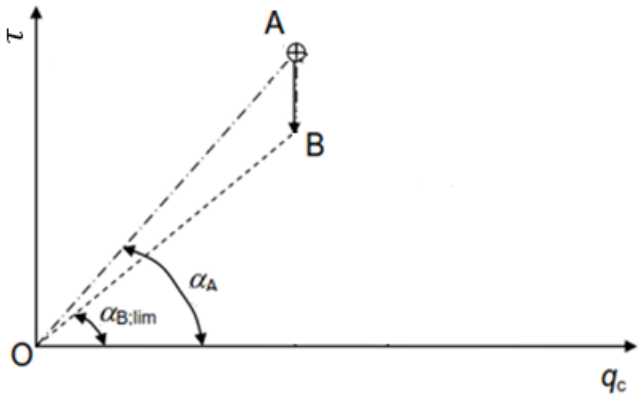

Figure 4-5: Effect of applying the limit value for the slope (α_t)

4.2 Limit values vs. data

In Appendix B, the limit values are compared to the available data. For this comparison, data from the Appendix of CUR 236 is added to the data from the Drachtsterweg in order to get a broader range in data.

The main thing that could be observed in the combined data set of CUR 236 and the Drachtsterweg, is that for micropile types B, C and D, the observed relation between average cone resistance and maximum mobilized shear stresses does not stop at the limit value for the cone resistance. This limit was set in CUR 236. For cone resistances higher than the limit value, the relation seemed to increase up to a certain maximum for $\tau_{mob;max}$, or to where the data stopped. The height of the limit values for the cone resistance is thus, in its current state, not correct according the data.

The use of limit values for the maximum mobilized shear stress showed that the height of the limit values are not always realistic for different pile types. The investigated pile types showed maximum values around 600, 350 and 300 kN/m^2 for respectively type B, C and D.

The limit value of 0.025 for the slope or α_t value was not reached for types C and D. For type B, there were several points that had a steeper slope. For type B, the height of this limit seemed slightly too low. For Types C and D, too high.

4.3 Conclusion

The limit values are thus applied in order to prevent unrealistic designing based on performed failure tests. The limit values restrict capacities which are above a level which is assumed to be unrealistic, and this basically based on experience in the form of previous tests. This is done by three different limit values, for the cone resistance (q_c), the maximum mobilized shear stress ($\tau_{mob;max}$) and the tensional shaft friction coefficient (α_t).

According to the effect that limit values have on the design method, it is useful to have them. Complete removal of the limit values can lead to conservative designing (limit value for q_c) or possible overestimation of the capacity (limit values for $\tau_{mob;max}$ and α_t). It is then important that the limit values are placed at the optimal positions relative to the data.

Comparison between current limit values and available data (combined dataset of Drachtsterweg and CUR 236) showed that the current limit values do not suit the data. Use of such values will not always prevent unrealistic designing, or may even result in conservative designing. New limit values are therefore needed

5 Limit value proposal

In the previous chapters, first the use or height of the currently applied limit values was questioned. The limit values were then evaluated based on data and a theoretical evaluation of the effects of the values. This showed that limit values are useful in the design method but not in the form in which they currently are.

This is mainly due to how the limit values were established in CUR 236. In CUR 236 a limit to the cone resistance was chosen based on general data interpretation. The maximum value for α_t was chosen to be 2.5%. These two limit values combined led to the limit value for the maximum mobilized shear stress: 2.5% of the limit value for the cone resistance.

The current limit values could thus use some improvement. Differences in data shape gave also reason to more pile type specific limit values, instead of general values that are applied to all piles; as was the case for the limits for α_t (2.5%)and $\tau_{mob;max}$ (2.5% of $q_{c;lim}$). In this chapter, different limit values are proposed based on the available data.

5.1 Methodology limit values

Based on the evaluation of the limit values, proposals for new values are given. The proposals are based on general data interpretation and basic statistics, as can be seen in Appendix C. Furthermore are the limit values de-linked from each other as is currently the case (Limit for the q_c and α_t, from which the $\tau_{mob;max}$ limit follows). A summary of the current limit values and the proposed limit values can be found in Table 5-1.

Limit values for the cone resistance are based on the location of the inflection point. This point basically shows the end of the relation between the maximum mobilized shear stress and the average cone resistance. The location of this point is estimated based on two different types of data visualization.

The first one is the $\tau_{mob;max} - q_{c;avg}$ plot which is used to estimate the point where $\tau_{mob;max}$ roughly has reached an average maximum mobilized shear stress. The second one is based on the $\alpha_t - q_{c;avg}$ plot. In this plot the point where α_t starts decreasing is used.

The reason why these points are used to base the limit value of q_c on, comes from the expected shape of the relation between $\tau_{mob;max}$ and q_c which can be seen in the example in Figure 5-1. In the first part, $\tau_{mob;max}$ increases linearly with the average cone resistance. After a certain cone resistance is reached, this increase flattens out. This point can then be used as the limit value for the cone resistance, because afterwards, no significant additional shear stresses are developed. Using a higher or lower limit value can result in under- and overestimation of the pile capacity as was discussed in section 4.1. If this is plotted in terms of α_t which is the slope of the linearly increasing trend, it would show a horizontal line which decreases after the limit value is reached. This because α_t is basically the derivative of the $\tau_{mob;max} - q_c$ trend. Both plots are used to determine the limit value for q_c, in order to get a better view on the behaviour of the trend.

The limit values for the maximum mobilized shear stress and α_t are then determined based on respectively the data points below and above the limit value for q_c, indicated by respectively circle 1 and circle 2 in Figure 5-1. This is done by taking the mean and standard deviation of the data points. The limit value is then placed around the 95% coverage. The way to determine the value at 95% of the data can be found in section 2.7. For the complete elaboration of this, see Appendix C.

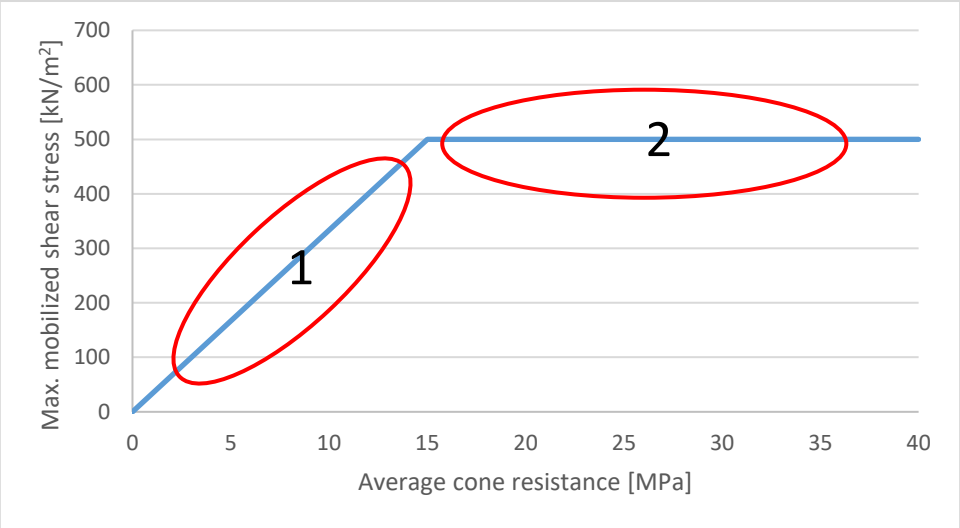

Figure 5-1: Example of the expected relation between $\tau_{mob;max}$ and $q_{c;avg}$

5.1.1 Cone resistance

The limit values for the cone resistance are moved to respectively 25, 22.5 and 20 MPa for pile types B, C and D. See Appendix C for further elaboration.

5.1.2 Maximum mobilized shear stress

From the data it could be seen that the current limits for $\tau_{mob;max}$ were not always realistic compared to the location of the data points. The limit of type B was too low and the limit of C too high. The limit value of type D was also too high compared to the available data, but the amount of data points at q_c >20 MPa is relatively sparse, which made it difficult to see a clear upper boundary. The limit for type D is, due to this low amount of available data points, based on the α_t limit.

Proposed limit values are 600 kN/m^2 for type B and 350 kN/m^2 for types C and D. Determination of these values can be found in Appendix C.

5.1.3 α_t

The current limit value for α_t was only exceeded by data point of type B piles. For this pile type the limit value is increased to 3%. For types C and D, all points were far below the limit value. Therefore the limit values for C and D are reduced to 1.75%.

Table 5-1: Summary of the current used limit values and the proposed ones

	$q_{c;lim}$ $[MPa]$		$\tau_{mob;lim}$ $[kN/m^2]$		$\alpha_{t;lim}$ $[-]$	
Type	CUR 236	proposed	CUR 236	proposed	CUR 236	proposed
A	20	*	500	*	0.025	*
B	20	25	500	600	0.025	0.0300
C	20	22.5	500	350	0.025	0.0175
D	15	20	375	350	0.025	0.0175
E	15	*	375	*	0.025	*

* No values proposed due to lack of data

5.2 Shape of the proposed limit boundaries

When the in Table 5-1 proposed limit values are applied, the boundaries for pile types B, C and D get the shape which can be seen in respectively Figure 5-2, Figure 5-3 and Figure 5-4. It can be seen that the boundaries set by the proposed limit values, better suit the shape of the data points. Note that these are just the boundaries. All points outside the boundaries should be moved inside the area within

them, before being applied in a design or α_t determination from failure tests. The top boundaries can be described by the following equation:

$$\tau_{mob;max} = \alpha_{t;lim;X} \cdot q_c \leq \tau_{mob;lim;X} \qquad 5\text{-}1$$
$$q_c \leq q_{c;lim;X}$$

With:

$\alpha_{t;lim;X}$	Limit value for α_t for a certain pile type X (See Table 5-1) [−]
$\tau_{mob;lim;X}$	Limit value for $\tau_{mob;max}$ of pile type X (See Table 5-1) [kN/m^2]
$q_{c;lim;X}$	Limit value for q_c of pile type X (See Table 5-1) [MPa]

The right boundary is added in order to give an indication of the area in which the data points have to be (after limit values are applied) when a design is made, or α_t has to be determined.

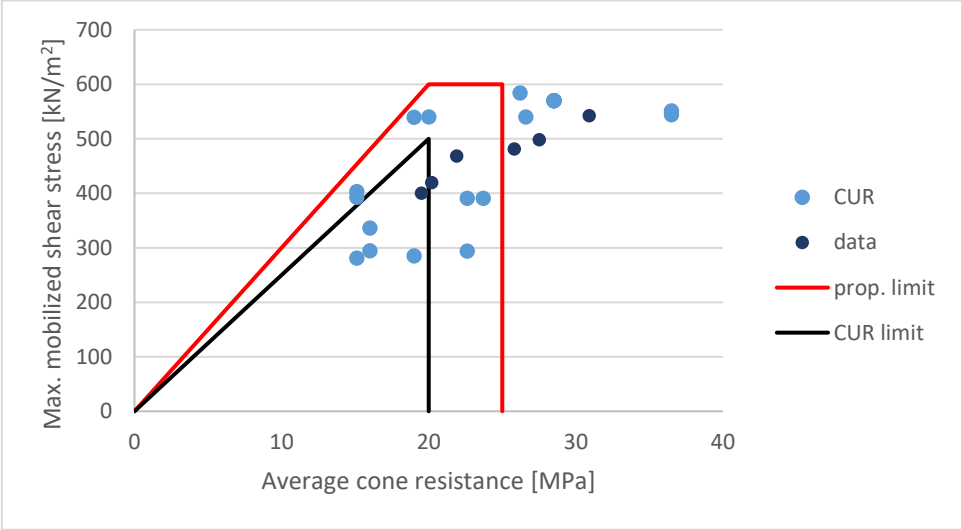

Figure 5-2: Boundaries set by the current and proposed limit values for type B, relative to the data points

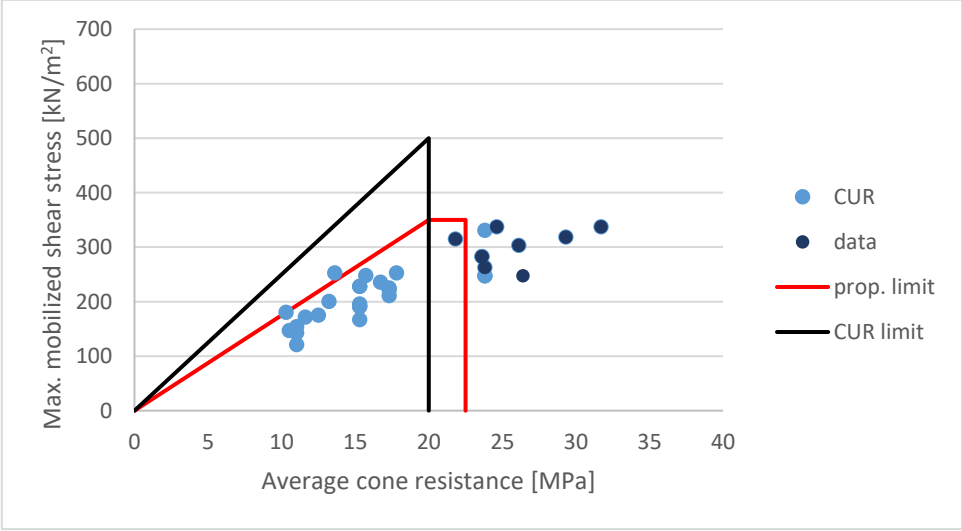

Figure 5-3: Boundaries set by the current and proposed limit values for type C, relative to the data points

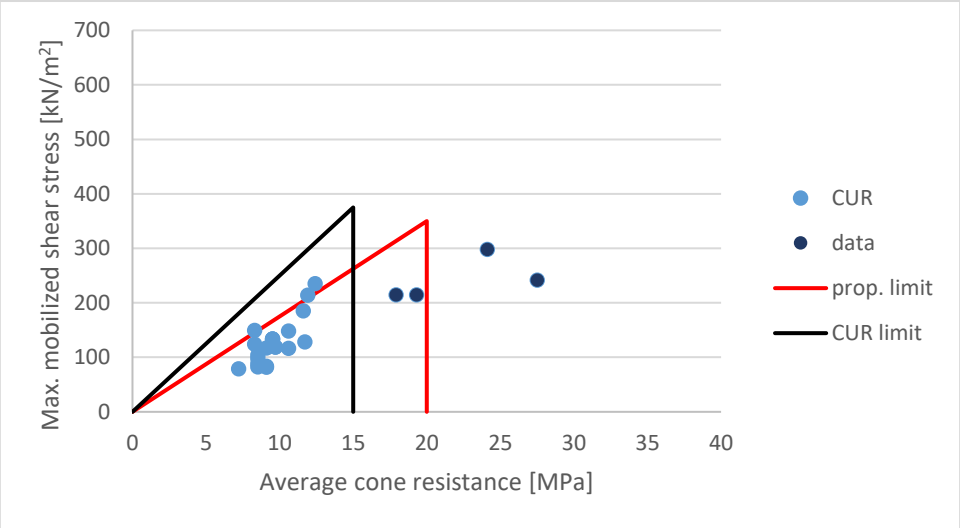

Figure 5-4: Boundaries set by the current and proposed limit values for type D, relative to the data points

5.3 Explanation and effects of the proposed limit values

In the previous section, new limit values were proposed. The effects that the limit values in this form have on a possible design or α_t value, are discussed below.

5.3.1 Cone resistance

From the data it could be seen that the maximum mobilized shear stresses increase with an increasing cone resistance, up to a certain point where the increase slows down and flattens out. The limit for q_c is carefully chosen in the part where the trend flattens out, this in order to prevent both an unsafe- and a conservative design.

If the limit is set too low, and failure tests are performed to derive an α_t value from, this would result in a higher α_t value. When this value is used in a design with cone resistances below the limit value, this leads to a minor overestimation of the amount of shear stresses that can be mobilized and thus a less safe design. This phenomena was also discussed in section 4.1.1.

When the limit value is set too high or even completely removed, this can lead to a more conservative design. The reason for this is that cone resistances are used which are not in the range where $\tau_{mob;max}$ increases with q_c, Outside the boundaries within a relation between the two is proved thus. When α_t is determined based on such higher value, it results in a lower value. This value applied in a design with cone resistances lower than encountered at the failure tests, will result in an underestimation of the maximum mobilized shear stresses.

It is interesting to know the exact location of the limit value in order to optimize the design. Safe enough, but also not too conservative.

5.3.2 Maximum mobilized shear stress

The limit values for the maximum mobilized shear stress are chosen based on the 95% data coverage of the data sample, except for type D due to the low amount of data.

The proposed limit values follow the top part of the data, and make sure that a design will not end up too conservative as was for example the case with type B where $\tau_{mob;max}$ was increased from 500 to 600 kN/m^2.

For types C and D, the limits were reduced because they were relatively too high compared to the data points. When a limit is set too high, it has no use in preventing unrealistically high values. Having such limit is thus useless.

The effects of the proposed limit values have again two effects. One to prevent too conservative designs, and the other to prevent unsafe designs. Again an optimum based on the data points was sought, for the same reasons as stated in 5.3.1.

5.3.3 α_t

The proposed limits for α_t were changed in both ways: increased and reduced. It is important that the value is not too low to prevent conservative designing, and also not too high to keep the value useful.

The α_t limit for Type B piles is increased to 3.0% due to several points outside the limit boundary following CUR 236. The increase of this limit prevents unnecessary conservative designs. For types C and D however, the limit value is reduced to 1.75%. The limit value of 2.5% was never reached in the data, which already gave an indication that this value was too high. Statistical investigation of the data showed that 1.75% was a more suitable limit.

The α_t difference between the pile types might have to do with the way how grout is applied, and the height of the applied pressures. This was however not investigated into depth in this thesis.

6 Expectancy and lower bound values

In the previous chapter, new limit values were proposed based on a statistical approach of the data. The necessity of limit values was shown in chapter 4, where the limit values were evaluated. Next to new limit values, it is useful to re-evaluate all current values. Also the expectancy or average values on which failure tests are based, and the lower bound which have to be applied when no testing before installation is done, thus. In this chapter, the expectancy and lower bound values are added to complete the new value proposal.

6.1 Methodology

The way of determining of the average and lower bound values is the same as for the limit values. The inflection point is determined based on general data interpretation of the $\alpha_t - q_c$ and the $\tau_{mob;max} - q_c$ plots. This is in principal the same as for the limit values, because the relation is still assumed to increase linearly up the limit for the cone resistance. The limit for q_c yields thus also for the expectancy and lower bound values.

Then, based on a statistical data analysis of the data points above and below the limit value for q_c, the values for respectively $\tau_{mob;max}$ and α_t are determined. For the average or expectancy values the mean is used, and for the lower bound values, the 5% lower fraction following respectively:

$$\bar{X} = \frac{1}{n}\sum_{i=1}^{n} X_i \qquad 6\text{-}1$$

$$\bar{X}_{frac;95\%} = \bar{X} - t_{0.05;n-1} \cdot \frac{S}{\sqrt{n+\frac{1}{n}}} \qquad 6\text{-}2$$

With:

$\bar{X}$	Sample mean [$*$]
X_i	A certain data point i [*]
S	Sample standard deviation [*]
n	The number of data points in the sample [$-$]
$\bar{X}_{frac;95\%}$	Lower bound which has a 95% chance on exceedance [*]
$t_{0.05;n-1}$	Value of t-distribution [$-$]

* dependent on the unit of the data

6.2 Proposed values

Based on the previously presented statistics, the values in Table 6-1 were derived. Those values were however not always equally convenient to use as design values or in the code due to the irregular form and specific digits (i.e. 0.0208 or 0.0083). Therefore were the values adapted to more convenient values to use, and more easy to remember than for example a very specific value with several digits.

The relatively big difference between the average and lower bound $\tau_{mob;max}$ values for type D is due to the low amount of data points in the range above the limit value

Table 6-1: Summary of the values obtained from a statistical data analysis

	Type B		**Type C**		**Type D**	
	$\tau_{mob;max}$	α_t	$\tau_{mob;max}$	α_t	$\tau_{mob;max}$	α_t
Average	549.2	0.0208	295.0	0.0140	270.2	0.0130
Lower bound	495.3	0.0126	233.1	0.0108	64.2	0.0083

The adapted values are then presented in Table 6-2. For the average or expectancy values, statistics and adapted values are relatively close to each other. The maximum mobilized shear stress of the

lower bound values is based on α_t and the limit value for the cone resistance. This In order to prevent a jump in the line that describes the assumed relation.

For a complete elaboration, see Appendix 78C.

Table 6-2: Summary of the adapted statistical values

	Type B		Type C		Type D	
	$\tau_{mob;max}$	α_t	$\tau_{mob;max}$	α_t	$\tau_{mob;max}$	α_t
Average	525	0.0210	300	0.0135	250	0.0125
Lower bound	300	0.0120	225	0.0100	150	0.0075

6.3 Shape of the proposed values

Finally the relations that are described by the proposed values are visualised in Figure 6-1, Figure 6-2 and Figure 6-3 together with the data point on which they are based. The relations are described by the following equations.

For $q_c \leq q_{c;lim;X}$:

$$\tau_{mob;max} = \alpha_{t;X} \cdot q_c \qquad 6\text{-}3$$

For $q_c \geq q_{c;lim;X}$:

$$\tau_{mob;max} = \alpha_{t;X} \cdot q_{c;lim;X} \qquad 6\text{-}4$$

With:

$\alpha_{t;X}$	Tensional shaft friction coefficient for a certain pile type X $[-]$
$\tau_{mob;X}$	Maximum mobilized shear stress of pile type X $[kN/m^2]$
q_c	Cone resistance $[MPa]$
$q_{c;lim;X}$	Limit value for q_c of pile type X $[MPa]$

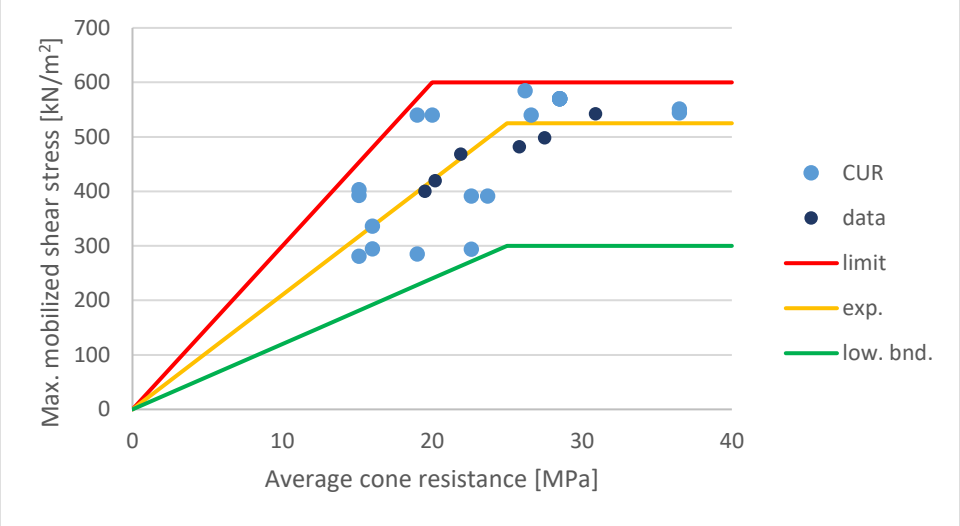

Figure 6-1: Proposed limit values type B with respect to the data points

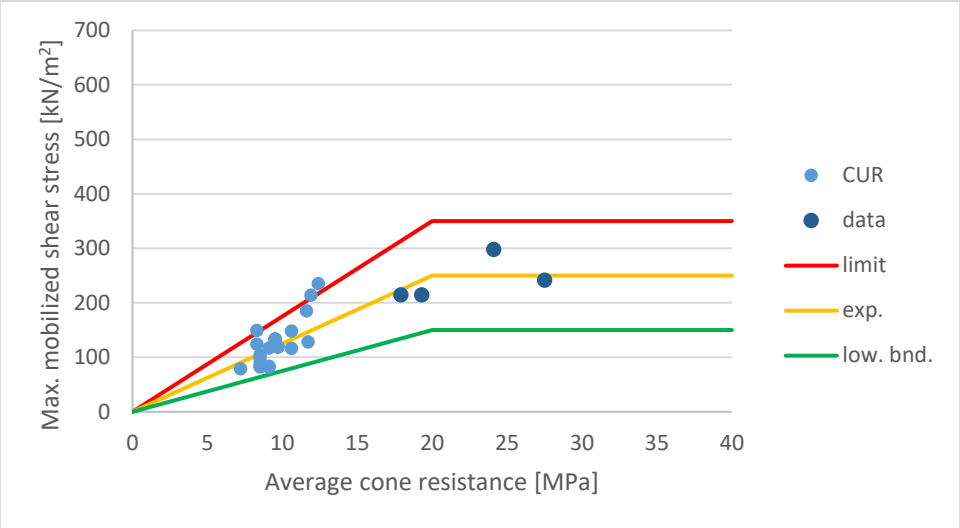

Figure 6-2: Proposed limit values type C with respect to the data points

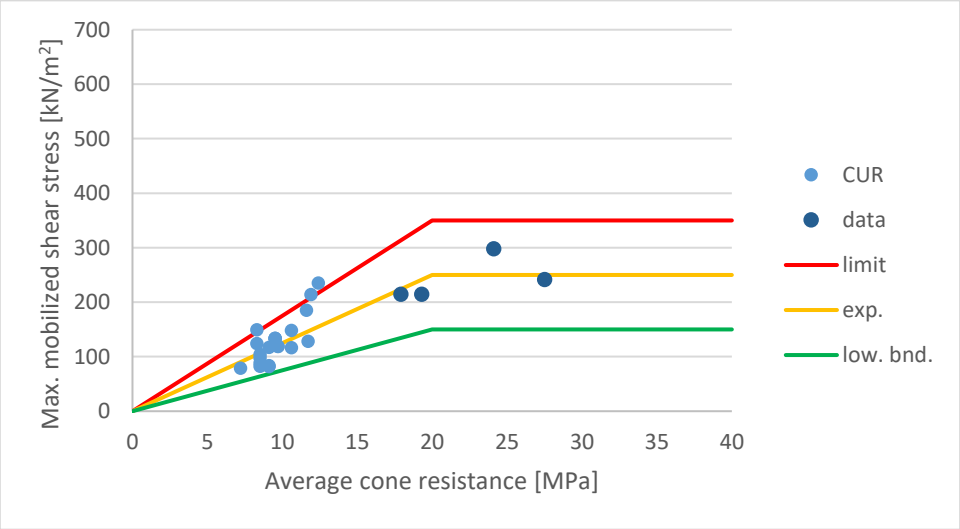

Figure 6-3: Proposed limit values type D with respect to the data points

7 Consequences of the proposed values for the design process

In this thesis, the limit values that are currently applied in the design process op micropiles were evaluated. This showed that there was room for improvement because the current values were sometimes too conservative, and for other pile types too high. Therefore new values that replace the current limit values and values in Table 6.1 from CUR 236 were proposed in the previous two chapters. The proposed values are based on a statistical approach of the available data. Additional data might thus result in slightly different values.

There is however, sometimes confusion about how the values must be used or when different values have to be applied. In this chapter, the design method and the way how to apply the limit values is clarified.

7.1 Design scheme

In the literature review it was already mentioned that there are two methods of design a micropile foundation. The first one it to take the lower bound values, and use them in the formula presented in equation 7-1 in order to determine the pile capacity. This will however lead to a conservative design.

The second option is to make an optimized design. This can be done by installing micropiles in a layer with a high bearing capacity, usually sand, and test them. From the failure load a value for the tensional shaft friction coefficient α_t can be derived following the scheme presented in section 2.4, equations 2-4 to 2-11. When values received from this scheme are higher than the limit values, they have to be reduced to that specific, exceeded limit value. Next to failure tests, validation tests and execution control must be applied to the production piles.

α_t values received from failure testing are specific for the pile type, project and soil layer in which the test piles were installed. They are not allowed to be used in other projects or different soil layers at the same project location.

In sections 7.1.1 to 7.1.3, the individual values will be explained in more detail.

7.1.1 Lower bound values

The lower bound values must thus be used in a design when no failure tests are performed. The reason for this is to ensure a design that is safe enough.

7.1.2 Average or expectancy values

The average or expectancy values are used when an optimized design is preferred. Based on the average values, an expected failure load is determined for the test piles. This failure load is then used to determine the height and increments of the loading procedure as described in section 2.3. The average and expectancy values have no further use in the design process.

7.1.3 Limit values

From the failure tests, a layer and project specific α_t value is derived. When this value is higher than the limit value, it should be reduced to the limit value. It must furthermore be checked that values for the cone resistance and maximum mobilized shear stress do not exceed their limit value. If they do, they should be reduced to the limit value.

The use of limit values is to prevent unrealistic and unsafe designs, based on data from previous projects. Based on the values that were received in those projects, it can be said that ‘compared to previous projects’, the values for a new project are unrealistically high and therefore should be reduced to ensure the design safety. The limit values are thus no hard truth about the upper boundary, but more an indication based on experience.

7.1.4 Lower bound or optimized design

The question rests whether to use the lower bound values, or to make an optimized design. The consideration mainly rests on what the most economical solution is. When lower bound values are used, one is almost certain that over designing has taken place, which makes the project less cost-effective. But for an optimized design, failure tests have to be performed which also cost a certain amount of money ($\pm$ €30.000 for 3 piles plus testing).

From an economic point of view and the current values in CUR 236, the turning point between the first (lower bound) and the second (optimized) design option, lies around 100 piles. When over 100 piles have to be installed, it is often more economic to perform failure tests and optimize the design. Below the 100 piles, a conservative design based on the lower bound values suits better. This is however just a rough indication. During a design, a more detailed cost-consideration should be made.

7.2 Consequences of the proposed values

The proposed values do not have significant effects on the design method, except that more carefulness is needed when filling in α_t and $q_{c;avg}$ in the formula presented in equation 7-2. This due to the shape of the limit boundary where the limit of $\tau_{mob;max}$ is already reached before the limit for the cone resistance. In some cases, the limit for $\tau_{mob;max}$ can thus be exceeded by the multiplication of both an α_t- and a $q_{c;avg}$ value close to their limit value.

7.3 Further reduction of the capacity

The capacity that is received from equation 7-3 is the design capacity, indicated in Figure 7-1 by 'R_d'. No further application of partial load- or resistance factors is needed because they are already implemented in the formula via respectively $\gamma_{m;var;qc}$ and $\gamma_{s;t}$ (See also section 2.2). The formula in equation 7-4 corrects the characteristic values for the load and resistance, S_k and R_k, thus already to design values S_d and R_d.

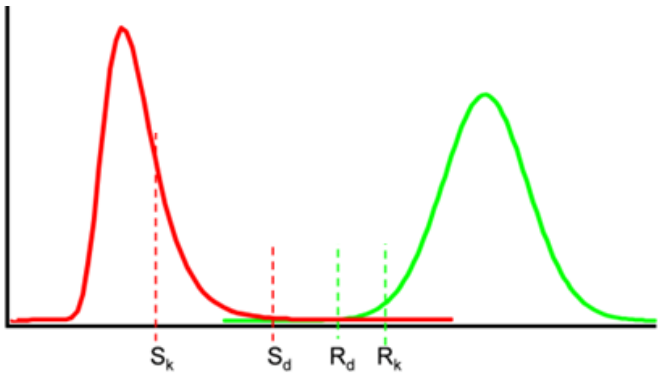

Figure 7-1: Probability density functions showing the variations in load (red) and resistance (green) (Jonkman, Steenbergen, Morales-Nápoles, Vrouwenvelder, & Vrijling, 2015)

7.4 Reduction for overconsolidated soils

In the design process, it is not necessary to reduce for overconsolidation of the soil. In principal is the OCR already taken into account when the α_t value was determined for a certain layer of soil at a certain project site. The α_t value is at that time, a characteristic value for that specific, over consolidated layer.

Following CUR 236, the only exception to this is pile type E, due to the vibrations that are caused during installation.

8 Conclusion and Recommendations

The primary goal of this thesis was the analysis of a dataset provided by Heijmans. The dataset contained information of failure tests performed on four different types of micropiles, including CPT data, test data and the installation logs. The idea was to use the information in this dataset to find relations between installation aspects and the final pile capacity. This was turned out to be impossible due to the lack of data in- and the varying quality of the installation logs. The goal of the thesis was then changed in the direction of one of the findings of the performed data study, which is the evaluation of the limit values from CUR 236; and if necessary, a proposal for better values.

To reach this new goal, the research question ("**Is optimization of the current limit values in CUR 236 possible?"**) was used, which was split up into three parts. An additional data study, an evaluation and a conclusion. In the complete data study (initial and additional study performed on the limit values), answers to the following sub-questions were sought:

1. How do different pile types relate to each other?
2. How does raw data relate to data adapted according limit values stated in CUR 236?
3. How does the data (raw and adapted) relate to values presented in CUR 236 Table 6.1?

Parts of the initial data study are left out because they were no longer relevant for the changed scope.

The second step was an evaluation of the findings in a combined data set of the Drachtsterweg data and data from CUR 236. Based on the evaluation, a conclusion in the form of a proposal for new values is given.

8.1 Data study

First of all did the data study show that the values for micropile type E were not reliable to use in further research. The data was not logged correctly and CPT's were taken after installation of the piles and did therefore not show the initial soil conditions, as was the case for all other piles. The data for types B, C and was mostly good, and was used for further elaboration. Data for type D showed that most of the piles were not correctly installed in the sand layer, and therefore not suitable to compare with piles that are fully installed in sand. Those piles were left out of consideration as well. Furthermore was it observed that almost all installation logs did not suit the guidelines for aspects that have to be logged during installation, presented in chapter 9 of CUR 236. There was in principle enough information in the logs to determine if a pile was not installed correctly, but it did not follow the design guides, which it should have. Execution control happens thus not always for all piles according to the guidelines.

Interpretation and elaboration of the data showed significantly higher values for $\tau_{mob;max}$ and α_t at type B piles, than for piles of types C and D. The possible explanation for this are in the height of the applied grout pressures, the way how grout is applied and the installation method.

For type B, significantly higher grout pressures are applied: 10 to 25 Bar against 0 to 6 Bar for types C and D. Furthermore the way how grout is applied. For type B, the pressure put directly on the soil around the pile while the casing is pulled upwards. For types C and D, grout is ejected from the pile tip and flushes away the soil, or is mixed with it.

Installation of the piles differs mostly in the way of boring. Types C and D are bored and screwed in respectively. Together with boring or screwing, grout is ejected from the tip which flushes away the soil. For type D, the soil is then mixed with the grout to form an anchor body. This basically answers the first sub-question. Further investigation was not performed due to the scope which focussed on a limit value evaluation.

The next step was a comparison between the raw data and data adapted according the limit values given in CUR 236. CUR 236 states that limit values have to be applied in a design and when α_t is determined. The limit values for the cone resistance are 20 MPa for types B and C, and 15 for type D. The limit for α_t is 2.5% for all pile types, and the maximum mobilized shear stress limit is 2.5% of the cone resistance limit.

Comparison between the data processed according the limit values and the raw data showed significantly lower α_t values for the raw data. A quick evaluation what this meant for the final capacity of the pile, showed no significant differences. The use of limit values heightens thus unnecessarily the α_t value. Due to this, α_t loses its physical meaning and might give an initial idea that a pile has a much higher capacity than it actually has.

Comparison of the data with the values stated in CUR 236 Table 6.1, showed that the raw data was more in line with the expected values from Table 6.1. Adapted data following the limit values, showed again significantly higher values.

8.2 Evaluation

The findings of the data study gave rise to the second part which was an evaluation of the currently applied limit values. This was done by combining the data from the Drachtsterweg with data from the one of the appendices of CUR 236. The data in that appendix was used to base the design values (expected- and lower bound values) in CUR 236 on. Data from the Drachtsterweg was an addition to that data which broadened the range in cone resistance up to about 25-30 MPa. From the CUR data however, much less data details were known.

Visual evaluation of the combined data showed that the limit values for q_c were relatively low for all three considered pile types. For Type B, the limit values for $\tau_{mob;max}$ and α_t were also low compared to the data. For types C and D however, the limits for $\tau_{mob;max}$ and α_t seemed to be too high. Further investigation of the effects of the limit values, showed that they are useful for the design process, but not in its current form.

8.3 Conclusion

Evaluation of the limit values showed that the current limit values in CUR 236, did not suit the data best compared to the available data. Some of the values were relatively high, other values relatively low compared to the data points. In this thesis new values were proposed for three of the five micropiles. A complete new design strategy based on a theoretical approach might also be possible, but that will be discussed in the next section with the recommendations. For two types of micropiles, no values were proposed due to the lack of data on those particular piles.

The new proposed values are based on a statistical data analysis where the limit values are placed at a 5% upper fraction. Average and lower bound values are also added for completeness. Current values can be found in Table 8-1, and the proposed values in Table 8-2.

Table 8-1: Summary of the current micropile design values (CUR236, 2011)

	Type B		**Type C**		**Type D**	
	$\tau_{mob;max}$ $[kN/m^2]$	α_t $[-]$	$\tau_{mob;max}$ $[kN/m^2]$	α_t $[-]$	$\tau_{mob;max}$ $[kN/m^2]$	α_t $[-]$
Limit	500	0.0250	500	0.0250	375	0.0250
Average	340	0.0170	240	0.0120	180	0.0120
Lower bound	220	0.0110	160	0.0080	120	0.0080

Table 8-2: Summary of the prosed micropile design values

	Type B		Type C		Type D	
	$\tau_{mob;max}$ $[kN/m^2]$	α_t $[-]$	$\tau_{mob;max}$ $[kN/m^2]$	α_t $[-]$	$\tau_{mob;max}$ $[kN/m^2]$	α_t $[-]$
Limit	600	0.0300	350	0.0175	350	0.0175
Average	525	0.0210	300	0.0135	250	0.0125
Lower bound	300	0.0120	225	0.0100	150	0.0075

8.4 Discussion

A proposal for new limit- and design values was thus presented in this thesis. It is however important to know the limitations of this proposal. The limitations can be split up into two parts: a statistical part which concerns mainly the reliability and density of the data, and a part which deals with the applicability of the proposed values. The first part about the data is again subdivided in the reliability of the data, data density and comparability of the data.

8.4.1 Reliability of data

The first limitation lies in the reliability of the data. For a reliable outcome of the statistical analysis, reliable data is needed. The proposal in this thesis was based on data from the Drachtsterweg and data from the Appendix of CUR 236. A data reliability check was only partially possible due to the availability of detailed data on the part from CUR 236. Therefore are the data points which were neglected in the statistical analysis of CUR 236 also neglected in the proposal in this thesis; except for values above the limit value of q_c. The reason for neglecting this part was that it is assumed that the authors of CUR 236 had good reasons to neglect that part of the data. The part above the limit value for q_c was however neglected because it was above the limit value for q_c. Values neglected for that reason, were included in this thesis because a new limit value for the cone resistance was sought. Using already adapted data would result in biased findings.

From the part of the Drachtsterweg data which could be checked, several piles were neglected because they were not fully installed in the layer of sand, but also in the clay layer above it. Those piles were therefore assumed to be not realistic for a comparison in terms of capacity, to piles which were installed completely in the sand. Data of those piles was not taken into account in the proposal.

Not all data used for the proposal could thus be checked on reliability and usefulness. This does not mean that a part of the data was incorrect, only that there is a slight uncertainty in the proposal, based on the used data points.

8.4.2 Data density

The next aspect regarding data and statistical analysis of the data is the data density. The higher the data density, the more certain and smaller the range in possible outcomes, based on statistics. If the available data is seen as a sample on which statistically a prediction is made on the range of the capacity expressed in α_t or $\tau_{mob;max}$, then the prediction is more certain when more data points are available. Following the table in Appendix E, the distribution converges towards the normal distribution around 10-20 data points. This number was however not always reached, especially for micropile type D in the higher cone resistance range.

Furthermore was the continuity of the data not always optimal. Sometimes gaps were present in the data, which made determination of the limit value for q_c more difficult. This was again mainly the case for type D were especially in the higher cone resistance range, only few data points were available. The certainty of the value proposal for type D micropiles is thus lower than for types B and C.

8.4.3 Comparability of data

Furthermore is it not certain if all data points are comparable to each other. In other words: it is not sure that a pile A, installed at depth X, can be compared to pile B installed at depth Y, due to the different stress state of the soil. This stress-state is partially taken into account in the cone resistance which generally gets higher over a depth increase, but not completely. Next to the stress-state of the soil are there other aspects that might influence the final capacity which make piles at different locations and depths, less comparable to each other. Such aspects are for example the shape and size of the grains and the grain distribution from the side of the soil, and from the installation side for example the height of the grout pressure or the length of the grout body.

8.4.4 Applicability of the limit values

What also follows from the possible differences in stress-state of the soil in which a certain pile is installed, and this not directly taken into account with the limit values. Is that it is possible that at greater depths more shear stresses can be mobilized than allowed by the limit values. Most piles however, are installed at a roughly similar depth range. For those piles the proposed limit values are assumed to not directly lead to a significant reduction of the capacity due to the limit value application.

8.5 Recommendations

The recommendations can be split up in three parts. The first one regarding the practical aspects around performed failure tests, the second regarding the limit- and design value proposal and the final one about a different method to estimate the shear stresses in the design method.

8.5.1 Practical aspects

The first recommendation is based on the observed quality of the installation logs. Those logs were often not filled in correctly according to chapter 9 of CUR 236 which describes all aspects that have to be logged during installation. Example of observed defects in the logs were: aspects not logged, exactly similar values for different piles which is almost impossible (grout pressures, volume grout used) and pressures and torque not logged per prescribed 25 cm.

This thesis does not go into details on if those aspects are useful to log, solely on the fact that logging of those aspects is required in the guidelines and that it is not done properly in practice. (Sub)contractors that install micropiles should be asked for the complete installation logs by the client, or, if it is not possible to log certain aspects, a solid explanation why it deviates from the guidelines.

8.5.2 Limit- and design value proposal

The next recommendations are on the value proposal. The current proposal is in this form not completely suitable to replace the values in CUR 236. It is therefore advised to add limit- and design values for pile types A and E, in order to have a complete proposal. Values for those pile types should be derived in a similar, statistical way as was done for types B, C and D.

In the discussion it was seen that the data density and the continuity of the data were important factors for a obtaining a reliable result. A data set which is used to base values on, should satisfy those two aspects as well as possible. Based on the density of the data in the higher cone resistance range, is it also advised to re-elaborate, or at least check, the proposal for type D micropiles.

Furthermore is it advised to validate the proposed values by means of a different dataset in order to prove the proposal suitable or not. It might also be useful to create a database with pile tests all around the Netherlands, in order to gather data which can be used to compare to the limit- and design values every once in a while. If, at some point, the values do not suit the data anymore, it must be analysed why this has changed before coming up with new values.

8.5.3 Different design approach

The final recommendation is on the method how the shear stresses that can be mobilized, are determined. Currently there are two methods used to do so. The first one is to use the lower bound α_t values form Table 6.1 from CUR 236 and multiply them with the measured cone resistance. The second one is to perform failure tests, derive an optimized α_t value from those tests and multiply that α_t value with the measured cone resistance; basically a full-scale test on which a design is based thus. *(limit values have to be applied first when the measured value is higher than the limit value)*.

Designing on lower bound values results however in a relatively conservative design, and performing failure tests cost additional money ($\pm$ €30.000 for three piles + testing). A different way to estimate the shear stresses that can be mobilized might therefore offer a solution.

In the past several methods to estimate the frictional capacity of micropiles were proposed. In Figure 8-1 a part of the summary of the β-method presented by Juran et al. in 1999, is given. The part concerns the method for cohesionless soils. Note that the pile types in the figure are not equal to the pile types defined in CUR 236 and also this thesis.

	Micropile type		
Soil type	Type A Tremie-grouted	Type B Pressure-grouted	Type C, D Post-grouted
Cohensionless	β method $f_s = \beta\sigma'_{vz}$ $\beta = K\tan\phi'$ $K = K_0 = (1 - \sin\phi')\mathrm{OCR}^{\sin\phi'}$ $K = 0{\cdot}7$	$f_s = p_g \tan\phi'$ $f_s = \beta\sigma'_{vz}$ $\beta = K_1 K_2 \tan\phi'$ $K_1 = 1{\cdot}4$ to $1{\cdot}7$ $K_2 = 1{\cdot}2$ to $4 \longrightarrow$ { 1·2–1·5 (DS); 1·5–2·0 (MS); 3–4 (G) } $K = 4$ to 7 (Turner, 1995)	Ostermayer and Scheele (1978) CCTG (1993)

* DS, dense sand; MD, medium sand; G, gravel.

Figure 8-1: Part of the summary of available recommendations for preliminary design of micropiles (Juran, Bruce, Dimillio, & Benslimane, 1999)

In other design methods, design values for the ultimate friction-capacity were presented based on the pile- and soil type by Cheney (1984), Lizzi (1982), Nicholson (1989-1992), the French code CCTG (1993), Solentanche (1992), Jorge (1984) and Ostermayer (1977) (Juran, Bruce, Dimillio, & Benslimane, 1999).

The approach that is recommended to investigate is based on the mobilization of a passive load state of the soil, due to the application of grout under pressure. The general relation for the ultimate unit skin friction of the pile (f_s) is based on the general formula for piles presented by the American Petroleum Institute and an empirical relation for the friction angle (ϕ'):

$$f_s = K \cdot \sigma'_v \cdot \tan(\phi') \qquad 8\text{-}1$$

$$\phi' = tan^{-1}[0.1 + 0.38 \cdot log\left(\frac{q_t}{\sigma'_v}\right)] \qquad 8\text{-}2$$

With:

f_s	Ultimate unit skin friction $[kPa]$
σ'_v	Effective overburden pressure $[kPa]$
K	Lateral earth pressure coefficient $[-]$
ϕ'	Drained friction angle [°]
q_t	Corrected cone resistance $[kPa]$

The relation in equation 8-1 presents a parabolic relation between the cone resistance and the ultimate unit skin friction, where the increase in friction flattens out over increasing cone resistance. From this relation, all parameters except for K, can easily be determined or derived from CPT data. K must be calibrated based on data.

The data that is needed for such calibration must come from failure tests performed on piles from a certain pile type, installed at several depths with similar lengths of anchor body, while a constant grout pressure is applied during installation of all piles. This should in principal lead to a roughly equal capacity per depth variation (i.e. 15-20 m, 25-30 m and 35-40 m).

By fitting the relation curve on the data points, K can then be estimated, from which together with the vertical soil stresses and the applied grout pressures, a relation between the three can be sought.

The reason why different depth levels are needed is because a higher vertical soil stress might also need a higher grout pressure in order to reach a similar load state of the soil, thus making K a function of the depth and applied grout pressures.

With the calibrated fit, the parabolic relation might then be used to design based on depth, grout pressure and cone resistance. Several other aspects (i.e. grain size/shape, water/cement-ratio etc.) might also have their effects on the ultimate skin friction between soil and pile, but grout pressure and depth are assumed to be the most decisive in this.

It is however uncertain if this approach yields for all micropile types due to the unpredictability of the anchor body shape for some types. Furthermore is it, due to the huge uncertainties that accompany the in-situ installation of micropiles, not sure if research on the method where K is calibrated with data points will result in a useful outcome. Research on the other methods which try to estimate the frictional capacity had to concluded the following:

"*The broad conclusion to be drawn from this study is that micropile construction techniques greatly affect the axial loading capacity, and so raise significant limitations with regard to the use of empirical design rules. Therefore, the design of micropile systems relies essentially upon filed loading tests, which are of paramount importance for on-site evaluation and optimization of the design and construction of the micropile systems and for establishing the actual factors of safety.*" (Juran, Bruce, Dimillio, & Benslimane, 1999).

The best way to design micropiles is thus still via testing of piles from which an grout-soil interface parameter is derived, which then is used for the final design.

9 Bibliography

Bartlett, S. (2011, March 11). *Earth Pressure Theory.* Retrieved from Civil and Environmental Engineering, University of Utah: http://www.civil.utah.edu

Bauer Funderingstechniek BV. (2016). *Type B - 16-02-MEM-001 Leeuwarden Drachtsterweg - aanbrengen testpalen dd 30-06-1...* Bauer Funseringstechniek.

Bauer Funderingstechniek BV. (2016). *Type B - 16-02-RAP-001 Rapportage bezwijkproeven rev 0 21-07-2016.* Bauer Funderingstechniek.

CUR Bouw & Infra. (2008). *Van onzekerheid naar betrouwbaarheid - Handreiking voor geotechnisch ontwerpers.* Delft: CUR Bouw & Infra.

CUR166. (2012). *CUR 166 - Damwandconstructies, 6e druk, deel 2.* Gouda: Stichting CURNET.

CUR236. (2011). *CUR-Rapport 236 'Ankerpalen'.* Gouda: Stichting CURNET.

Dekking, F., Kraaikamp, C., Lopuhaä, H., & Meester, L. (2005). *A Modern Introduction to Probability and Statistics.* Delft: Springer.

Deltares. (2012). *C193 Verborgen Veiligheden.* Deltares.

Heijmans Integrale Projecten BV. (2016). *Grondonderzoek - Project Verdiepte Ligging Drachtserweg.* Rosmalen: Heijmans Integrale Projecten B.V.

Ingenieursbureau Harmelen BV. (2015). *2e Beproevingstraject VF-palen aquaduct Drachtserweg moot 5.* Maarssen: Ingenieursbureau Harmelen B.V.

Jonkman, S., Steenbergen, R., Morales-Nápoles, O., Vrouwenvelder, A., & Vrijling, J. (2015). *Pobabilistic Design: Risk and Reliability Analysis in Civil Engineering - Lecture Notes CIE4130.* Delft: Delft University of Technology.

Juran, I., Bruce, D., Dimillio, A., & Benslimane, A. (1999). Micropiles: the state of practice. Part II: design of single micropiles and groups and networks of micropiles. *Ground Improvement*, 89-110.

Mayne, P. (2014). *Interpretation of geotechnical parameters from seismic piezocone tests.* Las Vegas: 3rd International Symposium on Cone Penetration Testing.

MOS Grondmechanica BV. (2014). *Realisatie Onderdoorgang Drachtserweg - R1303512-RH_5.* Leeuwarden: Mos Grondmechanica.

Nederlands Normalisatie-instituut. (2005). *NEN 6745-2 - Geotechniek - Proefbelansting van funderingspalen - Deel 2: Statische axiale belasting op trek.* Delft: Nederlands Normalisatie-instituut.

Nederlands Normalisatie-instituut. (2015). *NEN-EN 14199 - Uitvoering van bijzonder geotechnisch werk - Micropalen.* Delft: Nederlands Normalisatie-instituut.

Nederlands Normalisatie-instituut. (2016). *NEN 9997-1 Geotechnical design of structures - Part 1: General rules.* Delft: Nederlands Normalisatie-Instituut.

(2009). *NEN-EN-ISO 22476-12.* Delft: Nederlands Normalisatie-instituut.

Pelletier, et al. (1993). *Recommended Practice for Planning, Designing and Constructing Fixed Offshore Platforms.* API.

Robertson. (2012). *Guide to Cone Penetration Testing for Geotechnical Engineering.*

Robertson, P., & Campanella, R. (1983). Interpretation of cone penetration tests. Part 1: Sand. *Canadian Geotechnical Journal*, 718-733.

SBRCURNET. (2016). *Addendum bij SBRCUR 236 Ankerpalen, 1e druk.* Gouda: SBRCURNET.

U.S. Department of Transportation. (2006, March). *A Laboratory and Field Study of Composite Piles for Bridge Substructures.* U.S. Department of Transportation. Retrieved from https://www.fhwa.dot.gov/publications/research/infrastructure/structures

Verruijt, A. (1999). *Grondmechanica.* Delft: Delft University Press.

VertrekCPT. (2015, February 12). *Common Corrections in CPT Data Analysis.* Retrieved from VertrekCPT: http://www.vertekcpt.com

Appendices

A Data study

Based on the background information given in the Literature review, the data study is executed and presented in this Appendix. First α_t, $\tau_{mob;max}$ and q_c are determined for the individual pile types, where also the integrity of the piles is checked by means of installation logs. Then the received values are compared to each other's and to CUR 236. Before the data is investigated, the general layering of the subsoil at project location is presented.

A.1 General geological layering of subsoil at test site

To get a first idea of the subsoil in which the tested piles were installed, a report on soil investigation executed at the Drachtsterweg, Leeuwarden (NL), was investigated. Borings applied by Fugro sketched the following general layering of the subsoil (Heijmans Integrale Projecten BV, 2016):

Depth [NAP –m]	**Soil texture**
0-5	Clay
5-7	Sand, medium fine
6-13	Loam/Boulder clay
13-20	Sand, medium fine, slightly silty
20-30	Sand

The executed borings only reached to about NAP -20 m. the exact composition of layers below this level are thus unknown. From CPT profiles, it could be determined that there was another layer of sand present.

Most of the piles were installed in the more shallow sand layer between NAP -13 and -20 m. A layer which consist mostly out of medium fine sand. For future references, this layer will be called the 'first sand' or 'shallow' layer.

The other piles were installed between -23 and 30 m. These piles are also installed in a sand layer, but the exact composition of that layer is not fully known. For future references, this layer will be called the 'second sand' or 'deep' layer.

A.2 Type B

The first considered type is type B, a micropile which is bored into the soil with a single casing. After the GEWI-bar is placed, the casing is removed while grout is applied under high pressure.

Six test piles of type B were installed, three in the shallow layer between NAP -15 and -20, and three in the deep layer between NAP -23 and -30. The piles in the deep layer (P02, P04 and P06) were installed before the piles in the shallow layer.

A.2.1 Soil investigation

Prior to installation of the test piles, eight CPT's were performed close to the location where the piles were planned. Spacing between the pile and relevant CPT's can be seen in Figure A-1. About 15 meters to the left side of Figure A-1, a building pit was present. Seen the distance between them and the depth of the building pit, it is reasonable to assume that the building pit did not affect the test site.

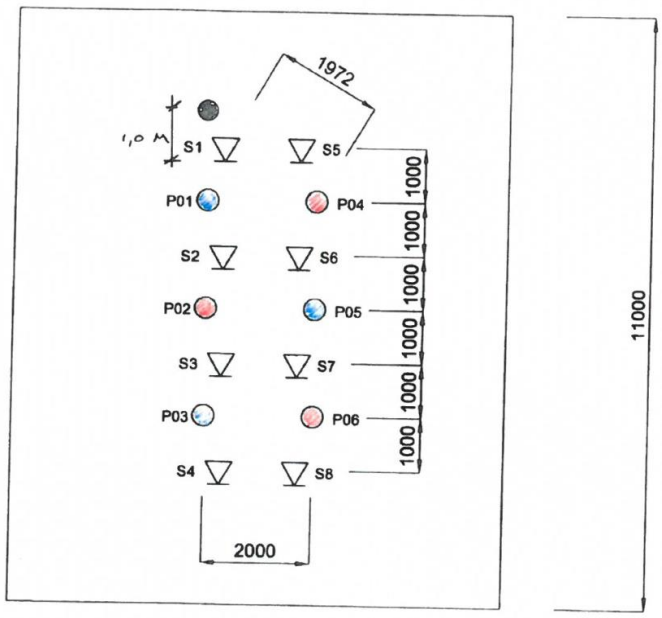

Figure A-1: CPT locations relative to the test piles (Bauer Funderingstechniek BV, 2016)

The average of the 4 CPT's within the 2 meter range, was used to determine the cone resistance q_c at pile location. Two CPT's with a distance to the pile of 1 meter, and 2 with a distance of roughly 2 meters.

CPT's in the shallow layer showed a generally strong layer. The deep layer is significantly weaker than the shallow layer, which can be seen by the lower values for the average cone resistance q_c. The average values for q_c per pile can be found in Table A-1; these values are an average of the cone resistances measured along the anchor length of the pile.

Table A-1: Average cone resistances per pile

Depth	**NAP -15 to -20m**			**NAP -23 to -30m**		
Pile name	P01	P03	P05	P02	P04	P06
$\boldsymbol{q\_c}$ **[MPa]**	30.9	27.5	25.8	19.5	21.9	20.2

A.2.2 Integrity of the installed piles

A.2.2.1 Installation logs

An overview of the relevant data registered during installation can be found in Table A-2.

Table A-2: Data registered in installation logs of Type B (Bauer Funderingstechniek BV, 2016)

General						
Pile name	P01	P03	P05	P02	P04	P06
Date	20-06-16	20-06-16	17-06-16	15-06-16	6-06-16	16-06-16
Bore depth [$mNAP$]	-19.93	-20	-19.95	-30.03	-29.91	29.98
Anchor length L_a [m]	5	5	4*	7	7	7
Free length [m]	15.33	15.40	16.35	24.43	23.31	23.38
∅ drill bit [mm]	180	180	180	180	180	180
∅ tube [mm]	133	133	133	133	133	133
∅ GEWI-bar [mm]	75	75	75	75	75	75
Couplings [$-$]	0	0	0	1	1	1
Grout and installation						

Cement type	CEM III B 42.5					
Specific weight[kg/L]	1.84					
Water/cement ratio	0.45					
Grout used [L]	500	550	650	650	600	700
Pressure [Bar]	10-24	9.5-25	9-22	15-16	7.5-18	10-20
Torque [Bar]	130-180	150-160	150-160	150-180	140-180	130-150

*Grouting of the final meter was unsuccessful, grout loss via borehole of P02

A.2.2.2 Time between installation and testing

In the installation logs, the date at which the piles were installed was logged. In the report on the analysis of the failure tests, no test dates were included. The only thing stated about the time between installation and testing was that it was at least two weeks. According to CUR 236, at least 10 to 14 days must have passed since installation, before the pile can be tested. This was thus done correctly, but could not be checked.

A.2.2.3 Pile tip

The shallow piles all had to be installed between NAP -15 and -20 meter, the deep piles between NAP -23 and -30 meter. The installation logs show that this was done correctly. Differences from this level are minimal as can be seen from the bore depth.

A.2.2.4 Casing, drill head and anchor steel

For all installed piles, the same casings and drill heads were used. The casings and drill heads had respectively a diameter of 133 and 180 mm.

Based on CUR 236, a 10 mm grout penetration zone on each side has to be taken into account which was also done in the report on failure testing of type B. The theoretical diameter of the anchor body is thus 200 mm. This zone is however more due to soil that is flushed away by the applied grout, than grout that penetrates into the soil. In general are the grout particles too big to enter the pores.

The anchor steel used for the shallow piles was a single GEWI-bar with a diameter of 75 mm. For the deep piles, the same bar type was used, except that these bars were made up out of 2 pieces connected by a coupling.

A.2.2.5 Water/cement ratio

For all piles, a water/cement ratio of 0.45 was used. The cement type used was CEM III B 42.5 N with a specific weight of 1.84 kg/L.

A.2.2.6 Conclusion pile integrity

All piles were installed as planned, except for one of the shallow piles which had a shorter anchor body length as can be seen in Table A-2. Reason for occurrence of the leakage is probably a local blow-out where a whole soil layer is locally lifted up, while grout flowed towards the borehole of pile P02. This explanation could however not be verified. For the anchor length of this pile, 4 meters will be used.

A.2.3 Test results

Testing of the type B micropiles resulted in values for the gross pile capacity. To determine the value at which soil mechanical failure occurs, these values were corrected for friction losses and head resistance; as was shown in equation 2-5:

$$R_{s;max} = F_{test;max;gross} - R_{s;fr} - R_{s,head} \qquad 2\text{-}5$$

Values for the friction and head losses as determined in the design can be found in Table A-3. The values for the pile head resistance ($R_{s,head}$) were assumed to be zero because the free length was

flushed out and wrapped into thick isolation material. Friction along the free length of the pile was determined based on the spring back of the pile when unloaded to the initial state (Bauer Funderingstechniek BV, 2016).

Based on the soil mechanical capacity ($R_{s;max}$) and the dimensions of the micropile, the mobilized shear stresses were determined following equation 2-6:

$$\tau_{mob;max} = \frac{R_{s;max}}{\pi \cdot \emptyset \cdot \mathrm{L_a}} \qquad 2\text{-}6$$

Table A-2 shows the value for the anchor length (L_a) and diameter of the drill bit and thus the borehole. Following CUR 236, and additional $20\ mm$ has to be taken into account due to penetration of the grout into the soil. The diameter becomes then $180 + 20 = 200\ mm$. The values for the mobilized shear stresses can be found in Table A-3.

Table A-3: Data received from testing of the piles (Bauer Funderingstechniek BV, 2016)

Pile name	**NAP -15 to -20m**			**NAP -23 to -30m**		
	P01	**P03**	**P05**	**P02**	**P04**	**P06**
$\boldsymbol{F_p}$ **[kN]**	1703	1677	1236	1859	2184	2210
$\boldsymbol{R_{s,head}}$ **[kN]**	0	0	0	0	0	0
$\boldsymbol{R_{s;fr}}$ **[kN]**	0	112	26	99	124	365
$\boldsymbol{R_{s;max}}$ **[kN]**	1703	1565	1210	1760	2060	1845
$\boldsymbol{\tau_{mob,max}}$ **[kN/m²]**	542.1	498.2	481.4	400.2	468.4	419.5

A.2.4 α_t determination

Based on the average cone resistances from Table A-1, and the maximum mobilized shear stresses from Table A-3; α_t can be determined following equation 2-7:

$$\alpha_{t;i} = \frac{\tau_{mob;max}}{q_{c;avg}} \qquad 2\text{-}7$$

The part of the formula that states that α_t has to be equal or below 2.5 % is neglected. This because the scheme is not followed in order to come to a design, but to come to a raw value which is needed for the data study. This is done because adapted values might give a wrong impression of the data when it comes to drawing conclusions. In Table A-4, the values for α_t can be found. It can be seen that the values for α_t in the deep layer are generally higher than in the shallow layer.

Table A-4: values for α_t and the values from which it is determined

Pile name	**NAP -15 to -20m**			**NAP -23 to -30m**		
	P01	**P03**	**P05**	**P02**	**P04**	**P06**
$\boldsymbol{\tau_{mob,max}}$ **[kN/m²]**	542.1	498.2	481.4	400.2	468.4	419.5
$\boldsymbol{q_c}$ **[MPa]**	30.9	27.5	25.8	19.5	21.9	20.2
$\boldsymbol{\alpha_t}$ **[−]**	0.0175	0.0181	0.0187	0.0205	0.0214	0.0208
	Average shallow:		**0.0181**	**Average deep:**		**0.0209**

A.3 Type C

Micropiles of type C are self-boring piles. A hollow tube with a drill bit that is several centimetres bigger than the tube itself is bored to depth. First water or a bore fluid is ejected at the tip to improve boring conditions. When anchor depth is reached, the bore fluid is replaced with grout and the anchor body is formed. It is possible that during grouting, volumes of soil around the pile are flushed out. This can give the anchor body a different than cylindrical shape.

For type C, three times three piles with different diameters were installed in the shallow layer between -13.5 and 18.5 $mNAP$, nine piles in total.

A.3.1 Soil investigation

CPT's were performed close to the piles before and after installation. Location of the CPT's can be found in Figure A-2. Average distances between pile and CPT were 1.5 meter. All piles and CPT's were performed before the project. No excavations or other interferences could have affected the results.

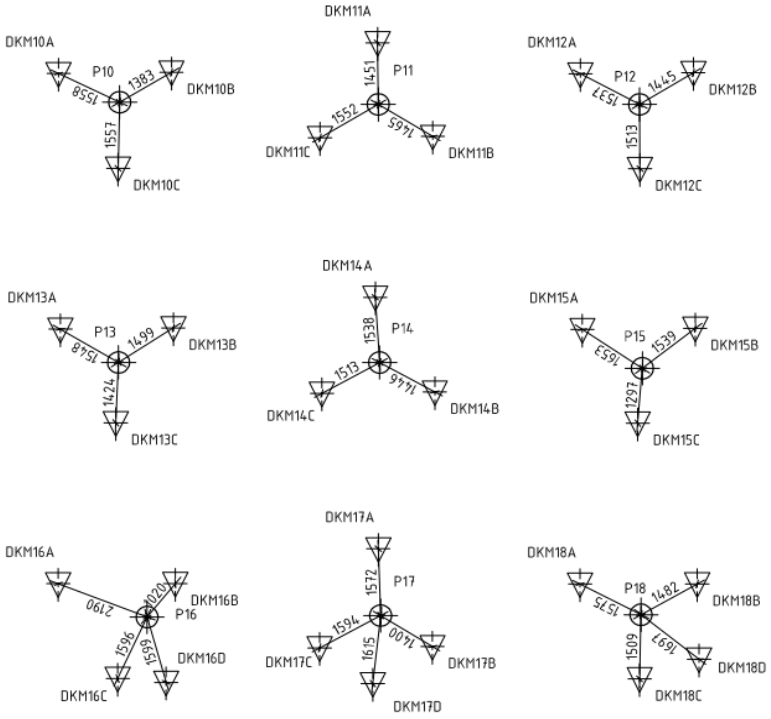

Figure A-2: CPT locations relative to the test piles (MOS Grondmechanica BV, 2014)

A.3.1.1 CPT's before and after installation

CPT's were performed before and after installation. Average values for the performed CPT's relevant for each pile are plotted in Figure A-3. It can be seen that for most piles, the data points before and after installation mostly lay in between each other's, except for piles 16 to 18. For piles 10 to 15, this means that the installation did not affect the soil 1.5 meters away from the pile in a significant way. For piles 16, 17 and 18, which have the biggest diameter (400 mm), it is unclear if the differences are due to installation, or also due to natural variability. Analysis of the individual CPT profiles did not provide a decisive answer to this either.

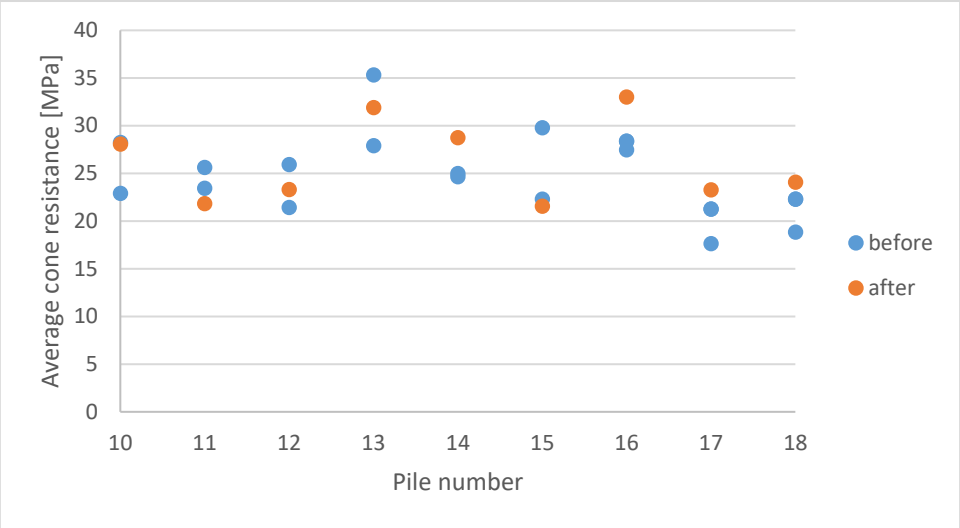

Figure A-3: Differences between CPT's performed before and after installation for type C

Based on the assumption that CPT's were not influenced by installation for the first six piles, the cone resistances were determined based on an average of the three surrounding CPT's. For the piles with a diameter of 400 mm, only the CPT's performed before installation are taken into account. This to be sure that possible effects by installation on the soil, do not give a distorted view on the values for α_t.

Table A-5: Average cone resistances per pile

Pile name	**P10**	**P11**	**P12**	**P13**	**P14**	**P15**	**P16**	**P17**	**P18**
q_c **[MPa]**	26.4	23.6	23.6	31.7	26.1	24.6	29.3	23.8	21.8

A.3.2 Integrity of the installed piles

A.3.2.1 Installation logs

An overview of the relevant data registered during installation can be found in Table A-6.

Table A-6: Data registered in installation logs of Type C (MOS Grondmechanica BV, 2014)

General									
Pile name	P10	P11	P12	P13	P14	P15	P16	P17	P18
Machine	Ecodrie								
Date install. 2014	19-02	19-02	18-02	19-02	19-02	19-02	20-02	17-02	17-02
Date testing 2014	27-03	26-03	25-03	24-03	21-03	20-03	19-03	18-03	17-03
Start time	9:20	8:10	14:20	13:30	12:00	10:40	12:30	16:25	15:05
End time	9:55	9:00	15:00	14:15	12:45	11:30	13:30	18:00	16:15
Install.time[min]	35	50	40	45	45	50	60	95	70
Pile tip [$mNAP$]	-18.5	-18.5	-18.5	-18.5	-18.5	-18.5	-18.5	-18.5	-18.5
Steel length [m]	21.5	21.5	21.5	21.5	21.5	21.5	21.5	21.5	21.5
Ø tube [mm]	101	101	101	101	101	101	101	101	101
Thickness [mm]	12.5	12.5	12.5	27.5	27.5	27.5	27.5	27.5	27.5
Ø drill bit [mm]	250	250	250	320	320	320	380	380	380
Ø pile [mm]	270	270	270	340	340	340	400	400	400
Steel type tube	M80	M80	M80	E470	E470	E470	-	E470	E470
Steel t. coupling	-	-	-	-	-	N80	-	-	-
Couplings [$-$]	5	5	5	4	4	4	4	4	4
Grout and installation									

W/C-ratio [$-$]	0.5	0.5	0.5	0.5	0.5	0.5	0.5	0.5	0.5
Bentonite use [L]	244	250	250	170	185	200	290	150	255
Grout use [L]	380	390	362	578	514	550	545	500*	864
Switch bentonite to grout [$mNAP$]	-12.5	-12.5	-12.5	-12.5	-12.5	-12.5	-12.5	-12.5	-12.5
Pressure [Bar]	4-5	1-5	1-5	1-5	1-5	2-5	1-5	2-6	2-5

*Dry boring over the final two meters due to pumping problems

The length of the anchor body (L_a) was assumed to be 5 meters for all piles, except for P17. P17 has a length of only 3 meters due to problems with the pumping system.

A.3.2.2 Installation machine

For installation of all type C micropiles, the Ecodrie 5500 machine was used (Figure A-4). This is a machine which is able to install micro- and Tubex piles. All piles were installed with the same machine

Figure A-4: Ecodrie 5500 (VermeulenHeiwerken)

During installation of P16, something was encountered in the soil around – 10.3 $mNAP$. CPT profiles around pile 16 did not show abnormalities. It is possible that a smaller boulder was encountered, because boulder clay was present in the layers closer to the surface. During excavation of the building pit, also boulders were found (Figure A-5).

Figure A-5: Excavated boulders encountered at the Drachtsterweg, Leeuwarden (NL) (Pictures Ir. Kimenai)

A.3.2.3 Time between installation and testing

All piles were tested about one month after installation as can be seen in Table A-7, which satisfies the 14 day demand of CUR 236.

Table A-7: Installation and test dates for type C

Pile name	**P10**	**P11**	**P12**	**P13**	**P14**	**P15**	**P16**	**P17**	**P18**
Date install. 2014	19-02	19-02	18-02	19-02	19-02	19-02	20-02	17-02	17-02
Date testing 2014	27-03	26-03	25-03	24-03	21-03	20-03	19-03	18-03	17-03
Number of days	36	35	35	33	30	29	27	29	28

A.3.2.4 Diameter of the drill head

Three different diameters were used during installation: 250, 320 and 380 mm. Based on CUR 236, a 10 mm grout penetration zone on each side had to be taken into account. The theoretical diameters became then 270, 340 and 400 mm. Due to the mechanism of installation however, it is possible that the effective diameter of the anchor body is bigger and different in shape. This could not be verified because the tested piles were not pulled out entirely.

Correction for the diameter was done when the maximum mobilized shear stresses were determined. Based on this correction, it was assumed that all piles can be put into a single data set.

A.3.2.5 Grout: Water/Cement ratio

For all piles a water/cement ratio of 0.5 of an unknown cement type was used.

A.3.2.6 Pile tip

All piles were installed between NAP -13.5 and -18.5 meter. Boring to depth above the anchor body was done with bentonite. The switch from bentonite to grout at the pump was done when NAP -12.5m was reached. Around NAP -13.5m, the bentonite was completely out of the system and lines; and grout was ejected from which the anchor body was formed.

A.3.2.7 Conclusion pile integrity

According to the installation logs, all piles, except P17, were installed correctly. During installation of P17 the grout pump broke down, due to which the anchor body was only 3 meters instead of the planned 5.

A.3.3 Test results

Testing of the type C micropiles resulted in values for the gross pile capacity. This value was in the report on type C directly the soil mechanical capacity $R_{s;max}$. Values for head resistance and friction along the free length of the pile were in the report in it, assumed to be zero. The argument for this assumption was that the free length of the piles was present in layers with softer soil types. No data was available to validate this assumption, in the data study it was thus assumed to be correct.

Based on the soil mechanical capacity ($R_{s;max}$) and the dimensions of the micropile, the mobilized shear stresses were determined following equation 2-6:

$$\tau_{mob;max} = \frac{R_{s;max}}{\pi \cdot \emptyset \cdot \mathrm{L_a}} \qquad 2\text{-}6$$

The determination of the maximum mobilized shear stresses did already take the diameter of a pile into account. It is therefore assumed that all installed piles can be compared to each other's as long as they are also installed in the same geological layer.

Table A-6 shows the value for the anchor length (L_a) and diameter of the pile. The values for the mobilized shear stresses can then be found in Table A-8.

Table A-8: Data received from testing of the piles

Pile name	P10	P11	P12	P13	P14	P15	P16	P17	P18
F_{design} [kN]	1500	1200	1200	1800	1620	1800	2000	990	1980
F_p [kN]	1050	1200	1200	1800	1620	1800	2000	990	1980
$R_{s,head}$ [kN]	0	0	0	0	0	0	0	0	0
$R_{s;fr}$ [kN]	0	0	0	0	0	0	0	0	0
$R_{s;max}$ [kN]	1050	1200	1200	1800	1620	1800	2000	990	1980
$\tau_{mob,max}$ $[kN/m^2]$	247.6	282.9	282.9	337.0	303.3	337.0	318.3	262.6	315.1

During testing of P14, one of the couplings failed before soil mechanical failure occurred. Although the soil mechanical failure load is probably higher than the load of 1620 kN, the actual load was used to determine the maximum mobilized shear stresses for P14.

Figure A-6: Failed coupling of a micropile at the Drachtsterweg, Leeuwarden (Pictures Ir. Kimenai)

A.3.4 α_t determination

Based on the average cone resistances and the maximum mobilized shear stresses from Table A-8; α_t was determined following:

$$\alpha_{t;i} = \frac{\tau_{mob;max}}{q_{c;avg}} \qquad 2\text{-}7$$

In Table A-9, the values for α_t can be found.

Table A-9: values for α_t and the values from which it is determined

Pile name	P10	P11	P12	P13	P14	P15	P16	P17	P18
$\tau_{mob,max}$ $[kN/m^2]$	247.6	282.9	282.9	337.0	303.3	337.0	318.3	262.6	315.1
q_c [MPa]	26.4	23.6	23.6	31.7	26.1	24.6	29.3	23.8	21.8
α_t [−]	0.0094	0.0120	0.0120	0.0106	0.0116	0.0137	0.0109	0.0110	0.0144
	Average:	**0.0111**		**Average:**	**0.0122**		**Average:**	**0.0121**	

From the average values the α_t it can be seen that no significant differences are present between the different diameters. From this it can be concluded that the assumption in section A.3.2.4 that all piles can be put into one single data set, was correct.

The average α_t value for the diameter of 340 mm, was determined based on only P13 and P15. This due to the coupling failure for P14.

A.4 Type D

Micropiles of type D are screwed into the soil. When the depth is reached at which the anchor body has to be created, grout is applied from the tip and mixed with the soil. The mixture of grout and soil forms the anchor body.

Nine piles with three different diameters were installed in the shallow layer. Not all pile tips were placed at the same level, carefulness with comparisons and conclusions based on it is thus needed.

A.4.1 Soil investigation

CPT's were performed close to the piles before and after installation. Location of the CPT's can be found in Figure A-7. The distance between pile and CPT was on average around 1.5 meters. Piles of type D were also installed and tested before the executional phase of the project, no project related aspects could have had influence on them.

Because the level of the pile tip differed between NAP -18.5 and -16.5 meters, it was not certain if all piles were installed in the sand bearing layer. Research on the CPT's showed that the top of the shallow sand layer was around NAP -13.5 meters. Several piles were thus only partially installed in the sand layer. More about this can be found in section A.4.2.6.

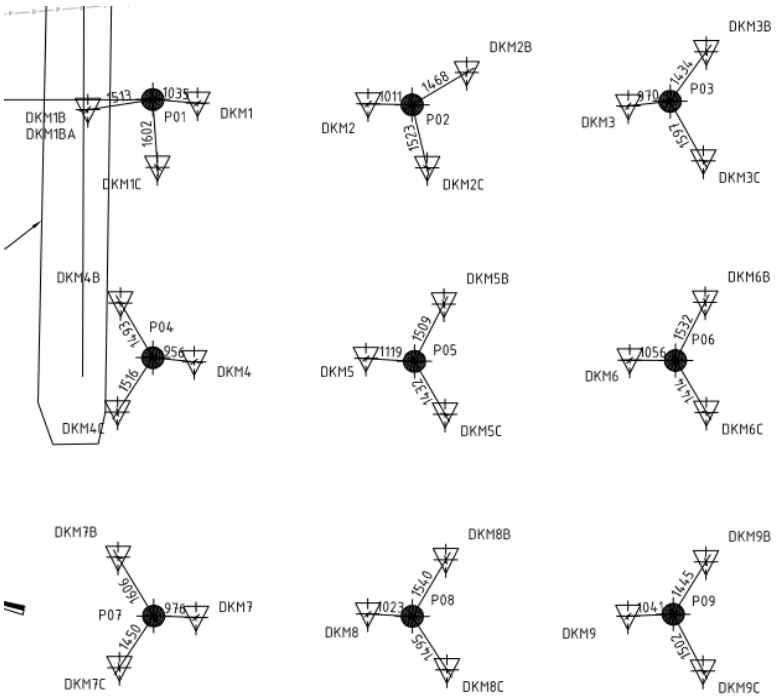

Figure A-7: CPT locations relative to the test piles (MOS Grondmechanica BV, 2014)

A.4.1.1 CPT's before and after installation

Again CPT's were performed before and after installation as can be seen in Figure A-8. For the first two piles even only after installation. The differences between CPT's before and after installation do not show a trend which indicates an effect of pile installation over the distance between pile and CPT. It is therefore assumed that all available CPT's around the pile can be used to determine the average value. Average values can be found in Table A-11.

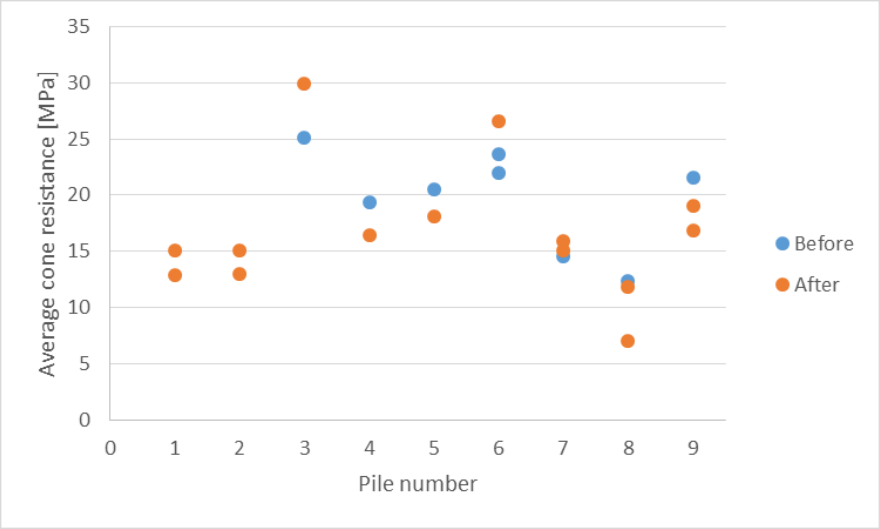

Figure A-8: Differences between CPT's performed before and after installation for type D

Table A-10: Average cone resistances per pile

Pile name	**P01**	**P02**	**P03**	**P04**	**P05**	**P06**	**P07**	**P08**	**P09**
q_c **[MPa]**	14.0	14.0	27.5	17.9	19.3	24.1	15.3	10.4	19.1

A.4.2 Integrity of the installed piles

A.4.2.1 Installation logs

Relevant logged information prior and during installation can be found in Table A-11.

Table A-11: Data registered in installation- and measurement logs of Type D (MOS Grondmechanica BV, 2014)

General									
Pile name	P01	P02	P03	P04	P05	P06	P07	P08	P09
Machine	Hutte		Ecodrie			-	Ecodrie		
Date install.	20-12-13		20-02-14			19-02-14	19-12-13		
Date testing	28-04	25-04	17-04	-	24-04	18-04 22-04	-	23-04	23-04
Start time	7:45	11:00	10:25	8:20	7:40	14:50	13:45	12:30	10:50
End time	9:45	12:00	11:05	9:20	8:20	15:40	14:50	13:15	11:30
Inst.time $[min]$	120	60	40	60	40	50	65	45	40
Grout$_{top}$$[mNAP]$	-11.5	-12	-13.5	-13.5	-13.5	-13.5	-12*	-12	-12.5*
Piletip $[mNAP]$	-16.5	-17	-18.5	-18.5	-18.5	-18.5	-17.5*	-17	-17*
Steel length $[m]$	19	19.5	21.5	21.5	21.5	21.5	20	19.5	19.5
Ø tube $[mm]$	60.3	60.3	60.3	82.5	82.5	82.5	101.6	101.6	101.6
Thickness $[mm]$	17.5	17.5	17.5	17.5	17.5	17.5	12.5	12.5	12.5
Ø screwbit $[mm]$	250	250	250	320	320	320	380	380	380
Ø pile $[mm]$	250	250	270	340	340	340	380	380	380

Steel type tube	STE460			N80					
Steel t. coupling	STE460		-	-	-	-	N80		
Couplings [−]	7	8	8	6	6	6	5	5	5
Grout and installation									
Cement type	-	-	-	-	-	-	-	-	-
W/C-ratio [−]	-	-	0.5	0.5	0.5	0.5	-	-	-
Bentonite use [L]	265	256	190	226	319	285	225	220	200
Grout use [L]	438	415	240	378	265	421	700	900	440
Switch bentonite to grout [$mNAP$]	-	-	-12.5	-12.5	-12.5	-12.5	-	-	-
Pressure [Bar]	1-5	1-6	1-5	2-6	1-5	1-5	1-6	1-5	1-6

* Contradictory values in installation logs and measurement sheets

A.4.2.2 Installation machine

For installation of the piles, 2 different machines were used. The first one was a the Hutte drilling machine. It is unknown which type within the Hutte series was used. The second machine used was again the Ecodrie which was also used for installation of Type C piles.

Piles P01 and P02 are the only piles installed with the Hutte machine, for the other piles the Ecodrie machine was used.

Figure A-9: Example of a Hutte drilling machine (directindustry.com)

Differences in specifications between the machines are unknown because only the type of machine used was logged, not the specific edition. Within a certain type, there are still lots of differences.

A.4.2.3 Time between installation and testing

Not all piles were installed around the same date, therefore significant differences are present between the date of installation and the date at which the piles were tested. In Table A-12 the installation- and test dates are presented, and also the amount of days between them. For P04 and P07, not test date was registered. It is assumed that those dates are close to the other test dates, values guessed for P04 and P07 are indicated with a ~.

Table A-12: Installation and test dates for type D

Pile name	P01	P02	P03	P04	P05	P06	P07	P08	P09
Date install.	20-12-13		20-02-14			19-02-14	19-12-13		
Date testing	28-04	25-04	17-04	-	24-04	18-04 22-04	-	23-04	23-04
Days to testing	129	126	56	~60	63	58	~125	125	125

For all piles, the timespan of 10 to 14 days between installation and testing was kept.

A.4.2.4 Diameter of the screw blades

Three different diameters were applied, 250, 320 and 380 millimetres in diameter. Based on CUR 236, no grout penetration depth has to be taken into account for piles of type D. Effective diameters are thus the same as the diameters of the screw blades.

For the different diameters is corrected when the maximum mobilized shear stresses are determined.

A.4.2.5 Grout: Water/cement ratio

For all piles a water/cement ratio of 0.5 has been used of an unknown cement type. Probably the same as for micropile type C because the piles were installed by the same contractor.

A.4.2.6 Pile tip

Not all piles were installed in the shallow layer in which they had to be installed. Comparing those piles to piles which were installed correctly might give a wrong impression of the data. The differences in how much the piles differ in this, are thus analysed first. In Table A-13 the level of the grout body top and bottom are presented.

There were some contradictory values for the pile tip and top part of the grout between the installation logs and measurement sheets for P07 and P09. The values in the installation logs are chosen to be decisive. This because they were filled in immediately during installation, the measurements sheets were filled in later. It is possible that in the measurement sheets the values for pile tips were accidently changed.

The grout top for P07 and P09 becomes the tip level plus 5 meters of anchor length.

Table A-13: Grout top and bottom for type D

Pile name	P01	P02	P03	P04	P05	P06	P07	P08	P09
Grout$_{top}$[$mNAP$]	-11.5	-12	-13.5	-13.5	-13.5	-13.5	-12	-12	-12
Piletip [$mNAP$]	-16.5	-17	-18.5	-18.5	-18.5	-18.5	-17.5	-17	-17

It can be seen that five of the nine piles were not installed in the shallow sand layer. Because slight fluctuations in the top of the sand layer were present, the CPT's around each pile are checked to see how much the anchor body top of the pile extended from the sand layer. Results are presented in Table A-14.

Table A-14: Extend of the grout top above the sand layer

Pile name	P01	P02	P03	P04	P05	P06	P07	P08	P09
Grout$_{top}$ [$mNAP$]	-11.5	-12	-13.5	-13.5	-13.5	-13.5	-12	-12	-12
Top sand layer [$mNAP$]	-13.1	-13.3	-13.4	-13.4	-13.5	-13.4	-13.2	-13.5	-13.3
Extend [m]	1.6	1.3	0	0	0	0	1.2	1.5	1.3

Five of the nine piles were thus installed incorrectly with between 1.2 to 1.6 of the 5 meters of anchor length in the boulder clay/loam above the shallow sand layer. For the piles completely installed in the sand layer, the distance between grout top and the shallow layer was less than the 1 meter that is needed for soil anchors following CUR 166.

Due to the significant differences in anchor body length present in the sand layer, the data set is, based on the differences, split up into 3 parts. The first part includes the correctly installed piles (P03 – P06), the second part the piles with an extend around 1.25 m (P02, P07 and P09) and the third part the piles with and extend into the soft layer around 1.5 m (P01 and P08).

A.4.2.7 Conclusions pile integrity

It was seen that five of the nine installed piles were not done correctly. Test data about those piles is not useful when making comparisons with other piles or with CUR 236. The other piles were installed more or less correctly.

A.4.3 Test results

Load values received from the failure test resulted immediately in the soil mechanical capacity ($R_{s;max}$) for the pile. Due to the same reason as for type C piles, the head resistance and friction along the free length were assumed to be zero.

Based on the soil mechanical capacity and the dimensions, the mobilized shear stresses were again determined following equation 2-6 and can be found in Table A-15.

$$\tau_{mob;max} = \frac{R_{s;max}}{\pi \cdot \emptyset \cdot \mathrm{L_a}} \qquad 2\text{-}6$$

The determination of the maximum mobilized shear stresses does already take the diameter of a pile into account. Therefore it is assumed that all installed piles can be compared to each other's, as long as they are also installed in the same layer. Used L_a for all piles was 5 meters, even for the two piles with contradictory values for top and bottom of the grout body.

Table A-15: Data received from testing of the piles

Extend [m]	**0**				**1.25**			**1.5**	
Pile name	P03	P04	P05	P06	P02	P07	P09	P01	P08
$\boldsymbol{F_{design}}$ **[kN]**	1000	1200	1200	1500	1000	1500	1800	800	1200
$\boldsymbol{F_p}$ **[kN]**	950	1080	1080	1500	800	1200	990	960	840
$\boldsymbol{R_{s,head}}$ **[kN]**	0	0	0	0	0	0	0	0	0
$\boldsymbol{R_{s;fr}}$ **[kN]**	0	0	0	0	0	0	0	0	0
$\boldsymbol{R_{s;max}}$ **[kN]**	950	1080	1080	1500	800	1200	990	960	840
$\boldsymbol{\tau_{mob,max}}$ **[kN/m^2]**	241.9	214.9	214.9	298.4	203.7	201.0	165.9	244.5	140.7

Piles P01, P02 and P03 were loaded until the maximum steel capacity was reached. No soil mechanical failure had occurred yet. Table A-15 shows thus probably an underestimated value for the soil mechanical capacity of the pile. Values are not corrected for because the amount of underestimation is unknown.

A.4.4 α_t determination

Based on the average cone resistance and maximum mobilized shear stresses, α_t can be determined according equation 2-7:

$$\alpha_{t;i} = \frac{\tau_{mob;max}}{q_{c;avg}} \quad 2\text{-}7$$

Results can be found in Table A-16.

Table A-16: values for α_t and the values from which it is determined

Extend $[m]$	**0**				**1.25**			**1.5**	
Pile name	P03	P04	P05	P06	P02	P07	P09	P01	P08
$\boldsymbol{\tau_{mob,max}}$ $\boldsymbol{[kN/m^2]}$	241.9	214.9	214.9	298.4	203.7	201.0	165.9	244.5	140.7
$\boldsymbol{q_c}$ $\boldsymbol{[MPa]}$	27.5	17.9	19.3	24.1	14.0	15.3	19.1	14.0	10.4
$\boldsymbol{\alpha_t}$ $\boldsymbol{[-]}$	0.0088	0.0120	0.0111	0.0124	0.0146	0.0132	0.0087	0.0175	0.0136
Average:	**0.0111**				**0.0121**			**0.0155**	

A.5 Type E

Type E micropiles are installed by means of vibrations and fluidisation. After installation depth is reached, anchor steel is placed and the tube is pulled while grout is applied under high pressure.

For type E, nine piles were installed. Three of them were installed in the shallow sand layer, three in the deep layer and three in both layers. The piles installed in both layers were installed prior to the other six piles. Following CUR 236, these piles were not representative to base a design on because they were installed in two different geological layers. Therefore six new piles in the shallow and deep layer were installed and tested.

In the data study, the piles installed through both layers are left out because they cannot be compared to piles of other types.

A.5.1 Soil investigation

Soil investigation for the test piles was quite sparse. Only a single CPT was taken close to where the pile location was planned. Distances between CPT's were too big ($> 2\ m$) to use an average of several CPT's. Furthermore were all CPT's performed after installation of the pile.

In Figure A-10 the locations of the available CPT's can be found. CPT DMKP818 was only one meter long. Due to an unknown reason this CPT was stopped and a new one was performed. The test site was located roughly 25 meters to the right of the building pit. The location of the CPT also indicates the location of the pile, because they were closely spaced.

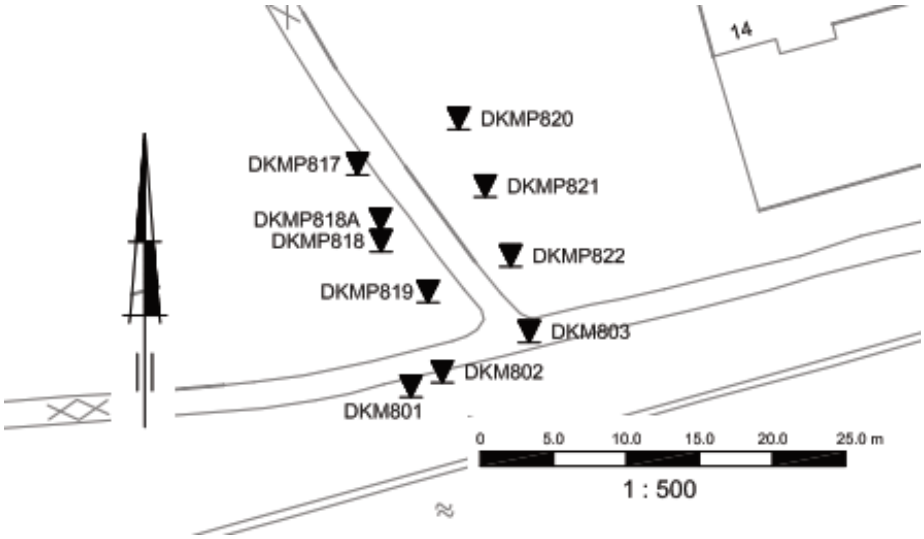

Figure A-10: Pile locations relative to the other's and their corresponding CPT's (Ingenieursbureau Harmelen BV, 2015)

The piles and their related CPT can be found in Table A-17. Because the average cone resistance values for the deep layer are lower than cone resistance values encountered by the analysis of type B, and due to the fact that CPT's were performed after installation, the values are compared to other CPT's for the shallow piles. It can be seen that those values are significantly higher than the values for CPT's performed close to the piles in the deep layer. The soil around those piles is thus probably influenced by the installation of the piles. Only the CPT for VF-7 shows a relatively normal average value. Results based on these CPT's are thus probably not reliable.

Table A-17: Piles and their corresponding CPT's

Depth	**NAP -15 to -20m**			**NAP -23 to -30m**		
Pile name	VF-9	VF-10	VF-11	VF-6	VF-7	VF-8
CPT name	DKMP817	DKMP819	DKMP821	DKMP818A	DKMP820	DKMP822
q_c **[**MPa**]**	23.6	28.4	23.2	7.8	14.4	9.3
q_c **'Deep' [**MPa**]**	16.0	12.5	16.4	7.8	14.4	9.3

A.5.2 Integrity of the installed piles

The information from the installation logs was relatively limited. Only few aspects were logged, and they were mostly the same for all piles as can be seen in Table A-18.

Table A-18: Data registered in installation- and measurement logs of Type E (Ingenieursbureau Harmelen BV, 2015)

Depth	**NAP -15 to -20 m**			**NAP -23 to -30 m**		
Pile name	VF-9	VF-10	VF-11	VF-6	VF-7	VF-8
Installation date	27-08-15	27-08-15	27-08-15	27-08-15	27-08-15	27-08-15
Test date	18-09-15	18-09-15	18-09-15	18-09-15	18-09-15	18-09-15
Pile tip [$mNAP$**]**	-20	-20	-20	-30	-30	30
Anchor length L_a **[**m**]**	5	5	5	7	7	7
∅ pile [mm**]**	250	250	250	250	250	250
∅ GEWI-bar [mm**]**	75	75	75	75	75	75
Water pressure [Bar**]**	0 → 15	0 → 15	0 → 15	0 → 15	0 → 15	0 → 15
Grout pressure [Bar**]**	10	10	10	10	10	10
Grout use [L**]**	345	345	345	440	440	440
Grout in system [L**]**	60	60	60	60	60	60

Grout per meter [L/m]	69	69	69	63	63	63

A.5.2.1 Conclusions pile integrity

The integrity check based on the installation logs turned out to be difficult. The data in the logs was the same for all piles in each layer, which is unlikely to be the case in reality. Furthermore were the CPT's not taken before, but after installation. It can be said that the installation logs of type E were not useful and not within line of CUR 236. Carefulness with using the data on type E piles is thus needed.

A.5.3 Test results

Testing of the piles resulted in gross values for the pile capacity. From the report in the failure tests on Type E piles, values for the head resistance and friction along the free length of the pile were found. With these values deducted from the gross, the nett value or the actual soil mechanical capacity ($R_{s;max}$) was found. From this capacity and following equation 2-6, the maximum mobilized shear stress was found. An overview of the values can be found in Table A-19.

Table A-19: Data received from testing of the piles

Depth	**NAP -15 to -20 m**			**NAP -23 to -30 m**		
Pile name	VF-9	VF-10	VF-11	VF-6	VF-7	VF-8
$\boldsymbol{F_{design}}$ **[kN]**	1621	1621	1621	1367	1993	1536
$\boldsymbol{F_p}$ **[kN]**	1783	2107	2107	1640	1993	1382
$\boldsymbol{R_{s,head}}$ **[kN]**	163.3	163.3	163.3	246.2	246.2	246.2
$\boldsymbol{R_{s;fr}}$ **[kN]**	28.3	28.3	28.3	28.3	28.3	28.3
$\boldsymbol{R_{s;max}}$ **[kN]**	1591.4	1915.4	1915.4	1365.5	1718.5	1107.5
$\boldsymbol{\tau_{mob,max}}$ **[kN/m^2]**	405.2	487.8	487.8	248.4	312.6	201.4

A.5.4 α_t determination

Based on the average cone resistance and maximum mobilized shear stresses, α_t can be determined according:

$$\alpha_{t;i} = \frac{\tau_{mob;max}}{q_{c;avg}} \qquad 2\text{-}7$$

Results can be found in Table A-20.

Table A-20: values for α_t and the values from which it is determined

Depth	**NAP -15 to -20 m**			**NAP -23 to -30 m**		
Pile name	VF-9	VF-10	VF-11	VF-6	VF-7	VF-8
$\boldsymbol{\tau_{mob,max}}$ **[kN/m^2]**	405.2	487.8	487.8	248.4	312.6	201.4
$\boldsymbol{q_c}$ **[MPa]**	23.6	28.4	23.2	7.8	14.4	9.3
$\boldsymbol{\alpha_t}$ **[$-$]**	0.0172	0.0172	0.0211	0.0317	0.0217	0.0217
	Average:	0.0185		**Average:**	0.0250	

Because the integrity of type E piles could not be verified and CPT's were taken afterwards, The data for type E is not used in further research. This in order to prevent unsure results and false conclusions.

A.6 Differences between pile types and CUR 236

In the previous sections, α_t values were determined based on raw data. In this section, the α_t values for different piles are compared to each other's and to values based on the design scheme from CUR 236, where limit values have to be applied. These limit values are 20 MPa for micropile types B and C; and 15 MPa for type D. The limit values for the maximum mobilized shear stresses are 2.5% of the maximum allowed cone resistance. The 2.5% is the limit value for the slope α_t.

A.6.1 α_t values according CUR 236

To compare the α_t values that were found based on raw data with values based on CUR 236, first the CUR 236 based values had to be determined. This was done according the design scheme that can be found in section 2.4: Test data interpretation. The main difference between them are the maximum values that are allowed to use for the cone resistance and the maximum mobilized shear stresses. The results can be found in Table A-21 for the shallow layer, and Table A-22 for piles installed in the deep layer. When α_t values determined following the reduced values, a maximum of 2.5% is used.

Table A-21: Overview of the maximum mobilized shear stresses, average cone resistance and α_t, received from respectively raw data and data adapted according CUR 236, for all piles installed in the shallow layer.

			Raw data			**CUR 236**		
Type	Name	Diameter $[mm]$	$\tau_{mob,max.}$ $[kN/m^2]$	q_c $[MPa]$	α_t $[-]$	$\tau_{mob,max.}$ $[kN/m^2]$	q_c $[MPa]$	α_t $[-]$
B	P01	200	542.1	30.9	0.0175	500.0	19.5	0.0250
	P03	200	498.2	27.5	0.0181	498.2	19.2	0.0250
	P05	200	481.4	25.8	0.0187	481.4	19.1	0.0250
C	P10	270	247.6	26.4	0.0094	247.6	12.9	0.0191
	P11	270	282.9	23.6	0.0120	282.9	17.3	0.0164
	P12	270	282.9	23.6	0.0120	282.9	18.1	0.0157
	P13	340	337.0	31.7	0.0106	337.0	18.9	0.0178
	P14	340	303.3	26.1	0.0116	303.3	16.9	0.0180
	P15	340	337.0	24.6	0.0137	337.0	17.0	0.0198
	P16	400	318.3	29.3	0.0109	318.3	19.2	0.0166
	P17	400	262.6	23.8	0.0110	262.6	15.6	0.0168
	P18	400	315.1	21.8	0.0144	315.1	16.1	0.0196
D	P01	250	244.5	14.0	0.0175	244.5	11.5	0.0213
	P02	250	203.7	14.0	0.0146	203.7	11.0	0.0185
	P03	250	241.9	27.5	0.0088	241.9	15.0	0.0161
	P04	320	214.9	17.9	0.0120	214.9	13.1	0.0163
	P05	320	214.9	19.3	0.0111	214.9	12.9	0.0167
	P06	320	298.4	24.1	0.0124	298.4	14.2	0.0210
	P07	380	201.0	15.3	0.0132	201.0	12.0	0.0167
	P08	380	140.7	10.4	0.0135	140.7	8.9	0.0158
	P09	380	165.9	19.1	0.0087	165.9	10.8	0.0154

Table A-22: Overview of the maximum mobilized shear stresses, average cone resistance and α_t, received from respectively raw data and data adapted according CUR 236, for all piles installed in the deep layer.

			Raw data			**CUR 236**		
Type	Name	Diameter $[mm]$	$\tau_{mob,max.}$ $[kN/m^2]$	q_c $[MPa]$	α_t $[-]$	$\tau_{mob,max.}$ $[kN/m^2]$	q_c $[MPa]$	α_t $[-]$
B	P01	200	400.2	19.5	0.0205	400.2	16.8	0.0239
	P03	200	468.4	21.9	0.0214	468.4	18.2	0.0250

	P05	200	419.5	20.2	0.0208	419.5	16.9	0.0248

Visualisation of these values can be found in Figure A-11 and Figure A-12 for respectively the raw data and data adapted according the limit values from CUR 236. The incorrectly installed piles of type D are left out of the visualization.

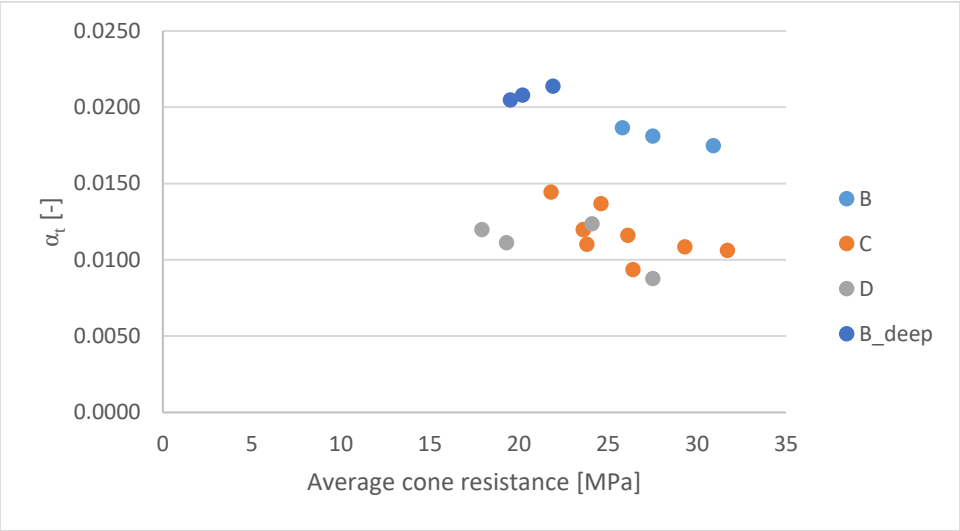

Figure A-11: α_t as function of the average cone resistance for all piles (based on raw data)

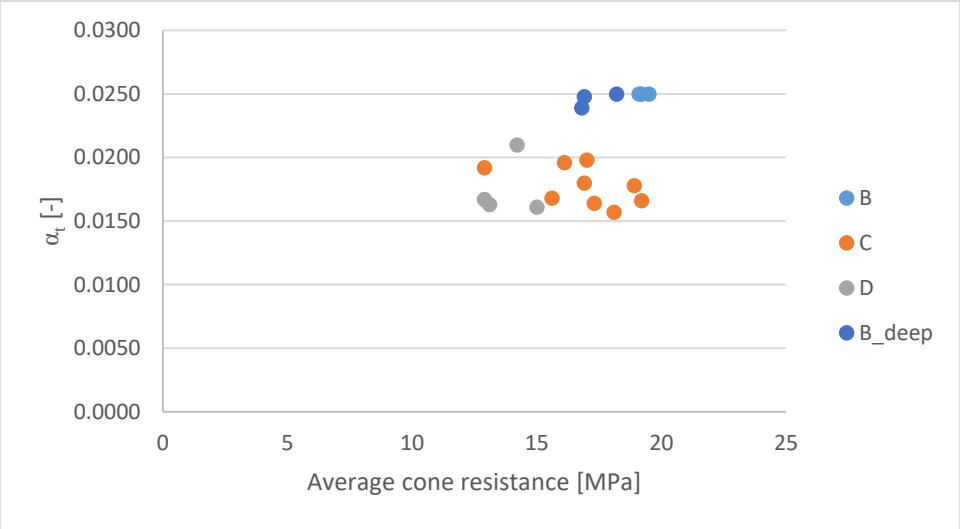

Figure A-12: α_t as function of the average cone resistance for all piles (based on CUR 236)

A.6.2 Comparison between different pile types

An interesting thing can be observed in Figure A-11, and that is that α_t values for micropiles C and D are generally lower than for type B. There are two possible explanations for this based on known differences in installation. The first option is that installation of types C and D disturbed the subsoil more than typ B. Piles of type C flush away the soil with high grout pressures. The hole that is created is then filled with grout. Type D completely remoulds the soil and mixes it with grout. The second explanation might be in the grout pressures.

Grout pressures applied at Types C and D are significantly lower than pressures applied at type B. Furthermore is the way how the grout is applied at C and D, different from B. For type C and D the grout

is applied at the tip and flushes away the- or is mixed with the excavated soil. For type B, the pressures are applied directly to the soil.

A.6.3 Comparison between raw values and values according CUR 236

In Figure A-11 and Figure A-12 values based on raw data and on the design scheme from CUR 236 were visualised. The main difference that can be seen is that values based on CUR 236 are generally higher than the raw values, as can also be seen in Table A-23.

Table A-23: Average values for α_t and the corresponding standard deviation

		Raw data		**CUR 236**	
	Type	μ [−]	σ [−]	μ [−]	σ [−]
Shallow	B	0.0181	0.00058	0.0250	0
	C	0.0117	0.00156	0.0178	0.00150
	D	0.0111	0.00161	0.0175	0.00223
Deep	B	0.0209	0.00046	0.0246	0.00059

These higher values are mostly caused by the limit value for the cone resistance. This value is 20 MPa for types B and C, and 15 MPa for type D. All measured values in the CPT's that were higher than the limit, were reduced to the maximum value.

α_t was determined by dividing the maximum mobilized shear stress by the average cone resistance as was stated in equation 2-7. Limit values for the maximum mobilized shear stress were barely needed to apply; only for pile P01 of type B. Limit values were respectively 500 kN/m^2 for types B and C, and 375 kN/m^2 for type D; 2.5% of the limit value for the cone resistance.

The question that now rises is what this means for a possible design. What are the differences in a design based on raw values and a design following the scheme in CUR 236 where limit values are applied. To estimate the differences, equation 2-1 is used:

$$R_{t,d} = \int_0^{L_a} \frac{O_{p;gem} \cdot f_1 \cdot f_2 \cdot f_3 \cdot \alpha_t \cdot q_{c;z;exc}}{\xi \cdot \gamma_{s;t} \cdot \gamma_{m;var;qc}} dz \qquad 2\text{-}1$$

In principal, the only values that vary are the average cone resistance, and the α_t value. All other parameters stay equal for the same considered pile. Therefore the bearing capacity of the pile during the comparison, can be expressed as the product of the two:

$$BC = \alpha_t \cdot q_{c;avg} \qquad A\text{-}1$$

With:

BC	Comparable bearing capacity [MPa]
α_t	Tensional shaft friction coefficient [−]
$q_{c;avg}$	Average cone resistance along the anchor body of the pile [MPa]

The comparable bearing capacity values that were found and the ratio between them, are displayed in Table A-24 and Table A-25 for piles in the shallow and deep layer respectively.

Table A-24: Comparable bearing capacity values for the raw- and CUR 236 based values for the 'shallow piles'

		Raw data			**CUR 236**			
Type	Name	q_c [MPa]	α_t [−]	$\boldsymbol{BC}$ **[$\boldsymbol{MPa}$]**	q_c [MPa]	α_t [−]	$\boldsymbol{BC}$ **[$\boldsymbol{MPa}$]**	BC ratio [−]
B	P01	30.9	0.0175	**0.54**	19.5	0.0250	**0.50**	1.11
	P03	27.5	0.0181	**0.50**	19.2	0.0250	**0.50**	1.04

	P05	25.8	0.0187	**0.48**	19.1	0.0250	**0.48**	1.01
C	P10	26.4	0.0094	**0.25**	12.9	0.0192	**0.25**	1.00
	P11	23.6	0.0120	**0.28**	17.3	0.0164	**0.28**	1.00
	P12	23.6	0.0120	**0.28**	18.1	0.0157	**0.28**	1.00
	P13	31.7	0.0106	**0.34**	18.9	0.0178	**0.34**	1.00
	P14	26.1	0.0116	**0.30**	16.9	0.0180	**0.30**	1.00
	P15	24.6	0.0137	**0.34**	17.0	0.0198	**0.34**	1.00
	P16	29.3	0.0109	**0.32**	19.2	0.0166	**0.32**	1.00
	P17	23.8	0.0110	**0.26**	15.6	0.0168	**0.26**	1.00
	P18	21.8	0.0144	**0.31**	16.1	0.0196	**0.32**	1.00
D	P01	14.0	0.0175	**0.24**	11.5	0.0213	**0.24**	1.00
	P02	14.0	0.0146	**0.20**	11.0	0.0185	**0.20**	1.00
	P03	27.5	0.0088	**0.24**	15.0	0.0161	**0.24**	1.00
	P04	17.9	0.0120	**0.21**	13.1	0.0163	**0.21**	1.01
	P05	19.3	0.0111	**0.21**	12.9	0.0167	**0.22**	1.00
	P06	24.1	0.0124	**0.30**	14.2	0.0210	**0.30**	1.00
	P07	15.3	0.0132	**0.20**	12.0	0.0167	**0.20**	1.00
	P08	10.4	0.0135	**0.14**	8.9	0.0158	**0.14**	1.00
	P09	19.0	0.0087	**0.17**	10.8	0.0154	**0.17**	1.00

Table A-25: Comparable bearing capacity values for the raw- and CUR 236 based values for the 'deep piles'

		Raw data			**CUR 236**			
Type	Name	q_c $[MPa]$	α_t $[-]$	$\boldsymbol{BC}$ $\boldsymbol{[MPa]}$	q_c $[MPa]$	α_t $[-]$	$\boldsymbol{BC}$ $\boldsymbol{[MPa]}$	BC ratio $[-]$
B	P02	19.5	0.0205	**0.40**	16.8	0.0239	**0.40**	1.00
	P04	21.9	0.0214	**0.47**	18.2	0.0250	**0.46**	1.03
	P06	20.2	0.0208	**0.42**	16.9	0.0248	**0.42**	1.00

It can be seen that the bearing capacity in almost all cases will end up the same. In only one case, the use of raw values leads to a significant overestimation compared to the capacity received from the design scheme in CUR 236.

In general both methods lead thus to the same bearing capacity of the pile. The differences in α_t do not result in a significant higher or lower pile capacity. Values based on CUR 236 show higher α_t values which might give a misleading view on the final pile capacity.

A.6.4 Comparisons with values stated in CUR 236

In CUR 236, design values for α_t are stated to come to a micropile design. It is however allowed to use values received from failure tests, as was also discussed in section 2.2: Pile design. When no failure tests are executed beforehand, the lower bound values have to be used in the design. The expected values can be used when failure tests are performed beforehand, validation tests after installation and execution control during installation. Different values found for α_t, are in such cases also allowed to be used. All values for α_t can be found in Table A-26.

Table A-26: α_t values based on raw data, the design scheme from CUR 236 and values presented in CUR 236

		Raw data	**CUR 236**	**CUR 236, Table 6.1 values**	
	Type	μ $[-]$	μ $[-]$	Lower bound	Expected
Shallow	B	0.0181	0.0250	0.011	0.017
	C	0.0117	0.0178	0.008	0.012

	D	0.0111	0.0175	0.008	0.012
Deep	B	0.0209	0.0246	0.011	0.017

It can again be seen that the values based on the design are significantly higher than the expected values from CUR 236. This is again due to division by a lowered average cone resistance. The values based on the raw data however, are relatively close to the expected values. This rises the idea that the expected values in CUR 236 are based on tests where raw data is used to determined α_t, or tests in soil conditions related to average cone resistances below the maximum allowed values.

A.7 Conclusion

Analysis of α_t values between different pile types showed significant lower values for types C and D, compared to type B. This difference is probably caused by the difference in pile mechanism. Types C and D are basically soil mix piles which might cause more disturbances in the soil directly around the pile. Furthermore are the applied grout pressures for type B significantly higher ($\approx$25 Bar) than the pressures applied at types C and D (0$-$6 Bar). The way how these pressures are applied are also different. For type C and D the grout is ejected under pressure at the pile tip, where it is mixed with the soil that was cut loose. For type B, grout is applied between the anchor steel and the soil around it. This grout is applied under pressure while the casing used for installation, is pulled out of the soil. These grout pressures act directly on the surrounding soil instead of via the soil-mix body.

Furthermore a comparison was made between α_t values based on raw data and based on the design scheme from CUR 236 where maximum values for the cone resistance and mobilized shear stresses are used. This showed that values based on CUR 236 are significantly higher. Evaluation what this means for the capacity showed no significant differences.

The final aspects that were compared, were the values received from the data (raw and flowing the design scheme) and values stated in Table 6.1 from CUR 236. In this table, lower bound and expected values for α_t in sand are presented. Values based on the design scheme from CUR 236 were significantly higher than the expected values in Table 6.1. The values determined based on raw data however, were relatively in the same range as the expected values. Designing failure tests for micropiles on the expected values in CUR 236 Table 6.1, will thus still lead to an underestimation of the actual pile capacity. At least, based on results received from piles tested at the Drachtsterweg, Leeuwarden. This does not necessarily have to mean the same for other project sites in- or outside the Netherlands.

B Data and limit values

In this appendix, the data received from failure test performed at the Drachtsterweg, Leeuwarden, are combined with the data from CUR 236 Appendix A. The whole data set is then plotted together with the limit values stated in CUR 236. This in order to see how the data points are located relative to the limit values which have to be applied if a design based on CUR 236 is made. All considered data points are based on raw data.

Comparisons are made for micropile types B, C and D. Types A and E are left out of consideration. A because this micropile type was not installed at the Drachtsterweg. Installation at the Drachtsterweg is important because relatively high cone resistances were measured there. These higher cone resistance values add worth to the data in CUR 236 because it extends the data with respect to the cone resistance.

Type E is left out because CPT's were taken after installation of the piles. These piles might influence the soil highly, due to the vibrations and fluidization which are used during installation. The integrity and usefulness of those CPT's is thus questionable.

B.1 Type B

To compare the location of the data point for type B, the data from the Drachtsterweg, Leeuwarden (NL) is combined with data from CUR 236 as can be seen in Table B-1. The values from the CUR can be identified by the '*B-*' in the name. Besides values for $\tau_{mob;max}$, q_c and α_t, also the diameter and the location of the test site can be found in the table. Note that for the diameter is corrected when $\tau_{mob;max}$ was determined.

Table B-1: Data available for type B (CUR236, 2011)

Name	Ø $[mm]$	$\tau_{mob;max}$ $[kN/m^2]$	q_c $[MPa]$	α_t $[-]$	Location
P01	200	542.1	30.9	0.0175	Drachtsterweg Leeuwarden (S)
P03	200	498.2	27.5	0.0181	Drachtsterweg Leeuwarden (S)
P05	200	481.4	25.8	0.0187	Drachtsterweg Leeuwarden (S)
P02	200	400.2	19.5	0.0205	Drachtsterweg Leeuwarden (D)
P04	200	468.4	21.9	0.0214	Drachtsterweg Leeuwarden (D)
P06	200	419.5	20.2	0.0208	Drachtsterweg Leeuwarden (D)
B-03	250	280.9	15.1	0.0186	De Spil, Houten
B-03	250	403.2	15.1	0.0267	De Spil, Houten
B-03	250	392.6	15.1	0.0260	De Spil, Houten
B-04	180	285.0	19.0	0.0150	Aquaduct Galamadammen
B-04	180	539.6	19.0	0.0284	Aquaduct Galamadammen
B-04	180	540.0	20.0	0.0270	Aquaduct Galamadammen
B-04	180	262.5	3.5	0.0750	Aquaduct Galamadammen
B-04	180	472.5	3.5	0.1350	Aquaduct Galamadammen
B-04	180	500.0	5.0	0.1000	Aquaduct Galamadammen
B-04	180	480.0	5.0	0.0960	Aquaduct Galamadammen
B-05	180	570.0	28.5	0.0200	St. Europaplein, Amsterdam
B-05	180	570.0	28.5	0.0200	St. Europaplein, Amsterdam
B-05	180	570.0	28.5	0.0200	St. Europaplein, Amsterdam
B-05	180	570.0	28.5	0.0200	St. Europaplein, Amsterdam
B-05	180	570.0	28.5	0.0200	St. Europaplein, Amsterdam
B-11	190	294.4	16.0	0.0184	Pannerdensch Kanaal

B-11	190	336.0	16.0	0.0210	Pannerdensch Kanaal
B-11	190	428.0	12.7	0.0337	Pannerdensch Kanaal
B-12	182	52.8	8.8	0.0060	Startschacht Hubertustunnel
B-13	200	57.4	7.0	0.0082	HSL Kunstwerken Dive-under
B-13	200	57.4	7.0	0.0082	HSL Kunstwerken Dive-under
B-13	200	64.9	9.4	0.0069	HSL Kunstwerken Dive-under
B-13	200	71.7	6.4	0.0112	HSL Kunstwerken Dive-under
B-13	200	68.6	6.6	0.0104	HSL Kunstwerken Dive-under
B-13	200	68.6	6.6	0.0104	HSL Kunstwerken Dive-under
B-15	180	106.2	11.3	0.0094	Betuweroute Zevenaar
B-15	180	105.8	12.9	0.0082	Betuweroute Zevenaar
B-15	180	106.6	13.0	0.0082	Betuweroute Zevenaar
B-15	180	105.3	11.2	0.0094	Betuweroute Zevenaar
B-15	180	105.3	11.2	0.0094	Betuweroute Zevenaar
B-18	200	293.8	22.6	0.0130	OG garage Anna v. Buerenpl.
B-18	200	391.1	23.7	0.0165	OG garage Anna v. Buerenpl.
B-18	200	391.0	22.6	0.0173	OG garage Anna v. Buerenpl.
B-18	200	551.2	36.5	0.0151	OG garage Anna v. Buerenpl.
B-18	200	543.9	36.5	0.0149	OG garage Anna v. Buerenpl.
B-18	200	584.3	26.2	0.0223	OG garage Anna v. Buerenpl.
B-18	200	540.0	26.6	0.0203	OG garage Anna v. Buerenpl.

The data in Table B-1 is then plotted in Figure B-1 to see how the points are located with respect to the boundary set by the limit values. Besides the limit boundaries, also the lower average and lower bound values from CUR 236 *Table 6.1* are plotted.

Note that there are some unrealistically high values present in the data of B-04. Such maximum mobilized shear stresses are logically seen, impossible to reach with an average cone resistance $\leq 5\ MPa$. Those data points are therefore neglected when comparing the data to the boundaries set by the limit values.

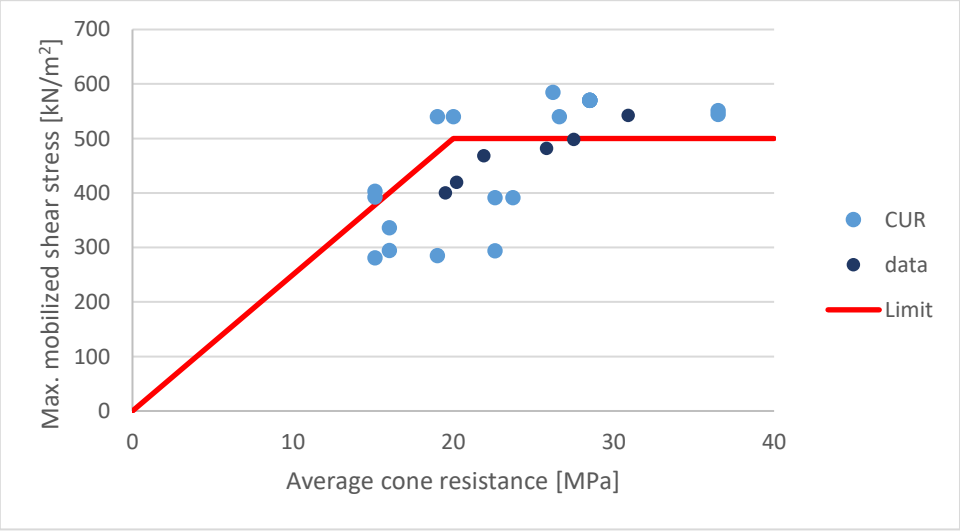

Figure B-1: Type B data points relative to the boundaries set by the limit values

The data compared to the boundaries set by the limit values show two interesting things. The limit of 20 MPa for the cone resistance is too low. The maximum mobilized shear stresses keep increasing with the cone resistance up to roughly 28 MPa. Furthermore is the limit of 500 kN/m^2 for the maximum mobilized shear stress also too low. There are also several data points with cone resistances below or at the limit value, but above the boundary for the maximum mobilized shear stress. These values indicate α_t values above the limit of 0.025. Although the general trend shows values below this slope, redefinition of this limit might be considered.

B.2 Type C

For type C the data from the Drachtsterweg was again combined with data from CUR 236 (Table B-2). The values from CUR 236 can be identified by the '*C-*' in the name. Besides values for $\tau_{mob;max}$, q_c and α_t, also the diameter and the location of the test site can be found in the table. Note that for the diameter is corrected when $\tau_{mob;max}$ was determined.

Table B-2: Data available for type C (CUR236, 2011)

Name	Ø $[mm]$	$\tau_{mob;max}$ $[kN/m^2]$	q_c $[MPa]$	α_t $[-]$	Location
P10	270	247.6	26.4	0.0094	Drachtsterweg Leeuwarden (S)
P11	270	282.9	23.6	0.0120	Drachtsterweg Leeuwarden (S)
P12	270	282.9	23.6	0.0120	Drachtsterweg Leeuwarden (S)
P13	340	337	31.7	0.0106	Drachtsterweg Leeuwarden (S)
P14	340	303.3	26.1	0.0116	Drachtsterweg Leeuwarden (S)
P15	340	337	24.6	0.0137	Drachtsterweg Leeuwarden (S)
P16	400	318.3	29.3	0.0109	Drachtsterweg Leeuwarden (S)
P17	400	262.6	23.8	0.0110	Drachtsterweg Leeuwarden (S)
P18	225	315.1	21.8	0.0144	Drachtsterweg Leeuwarden (S)
C-02	225	46.6	10.6	0.0044	Parkeergarage Bussum
C-02	225	46.6	10.6	0.0044	Parkeergarage Bussum
C-15	250	235.5	16.7	0.0141	Kw34 Betuweroute Hardinxv.-G
C-15	250	252.8	17.8	0.0142	Kw34 Betuweroute Hardinxv.-G
C-15	300	248.1	15.7	0.0158	Kw34 Betuweroute Hardinxv.-G
C-17	300	253.0	13.6	0.0186	Nieuwbouw Rabobank Utrecht
C-17	300	200.6	13.2	0.0152	Nieuwbouw Rabobank Utrecht
C-17	300	147.0	10.5	0.0140	Nieuwbouw Rabobank Utrecht
C-18	300	154.0	11.0	0.0140	Onderdoorgang Hapert
C-18	300	143.0	11.0	0.0130	Onderdoorgang Hapert
C-18	300	121.0	11.0	0.0110	Onderdoorgang Hapert
C19	370	175.0	12.5	0.0140	Proefbel. Werkendam
C19	370	171.7	11.6	0.0148	Proefbel. Werkendam
C19	370	180.3	10.3	0.0175	Proefbel. Werkendam
C-20	195	224.9	17.3	0.0130	Techniekkelder Rabobank
C-20	195	211.1	17.3	0.0122	Techniekkelder Rabobank
C-20	195	221.4	17.3	0.0128	Techniekkelder Rabobank
C-21	220	195.8	15.3	0.0128	Kunstwerk N201: 1st series
C-21	220	228.0	15.3	0.0149	Kunstwerk N201: 1st series
C-21	220	228.0	15.3	0.0149	Kunstwerk N201: 1st series
C-22	300	191.3	15.3	0.0125	Kunstwerk N201: 2nd series
C-22	300	166.8	15.3	0.0109	Kunstwerk N201: 2nd series

C-22	300	191.3	15.3	0.0125	Kunstwerk N201: 2nd series
C-23	220	247.5	23.8	0.0104	Onderdoorgang Peelo Zuid
C-23	220	247.5	23.8	0.0104	Onderdoorgang Peelo Zuid
C-23	220	330.8	23.8	0.0139	Onderdoorgang Peelo Zuid

The data from the table is then plotted in Figure B-2: Type C data points relative to the boundaries set by the limit values Figure B-2 in order to compare the data points with the limit value boundaries. Besides limit value boundaries, also the lower average and lower bound values as presented in CUR 236 *Table 6.1* are added to this figure.

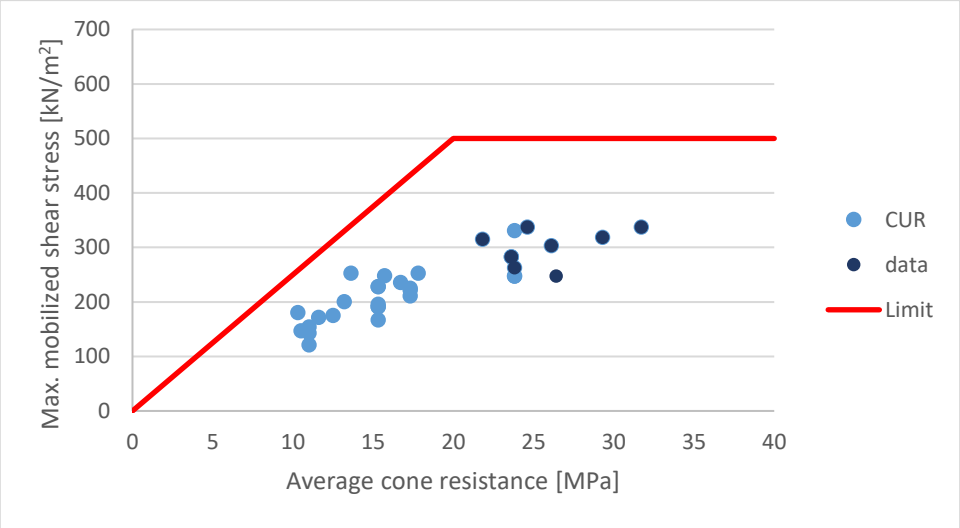

Figure B-2: Type C data points relative to the boundaries set by the limit values

The data point from tests on micropiles of type C show a general relation between q_c and $\tau_{mob;max}$. This trend increases up to roughly 25 MPa after which it seems to reach a maximum mobilized shear stress of around 350 kN/m^2.

It can be seen that the relation continues after the cone resistance limit of 20 MPa for is passed; this limit value for this is thus too low. The limit boundary for the maximum mobilized shear stress however, lies significantly above all data points. Based on the data the limit of 500 kN/m^2 is thus too high. Only about 350 kN/m^2 has been reached during testing up to failure.

B.3 Type D

The combined data set with data from the Drachtsterweg and data from CUR 236 can be found in Table B-3. From the Drachtsterweg data, five of the nine tested piles are left out. This due to the incorrect installation of the piles in the sand layer. Data from CUR 236 can be identified by the '*D-*' in the name.

Table B-3: Data available for type D (CUR236, 2011)

Name	**Ø $[mm]$**	**$\tau_{mob;max}$ $[kN/m^2]$**	**q_c $[MPa]$**	**α_t $[-]$**	**Location**
P03	250	241.9	27.5	0.0088	Drachtsterweg Leeuwarden (S)
P04	320	214.9	17.9	0.0120	Drachtsterweg Leeuwarden (S)
P05	320	214.9	19.3	0.0111	Drachtsterweg Leeuwarden (S)
P06	320	298.4	24.1	0.0124	Drachtsterweg Leeuwarden (S)
D-01	350	85.8	11.0	0.0078	Startschacht Hubertustunnel
D-01	350	55.0	11.0	0.0050	Startschacht Hubertustunnel
D-01	350	79.8	13.3	0.0060	Startschacht Hubertustunnel

D-03	300	134.0	9.5	0.0141	Ring A10 West, Amsterdam
D-03	300	134.0	9.5	0.0141	Ring A10 West, Amsterdam
D-03	300	134.0	9.5	0.0141	Ring A10 West, Amsterdam
D-04	350	81.9	9.1	0.0090	Sophiaspoortunnel
D-04	350	82.5	8.5	0.0097	Sophiaspoortunnel
D-04	350	88.4	8.5	0.0104	Sophiaspoortunnel
D-05	350	97.8	8.5	0.0115	Bouwdok Kaageiland
D-05	350	104.6	8.5	0.0123	Bouwdok Kaageiland
D-06	350	119.3	9.7	0.0123	Ijsbaan De Meent
D-06	350	119.3	9.7	0.0123	Ijsbaan De Meent
D-07	350	60.8	9.5	0.0064	Sophiaspoortunnel
D-07	350	48.5	9.5	0.0051	Sophiaspoortunnel
D-07	350	69.8	10.9	0.0064	Sophiaspoortunnel
D-08	180	454.7	39.2	0.0116	Uitbreiding gemaal Ijmuiden
D-08	180	462.6	39.2	0.0118	Uitbreiding gemaal Ijmuiden
D-08	180	478.2	39.2	0.0122	Uitbreiding gemaal Ijmuiden
D-08	180	466.5	39.2	0.0119	Uitbreiding gemaal Ijmuiden
D-10	400	141.3	15.7	0.0090	Ateliergeb. Rijksmus. A'dam
D-16	300	84.6	9.1	0.0093	Onderdoorgang Leidsstr.weg
D-16	300	93.0	8.3	0.0112	Onderdoorgang Leidsstr.weg
D-16	300	85.4	8.8	0.0097	Onderdoorgang Leidsstr.weg
D-18	450	117.4	9.1	0.0129	Overkappingsc. RW 28, Zeist
D-18	450	83.7	9.1	0.0092	Overkappingsc. RW 28, Zeist
D-19	400	79.2	7.2	0.0110	Woensdrecht
D-20	350	116.6	10.6	0.0110	Pijnacker
D-20	350	148.4	10.6	0.0140	Pijnacker
D-20	180	128.7	11.7	0.0110	Pijnacker
D-20	180	214.2	11.9	0.0180	Pijnacker
D-20	180	185.6	11.6	0.0160	Pijnacker
D-20	180	235.6	12.4	0.0190	Pijnacker
D-21	350	124.5	8.3	0.0150	Jeltesloot, 1e fase
D-21	350	149.4	8.3	0.0180	Jeltesloot, 1e fase

The data point are then plotted in Figure B-3, together with the boundary due to the limit values. Also the lower average and lower bound values are plotted in the figure, indicted by respectively the orange and green lines.

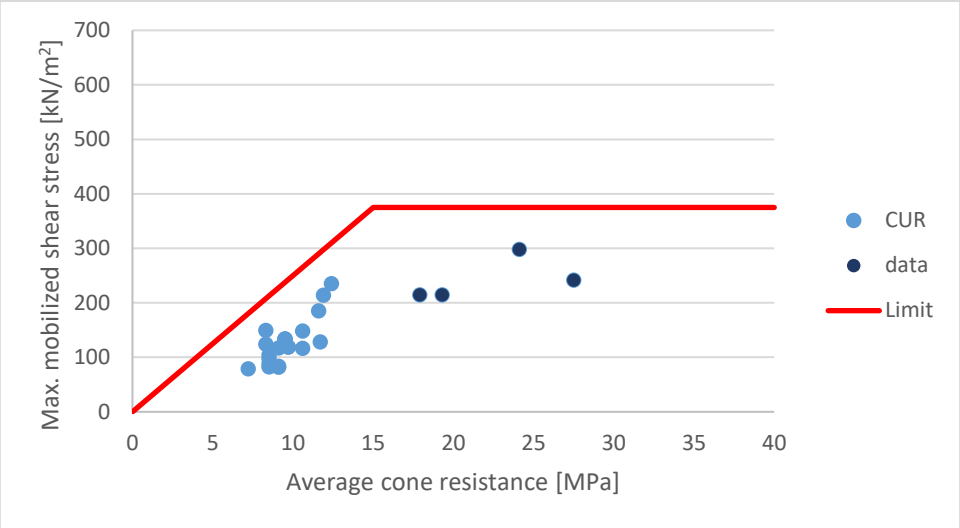

Figure B-3: Type D data points relative to the boundaries set by the limit values

The data points of type D micropiles were mostly installed in soils with an average cone resistance around 10 MPa. With the additional data from the Drachtsterweg, Leeuwarden (NL), also points above the limit value for q_c are added. From those points it can be seen that the relation between q_c and $\tau_{mob;max}$ continues after this limit up to roughly 20-25 MPa. There were also some points present close to a cone resistance of 39 MPa. It was possible to see a trend which continues up to there, but the gap in the data is assumed to be to significant to continue the observed relation.

The boundary set by the limit values for $\tau_{mob;max}$ is slightly too high. There are however not many available data points in the range above the limit for q_c, which make it difficult to see a clear maximum for the maximum mobilized shear stress. Furthermore can it be seen that the limit value for q_c is too low. In general continues the relation between the average cone resistance and the maximum mobilized shear stress up to roughly 20-25 MPa.

B.4 Conclusion

The main thing that can be concluded from the combined data set of CUR 236 and the Drachtsterweg, is that for micropile types B, C and D, the relation between average cone resistance and maximum mobilized shear stresses does not stop at the limit value for the cone resistance. This limit was set in CUR 236. For cone resistances higher than the limit value, the relation seemed to increase to a certain maximum for $\tau_{mob;max}$, or to where the data stopped. The use of limit values for the cone resistance is thus in its current state, not correctly applied according the data.

The use of limit values for the maximum mobilized shear stress can still be applied. Except that the height of the limit value is not always realistic for different pile types. The investigated pile types showed maximum values around 600, 350 and 300 kN/m^2 for respectively type B, C and D.

The limit value of 0.025 for the slope or α_t value was not reached for types C and D. For type B, there were several points that had a steeper slope. For type B, the height of this limit might thus be slightly too low. Carefulness with this changing this limit value is however needed.

C Statistical data analysis

In this appendix, limit values will be derived from the data by means of general data interpretation and statistics. This will be done for micropile types B, C and D. types A and E are left out due to insufficient data on them.

C.1 Methodology

For each pile type, first the limit value of the cone resistance will be determined. This is done by investigating the turning- or inflection point of α_t. After the turning point, the maximum mobilized shear stresses do not increase significantly with the average cone resistance anymore.

The limit for the maximum mobilized shear stress is then determined based on the data points above the limit value for the average cone resistance. This is done because $\tau_{mob;max}$ stays roughly equal, for an increasing average cone resistance. This can thus be used to statistically estimate the mean (equation C-1) and standard deviation (equation C-2) of those data points. The same will be done for α_t, but then in the data part below the limit for the average cone resistance, where the maximum mobilized shear stress is assumed to linearly increase with the average cone resistance. The available data can be seen as a sample which gives an estimation of the population. The population is in this case all micropiles that are, or will be installed for a similar pile type, in a similar way.

$$\bar{X} = \frac{\sum X_i}{n} \qquad \text{C-1}$$

$$S = \sqrt{\frac{\sum_{i=1}^{n}(X_i - \bar{X})^2}{n-1}} \qquad \text{C-2}$$

With:

$\bar{X}$	Sample mean [$*$]
S	Sample standard deviation [*]
X_i	A certain data point i [*]
n	The number of data points in the sample [$-$]

* dependent on the unit of the data

The limit values for $\tau_{mob;max}$ and α_t are then placed around the value where 95% of the data sample lies below. Following:

$$\bar{X}_{frac;5\%} = \bar{X} + t_{0.05;n-1} \cdot \frac{S}{\sqrt{n+\frac{1}{n}}} \qquad \text{C-3}$$

With:

$\bar{X}_{frac;5\%}$	Upper bound which has a 5% chance on exceedance [$*$]
$t_{0.05;n-1}$	Value of t-distribution dependent on sample size (See Appendix E) [$-$]

* dependent on the unit of the data

The limit value is not exactly taken at the calculated value, but at a round value close to it. This to make the limit values easier and more convenient to use and remember in practice.

Average values are determined, on which failure tests can be based in order to come to an optimized design. These values are based on the mean of the data. Finally also lower bound values are added which have to be applied when no failure tests are performed in order to come to an optimized design. Those values are based on:

$$\bar{X}_{frac;95\%} = \bar{X} - t_{0.05;n-1} \cdot \frac{s}{\sqrt{n+\frac{1}{n}}} \qquad C\text{-}4$$

With:

$\bar{X}_{frac;95\%}$ Lower bound which has a 95% chance on exceedance [*]

* dependent on the unit of the data

C.2 Type B

For type B, the data points presented in Table B-1 are used. The α_t value and the maximum mobilized shear stress of these points are subdivided in average cone resistance intervals of 2.5 MPa each (Table C-1 and Table C-2). This in order to plot α_t and $\tau_{mob;max}$ as function of the average cone resistance.

The data marked in red is data obtained from CUR 236, but was left out for unknown reasons while determining the statistical values on which Table 6.1 from CUR 236 is based. Contact with the author of CUR 236 on why these points were neglected in this matter, resulted in no clear answer. It is therefore assumed that those points were left out for good reason (not correctly installed, no pressure applied during grouting etc.), and are therefore also not fit to use for the statistical approach in this thesis.

Table C-1: $\tau_{mob;max}$ subdivided in average cone resistance intervals for type B

q_c [MPa]	0 – 2.5	2.5 – 5	5 – 7.5	7.5 – 10	10 – 12.5	12.5 – 15	15 – 17.5	17.5 – 20	20 – 22.5	22.5 – 25	25 – 27.5	27.5 – 30	30 – 32.5	32.5 – 35	35 – 37.5	37.5 – 40
N [−]	0	4	5	2	3	3	5	4	2	3	4	5	1	0	2	0
μ [kN/m^2]	-	-	-	-	-	-	341.4	441.2	444.0	358.6	526.0	570.0	542.1	-	547.5	-
σ [kN/m^2]	-	-	-	-	-	-	55.5	123.2	34.6	56.1	46.0	0	-	-	5.2	-
$\tau_{mob;max}$ [kN/m^2]		262.5	71.7	52.8	105.3	428.0	280.9	285.0	419.5	293.8	481.4	570.0	542.1		551.2	
		472.5	68.6	64.9	105.3	105.8	403.2	539.6	468.4	391.0	584.3	570.0			543.9	
		500.0	68.6		106.2	106.6	392.6	400.2		391.1	540.0	570.0				
		480.0	57.4				294.4	540.0			498.2	570.0				
			57.4				336.0					570.0				

Table C-2: α_t subdivided in average cone resistance intervals for type B

q_c [MPa]	0 – 2.5	2.5 – 5	5 – 7.5	7.5 – 10	10 – 12.5	12.5 – 15	15 – 17.5	17.5 – 20	20 – 22.5	22.5 – 25	25 – 27.5	27.5 – 30	30 – 32.5	32.5 – 35	35 – 37.5	37.5 – 40
N [−]	0	4	5	2	3	3	5	4	2	3	4	5	1	0	2	0
μ [−]	-	-	-	-	-	-	0.0221	0.0227	0.0211	0.0156	0.0198	0.0200	0.0175	0.0150	-	-
σ [−]	-	-	-	-	-	-	0.0040	0.0062	0.0004	0.0023	0.0019	0	-	0.0001	-	-
α_t [−]		0.0750	0.0112	0.0060	0.0094	0.0337	0.0186	0.00150	0.0208	0.0130	0.0187	0.0200	0.0175	0.0151		
		0.1350	0.0104	0.0069	0.0094	0.0082	0.0267	0.0284	0.0214	0.0173	0.0223	0.0200		0.0149		
		0.1000	0.0104		0.0094	0.0082	0.0260	0.0205		0.0165	0.0203	0.0200				
		0.0960	0.0082				0.0184	0.0270			0.0181	0.0200				
			0.0082				0.0210									

C.2.1 Cone resistance limit

The information from Table C-1 and Table C-2, where respectively the $\tau_{mob;max}$ and α_t data was sub-divided in average cone resistance intervals, is then used to plot both variables against the average cone resistance in order to find the turning point, and thus the limit for the cone resistance. Note that the values marked in red are left out of the visualizations in Figure C-1 and Figure C-2.

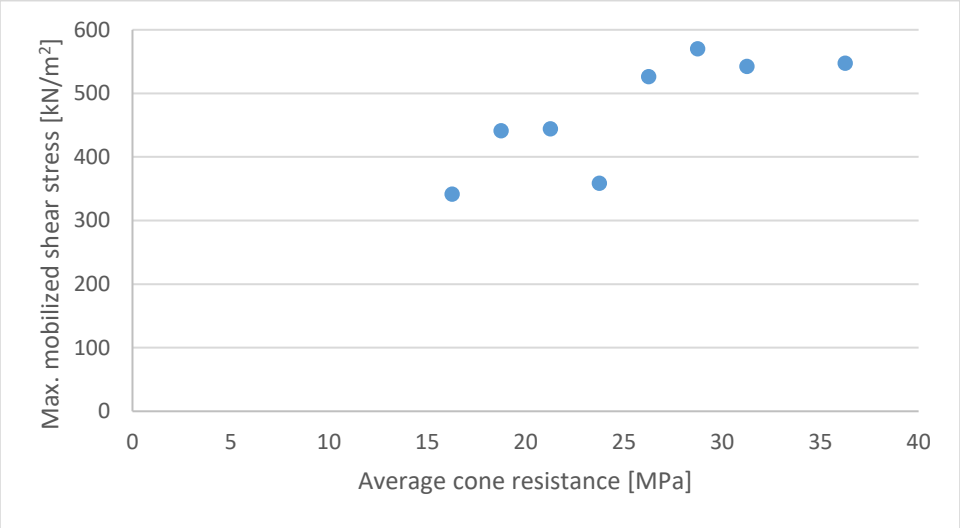

Figure C-1: the average values for $\tau_{mob;max}$ plotted as function of the average cone resistance intervals

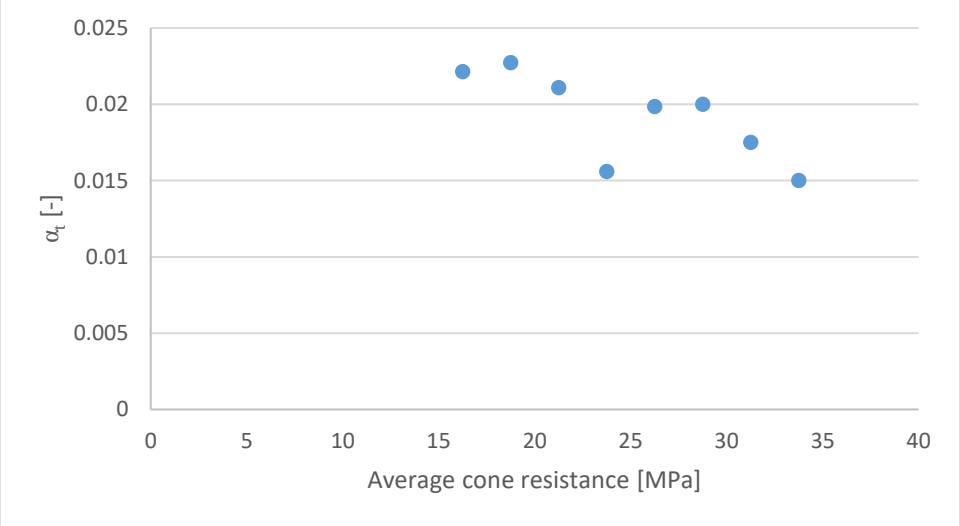

Figure C-2: the average values for α_t plotted as function of the average cone resistance intervals

It can be seen that the maximum mobilized shear stress reaches its average maximum around 25 MPa. Afterwards it stays about the same. For α_t, the maximum reduces significantly, slightly after 25-30 MPa. In both graphs, a dip in the curve can be seen between 20 and 25 MPa. This is due to the relative low amount of data points within each average cone resistance interval. Outliers have significant effects on the trend in such cases.

Based on the figures, the limit value for q_c is set at 25 MPa.

C.2.2 Maximum mobilized shear stress boundaries

The limit and lower bound for the maximum mobilized shear stress is then determined based on the values above the cone resistance limit of 25 MPa. These values are indicated in the red box in Figure

C-3. From those values, the mean and standard deviation are taken following equations C-1 and C-2. This resulted in the following values:

$$\bar{X}_{\tau_{mob;max}} = 549.2\ kN/m^2$$

$$S_{\tau_{mob;max}} = 31.3\ kN/m^2$$

The value below which 95% of the data lies becomes then:

$$\bar{X}_{\tau_{mob;max}} + t_{0.05;n-1} \cdot \frac{S\tau_{mob;max}}{\sqrt{1+\frac{1}{n}}} = 549.2 + 1.796 \cdot \frac{31.3}{\sqrt{1+\frac{1}{12}}} = 603.2\ kN/m^2$$

The value above which 95% of the data lies becomes then:

$$\bar{X}_{\tau_{mob;max}} - t_{0.05;n-1} \cdot \frac{S\tau_{mob;max}}{\sqrt{1+\frac{1}{n}}} = 549.2 - 1.796 \cdot \frac{31.3}{\sqrt{1+\frac{1}{12}}} = 495.3\ kN/m^2$$

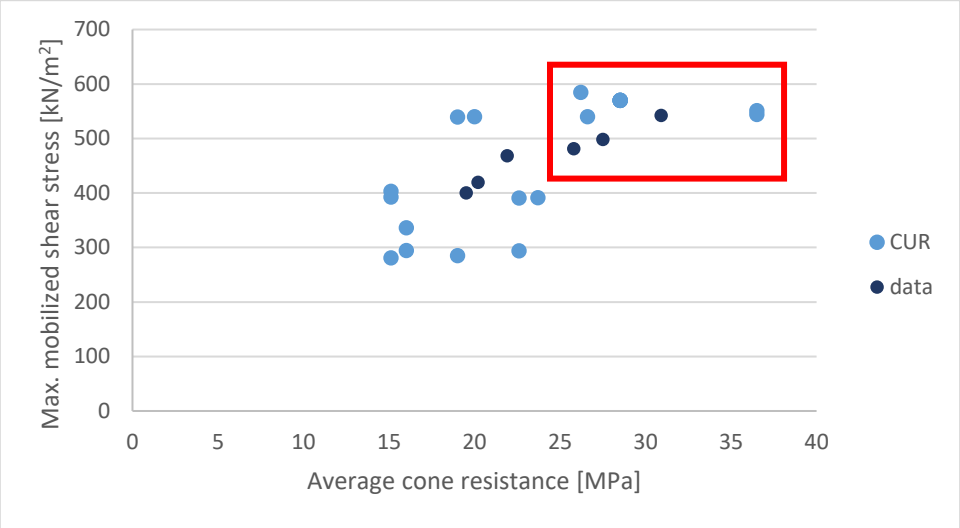

Figure C-3: Data points used for $\tau_{mob;max}$ limit determination of type B micropiles

C.2.3 α_t limit

The limit and lower bound for α_t are determined in the same way as for the maximum mobilized shear stress, except that the part of the data below the limit for the cone resistance is taken. In Figure C-4 the considered data points are indicated by the red box. The mean and standard deviation become then:

$$\bar{X}_{\alpha_t} = 0.0208$$

$$S_{\alpha_t} = 0.0048$$

The value below which 95% of the data lies becomes then:

$$\bar{X}_{\alpha_t} + t_{0.05;n-1} \cdot \frac{S\alpha_t}{\sqrt{1+\frac{1}{n}}} = 0.0208 + 1.771 \cdot \frac{0.0048}{\sqrt{1+\frac{1}{14}}} = 0.0289$$

The value above which 95% of the data lies becomes then:

$$\bar{X}_{\alpha_t} - t_{0.05;n-1} \cdot \frac{S\alpha_t}{\sqrt{1+\frac{1}{n}}} = 0.0208 - 1.771 \cdot \frac{0.0048}{\sqrt{1+\frac{1}{14}}} = 0.0126$$

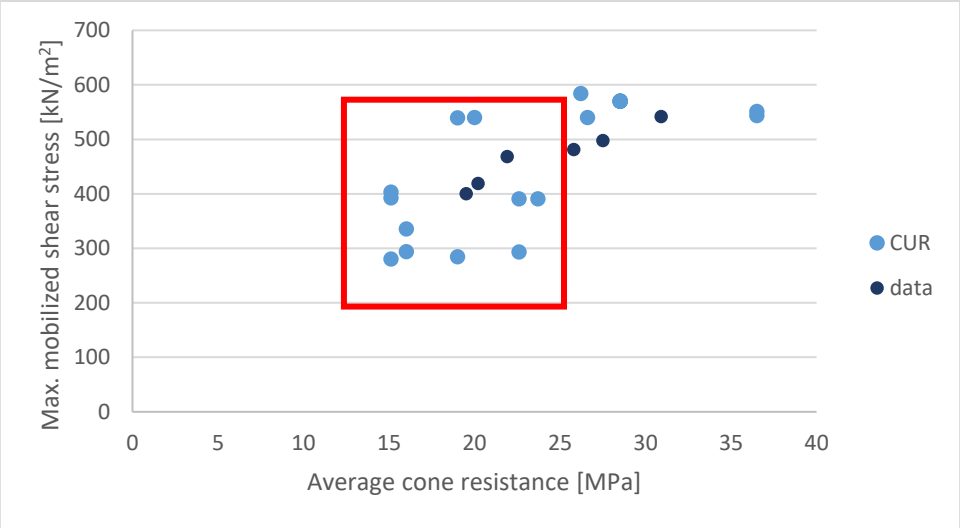

Figure C-4: Data points used for α_t limit determination of type B micropiles

C.3 Type C

For type C, the data points from Table B-2 are used. The α_t value and the maximum mobilized shear stress of these points are subdivided in average cone resistance intervals of 2.5 MPa each in respectively Table C-3 and Table C-4. Based on the subdivision, α_t and $\tau_{mob;max}$ can be plotted as function of the average cone resistance.

The data marked in red is data obtained from CUR 236, but was left out for unknown reasons while determining the statistical values on which Table 6.1 from CUR 236 is based. Contact with the author of CUR 236 on why these points were neglected in this matter, resulted in no clear answer. It is therefore assumed that those points were left out for good reason (not correctly installed, no pressure applied during grouting etc.), and are therefore also not fit to use for the statistical approach in this thesis.

Table C-3: $\tau_{mob;max}$ subdivided in average cone resistance intervals for type C

q_c [MPa]	0 – 2.5	2.5 – 5	5 – 7.5	7.5 – 10	10 – 12.5	12.5 – 15	15 – 17.5	17.5 – 20	20 – 22.5	22.5 – 25	25 – 27.5	27.5 – 30	30 – 32.5	32.5 – 35	35 – 37.5	37.5 – 40
N [−]	0	0	0	0	8	3	11	1	1	7	1	1	1	0	0	0
μ [kN/m^2]	-	-	-	-	152.8	209.5	210.6	252.8	315.1	284.5	303.3	318.3	337.0	-	-	-
σ [kN/m^2]	-	-	-	-	21.2	39.7	28.1	-	-	36.8	-	-	-	-	-	-
$\tau_{mob;max}$ [kN/m^2]					180.3	175.0	195.8	252.8	315.1	282.9	303.3	318.3	337.0			
					147.0	200.6	228.0			282.9						
					46.6	253.0	228.0			262.6						
					46.6		191.3			247.5						
					154.0		166.8			247.5						
					143.0		191.3			330.8						
					121.0		248.1			337.0						
					171.7		235.5									
							224.9									
							211.1									
							221.4									

Table C-4: α_t subdivided in average cone resistance intervals for type C

q_c [MPa]	0 – 2.5	2.5 – 5	5 – 7.5	7.5 – 10	10 – 12.5	12.5 – 15	15 – 17.5	17.5 – 20	20 – 22.5	22.5 – 25	25 – 27.5	27.5 – 30	30 – 32.5	32.5 – 35	35 – 37.5	37.5 – 40
N [−]	0	0	0	0	8	3	11	1	1	7	1	1	1	0	0	0
μ [−]	-	-	-	-	0.0141	0.0159	0.0134	0.0142	0.0144	0.0119	0.0116	0.0109	0.0106	-	-	-
σ [−]	-	-	-	-	0.0021	0.0023	0.0015	-	-	0.0014	-	-	-	-	-	-
α_t [−]					0.0175	0.0140	0.0128	0.0142	0.0144	0.0120	0.0116	0.0109	0.0106			
					0.0140	0.0152	0.0149			0.0120						
					0.0044	0.0186	0.0149			0.0110						
					0.0044		0.0125			0.0104						
					0.0140		0.0109			0.0104						
					0.0130		0.0125			0.0139						
					0.0110		0.0158			0.0137						
					0.0148		0.0141									
							0.0130									

							0.0122									
							0.0128									

C.3.1 Cone resistance limit

The average values per cone resistance interval from Table C-3 and Table C-4 for respectively $\tau_{mob;max}$ and α_t, is then plotted in order to find the limit value for q_c in Figure C-5 and Figure C-6. The limit value for q_c lies around the inflection point of the α_t trend, where it starts decreasing with increasing average cone resistance.

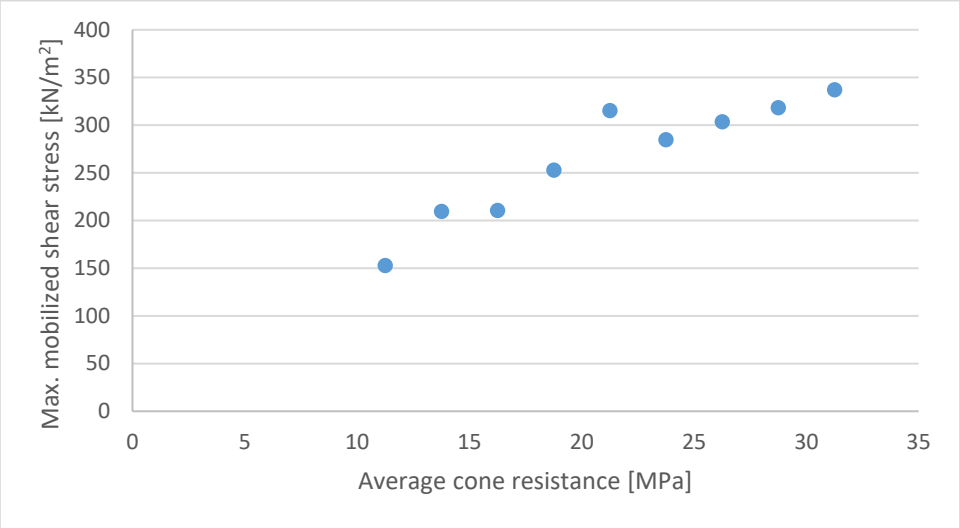

Figure C-5: Average values for $\tau_{mob;max}$ plotted as function of the average cone resistance intervals, type C

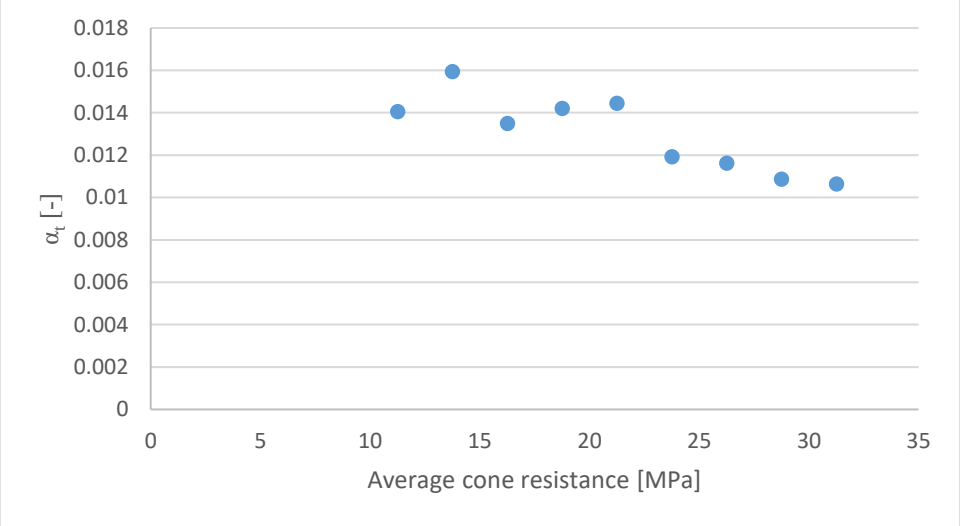

Figure C-6: Average values for α_t plotted as function of the average cone resistance intervals, type C

It can be seen that the maximum mobilized shear stress reaches its maximum between 20 and 25 MPa. For α_t, the maximum reduces significantly around the same point between 20 and 25 MPa. After the decrease, around 25 MPa, the α_t trend seems to stabilize again. Fluctuations in both curves are mainly due to the low amount of data points at some intervals. Outliers have in such cases significant effects on the location of the average data point.

Based on the figures, the limit value for q_c is set between 20 and 25 MPa, at 22.5 MPa.

C.3.2 Maximum mobilized shear stress limit

The limit and lower bound for the maximum mobilized shear stress are determined based on the values above the cone resistance limit of 22.5 MPa. These values are indicated in the red box in Figure C-3.

From those values, the mean and standard deviation are taken following equations C-1 and C-2. This resulted in the following values:

$$\bar{X}_{\tau_{mob;max}} = 295.0\ kN/m^2$$

$$S_{\tau_{mob;max}} = 35.4\ kN/m^2$$

The value below which 95% of the data lies becomes then:

$$\bar{X}_{\tau_{mob;max}} + t_{0.05;n-1} \cdot \frac{S\tau_{mob;max}}{\sqrt{1+\frac{1}{n}}} = 295.0 + 1.833 \cdot \frac{35.4}{\sqrt{1+\frac{1}{10}}} = 356.8\ kN/m^2$$

The value above which 95% of the data lies becomes then:

$$\bar{X}_{\tau_{mob;max}} - t_{0.05;n-1} \cdot \frac{S\tau_{mob;max}}{\sqrt{1+\frac{1}{n}}} = 295.0 - 1.833 \cdot \frac{35.4}{\sqrt{1+\frac{1}{10}}} = 233.1\ kN/m^2$$

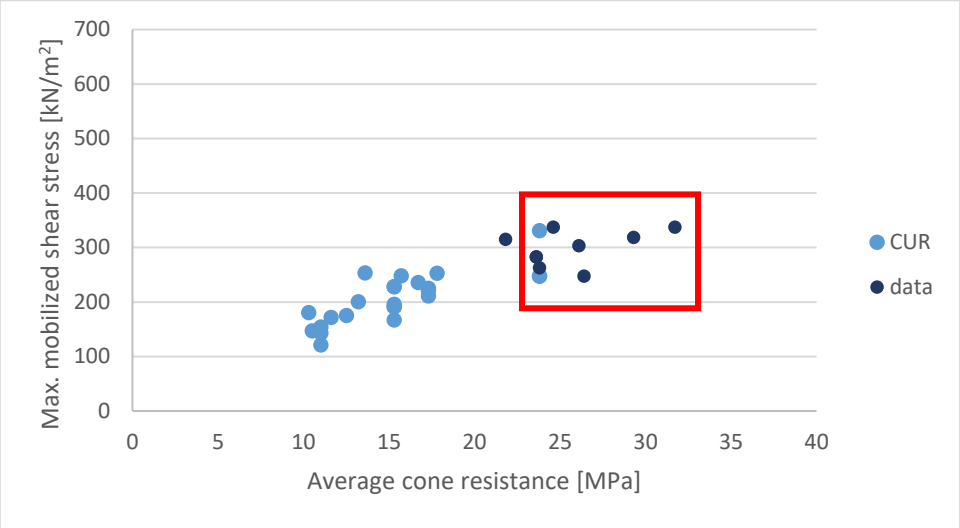

Figure C-7: Data points used for $\tau_{mob;max}$ limit determination of type C micropiles

C.3.3 α_t limit

The boundary values for α_t are determined in the same way as the ones for the maximum mobilized shear stress, except that the part of the data below the limit for the cone resistance is taken. The data below 22.5 MPa thus, as indicated in de red box in Figure C-9. This resulted in the following values:

$$\bar{X}_{\alpha_t} = 0.0140$$

$$S_{\alpha_t} = 0.0031$$

The value below which a 95% of the data lies becomes then:

$$\bar{X}_{\alpha_t} + t_{0.05;n-1} \cdot \frac{S\alpha_t}{\sqrt{1+\frac{1}{n}}} = 0.0140 + 1.721 \cdot \frac{0.0031}{\sqrt{1+\frac{1}{22}}} = 0.0171$$

The value above which a 95% of the data lies becomes then:

$$\bar{X}_{\alpha_t} - t_{0.05;n-1} \cdot \frac{S\alpha_t}{\sqrt{1+\frac{1}{n}}} = 0.0140 - 1.721 \cdot \frac{0.0031}{\sqrt{1+\frac{1}{22}}} = 0.0108$$

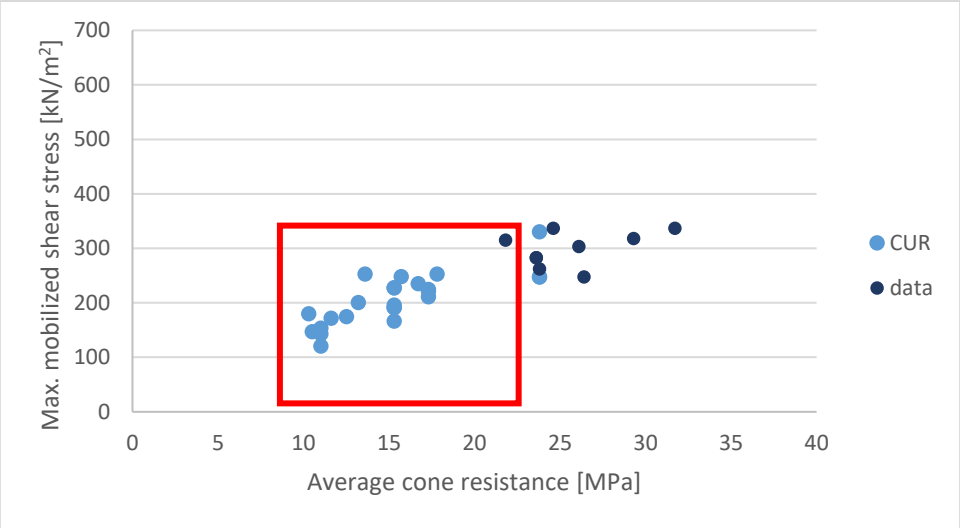

Figure C-8: Data points used for α_t limit determination of type C micropiles

C.4 Type D

For type B, the data points presented in Table B-3 are used. The α_t value and the maximum mobilized shear stress of these points are again subdivided in average cone resistance intervals of 2.5 MPa which is presented in Table C-5 and Table C-6. α_t and $\tau_{mob;max}$ are then plotted as function of the average cone resistance in Figure C-9 and Figure C-10.

The data marked in red is data obtained from CUR 236, but was left out for unknown reasons while determining the statistical values on which Table 6.1 from CUR 236 is based. Contact with the author of CUR 236 on why these points were neglected in this matter, resulted in no clear answer. It is therefore assumed that those points were left out for good reason (not correctly installed, no pressure applied during grouting etc.), and are therefore also not fit to use for the statistical approach in this thesis

Table C-5: $\tau_{mob;max}$ subdivided in average cone resistance intervals for type D

q_c $[MPa]$	0 – 2.5	2.5 – 5	5 – 7.5	7.5 – 10	10 – 12.5	12.5 – 15	15 – 17.5	17.5 – 20	20 – 22.5	22.5 – 25	25 – 27.5	27.5 – 30	30 – 32.5	32.5 – 35	35 – 37.5	37.5 – 40
N $[-]$	0	0	1	19	9	1	1	2	0	1	0	1	0	0	0	4
μ $[kN/m^2]$	-	-	79.2	107.8	158.7	-	-	214.9	-	298.4	-	241.9	-	-	-	-
σ $[kN/m^2]$	-	-	-	25.1	40.6	-	-	0	-	-	-	-	-	-	-	-
$\tau_{mob;max}$ $[kN/m^2]$			79.2	93.0	116.6	79.8	141.3	214.9		298.4		241.9				454.7
				124.5	148.4			214.9								462.6
				149.4	69.8											478.2
				82.45	85.8											466.5
				88.4	55.0											
				97.75	185.6											
				104.5	128.7											
				85.4	214.2											
				81.9	235.6											
				84.6												
				117.4												
				83.7												
				134.0												
				134.0												
				134.0												
				60.8												
				48.5												
				119.3												
				119.3												

Table C-6: α_t subdivided in average cone resistance intervals for type D

q_c [MPa]	0 – 2.5	2.5 – 5	5 – 7.5	7.5 – 10	10 – 12.5	12.5 – 15	15 – 17.5	17.5 – 20	20 – 22.5	22.5 – 25	25 – 27.5	27.5 – 30	30 – 32.5	32.5 – 35	35 – 37.5	37.5 – 40
N [−]	0	0	1	19	9	1	1	2	0	1	0	1	0	0	0	4
μ [−]	-	-	0.0110	0.0128	0.0140	-	-	0.01157	-	0.0124	-	0.0088	-	-	-	-
σ [−]	-	-	-	0.0031	0.0031	-	-	0.0006	-	-	-	-	-	-	-	-
α_t [−]			0.0110	0.0112	0.0110	0.0060	0.0090	0.0120		0.0124		0.0088				0.0116
				0.0150	0.0140			0.0111								0.0118
				0.0180	0.0064											0.0122
				0.0097	0.0078											0.0119
				0.0104	0.0050											
				0.0115	0.0160											
				0.0123	0.0110											
				0.0097	0.0180											
				0.0090	0.0190											
				0.0093												
				0.0129												
				0.0092												
				0.0141												
				0.0141												
				0.0141												
				0.0064												
				0.0051												
				0.0123												
				0.0123												

C.4.1 Cone resistance limit

The values from Table C-5 and Table C-6 are then plotted in Figure C-9 and Figure C-10 for respectively the maximum mobilized shear stress and α_t. Note that there are only few data points available at cone resistances higher than 20 MPa, which gives relatively a high insecurity about the location of the limit values based on them. The data point close to 40 MPa is neglected because the gap between that point and the rest of the data is too big.

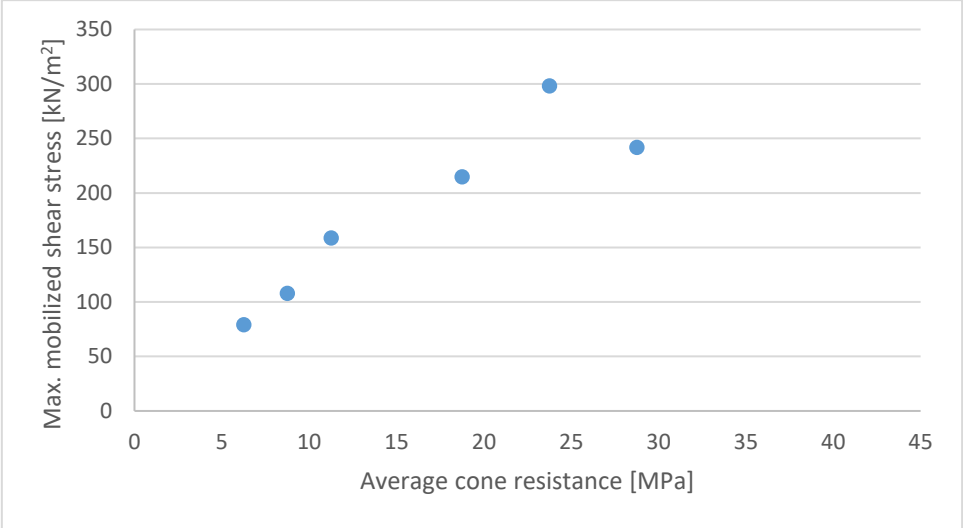

Figure C-9: Average values for $\tau_{mob;max}$ plotted as function of the average cone resistance intervals, type D

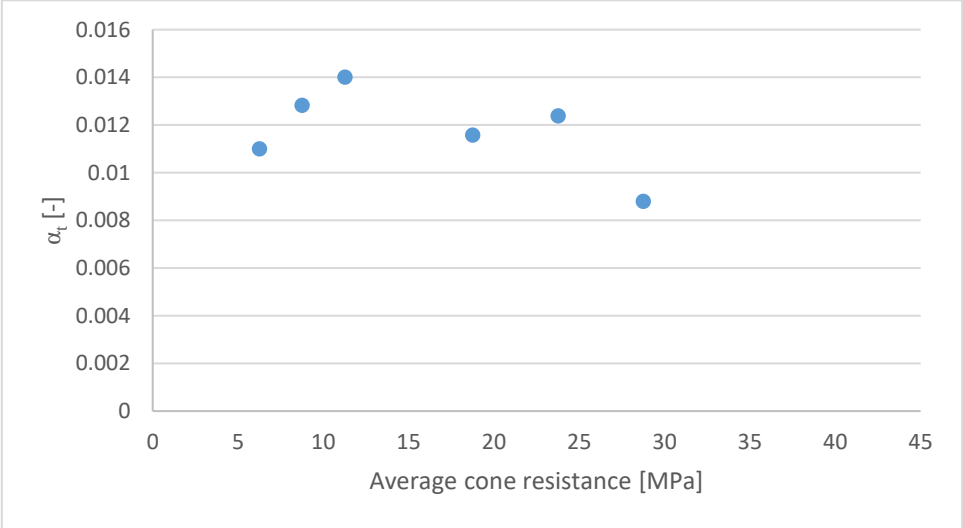

Figure C-10: Average values for α_t plotted as function of the average cone resistance intervals, type D

In general increases the maximum mobilized shear stress with the average cone resistance up to roughly 25 MPa, after which it decreases again. Those points are only based on two data points, which makes it difficult to see a clear trend. The inflection point in Figure C-10 is according the data also around 25 MPa. It is however possible that the maximum average $\tau_{mob;max}$ value is already reached at 20 MPa, and that the points at higher average cone resistance intervals are a natural scatter around the mean value. Furthermore is it important to remember that the data density after a cone resistance of 15 MPa, is sparse. This is accompanied by a higher insecurity of the exact trend.

The limit for q_c is therefore chosen to be at 20 MPa.

C.4.2 Maximum mobilized shear stress limit

The boundary values for the maximum mobilized shear stress are then determined based on the values above the cone resistance limit of 20 MPa. These values are indicated in the red box in Figure C-11. It can be seen that these values are based on only 2 data points, which is quite few and therefore is the reliability of this limit value questionable. From these two values however, the mean and standard deviation are taken following equations C-1 and C-2. Which resulted in the following values:

$$\bar{X}_{\tau_{mob;max}} = 270.2\ kN/m^2$$

$$S_{\tau_{mob;max}} = 40.0\ kN/m^2$$

The relative big uncertainty due to the presence of only 2 data points could also be seen in the relatively high value for the student-distribution factor $t_{0.05;n-1}$ of 6.314. The limit value becomes then:

$$\bar{X}_{\tau_{mob;max}} + t_{0.05;n-1} \cdot \frac{S\tau_{mob;max}}{\sqrt{1+\frac{1}{n}}} = 270.2 + 6.314 \cdot \frac{40.0}{\sqrt{1+\frac{1}{2}}} = 476.1\ kN/m^2$$

And the lower bound value:

$$\bar{X}_{\tau_{mob;max}} - t_{0.05;n-1} \cdot \frac{S\tau_{mob;max}}{\sqrt{1+\frac{1}{n}}} = 270.2 - 6.314 \cdot \frac{40.0}{\sqrt{1+\frac{1}{2}}} = 64.2\ kN/m^2$$

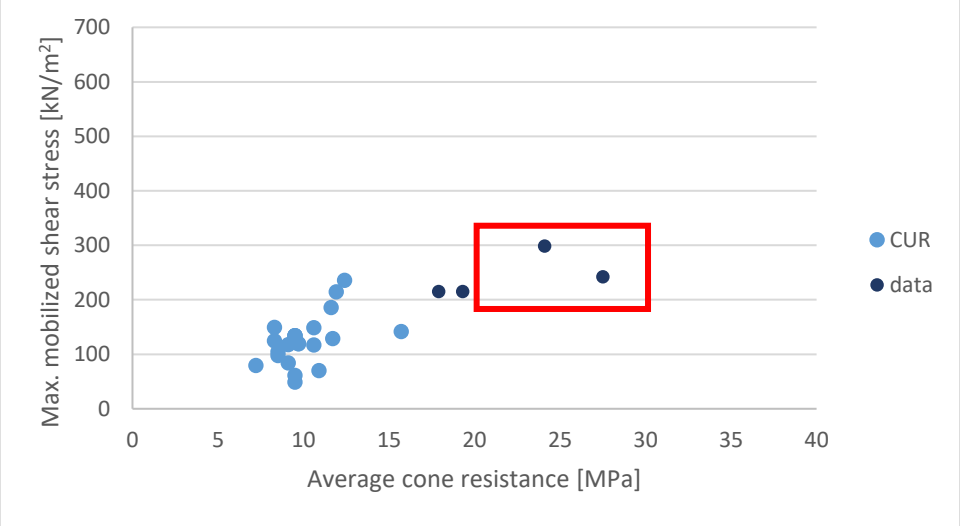

Figure C-11: Data points used for $\tau_{mob;max}$ limit determination of type D micropiles

C.4.3 α_t limit

The boundaries of α_t are then based on the data points below the cone resistance limit of 20 MPa, indicated with the red box in Figure C-12. This results in the following mean and standard deviation:

$$\bar{X}_{\alpha_t} = 0.0130$$

$$S_{\alpha_t} = 0.0028$$

The value below which a 95% of the data lies becomes then:

$$\bar{X}_{\alpha_t} + t_{0.05;n-1} \cdot \frac{S\alpha_t}{\sqrt{1+\frac{1}{n}}} = 0.0130 + 1.717 \cdot \frac{0.0028}{\sqrt{1+\frac{1}{23}}} = 0.0177$$

And the lower bound value:

$$\bar{X}_{\alpha_t} - t_{0.05;n-1} \cdot \frac{S\alpha_t}{\sqrt{1+\frac{1}{n}}} = 0.0130 - 1.717 \cdot \frac{0.0028}{\sqrt{1+\frac{1}{23}}} = 0.0083$$

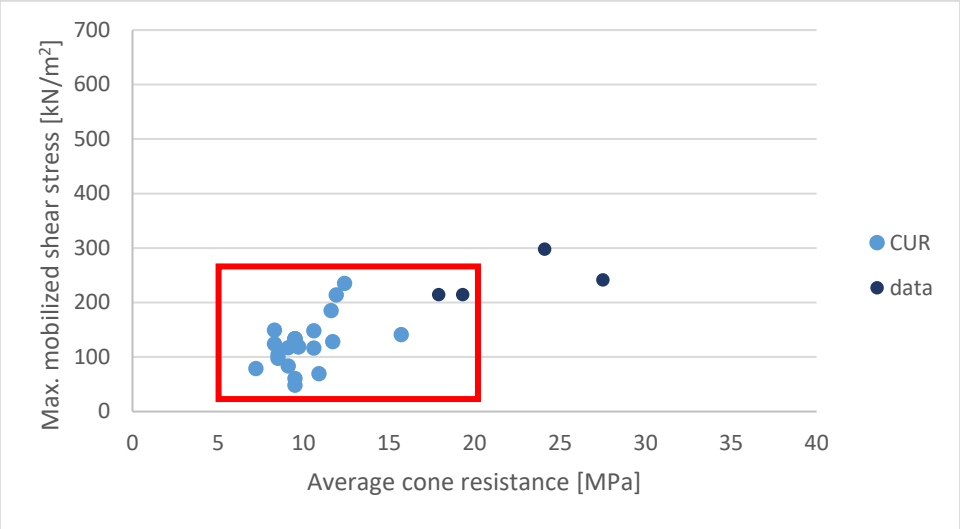

Figure C-12: Data points used for α_t limit determination of type D micropiles

C.5 Design values

In the previous sections, average and boundary values for $\tau_{mob;max}$ and α_t were determined based on a statistical approach. These values are however not always equally convenient to use in a design method, where rounded values are more easy to use and remember. Therefore the values are adapted to more suitable values. In Table C-7 an overview of the values received from the statistical approach can be found.

Table C-7: Summary of the values obtained from a statistical data analysis

	Type B		Type C		Type D	
	$\tau_{mob;max}$	α_t	$\tau_{mob;max}$	α_t	$\tau_{mob;max}$	α_t
Limit	603.2	0.0289	356.8	0.0171	476.1	0.0177
Average	549.2	0.0208	295.0	0.0140	270.2	0.0130
Lower bound	495.3	0.0126	233.1	0.0108	64.2	0.0083

C.5.1 Type B

The limit values for type B are changed from 603.2 to 600 kN/m^2 and 0.0289 to 0.0300 for respectively the maximum mobilized shear stress and α_t. This way, the maximum allowed $\tau_{mob;max}$ is reached at 20 MPa as can be seen in Figure C-13. Note that this is the upper boundary and not an assumed relation. Points above this border are assumed to be unrealistically high based on the available data. Those points should thus be reduced in the same way as is currently done in CUR 236.

The average value for α_t is changed from 0.0208 to 0.0210 to come to a round value. $\tau_{mob;max}$ is then reduced to 525 kN/m^2 in order to make the lines fit with the limit of 25 MPa for the cone resistance (25 MPa times 0.0210 equals 525 kN/m^2). Otherwise the relation would continue to after the point where the relation is assumed to end.

The average or expected line gives an idea of the 'to be expected' behaviour of a pile. This line is only used to base failure tests on which lead to an optimized α_t value for a design as was also discussed in section 2.2.

The lower bound values have to be applied when no failure tests are performed. These values are conservative in order to secure a safe design. Therefore is the maximum mobilized shear stress $\tau_{mob;max}$ based on α_t. The α_t value is rounded from 0.0126 to 0.0125. $\tau_{mob;max}$ becomes then 25 MPa times 0.0125, which is 312.5 kN/m^2. This value is reduced to 300 kN/m^2 to have a round and easy value.

The lines that are created by the proposed values are all visualized with respect to the data points in Figure C-13.

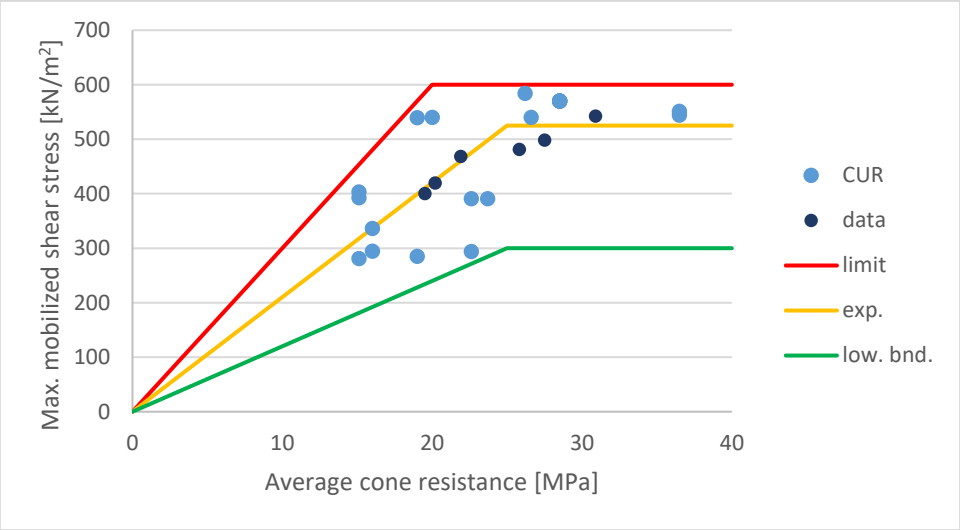

Figure C-13: Proposed limit values type B with respect to the data points

C.5.2 Type C

The limit values for type C are changed from 356.8 kN/m^2 and 0.0171 to 350 kN/m^2 and 0.0175 for respectively the maximum mobilized shear stress and α_t. The maximum allowed value for $\tau_{mob;max}$ is then reached at 20 MPa. The line from the limit values gives again the border above which values are believed to be unrealistic based on the available data.

The average values are changed from 295.0 to 300 kN/m^2 for the maximum mobilized shear stress, and for α_t from 0.0140 to 0.0135. α_t together with the limit for the cone resistance of 22.5 MPa, leads to about the value of 303.75 kN/m^2. The difference with the set value of 300 kN/m^2 is negligibly small, also with the knowledge what the average values are used for: making estimates for failure tests. An exact transition between the values was possible, but would lead to inconvenient values to use.

The lower bound values which were 233.1 kN/m^2 and 0.0108 for respectively the maximum mobilized shear stress and α_t are changed to 225 kN/m^2 and 0.0100. This in order to ensure a design that is safe enough according the data. These values should be applied in a design when no failure tests are performed.

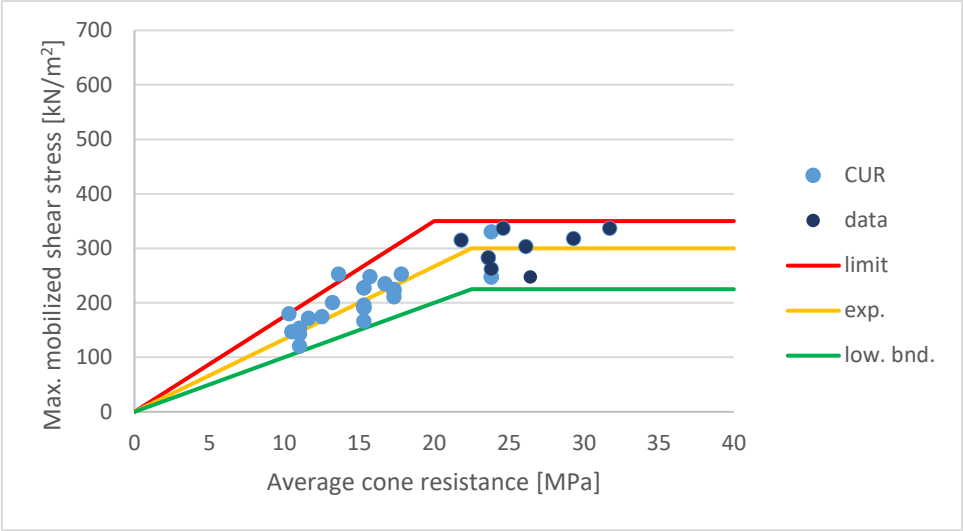

Figure C-14: Proposed limit values type C with respect to the data points

C.5.3 Type D

For type D, it was more complicated to determine reliable values for the maximum mobilized shear stress. This because only two point were available to use. This small amount of data points resulted in huge $\tau_{mob;max}$ range which would allow 'from an engineering point of view' unrealistically high values compared to for example type C micropiles. Therefore are the values for the mobilized shear stress based on the values for α_t and the cone resistance limit of 20 MPa.

The statistically determined values for α_t were respectively for the limit, average and lower bound, 0.0177, 0.0130 and 0.0083. These values are changed to the more round values of 0.0175, 0.0125 and 0.0075. These values combined with the limit value for the cone resistance of 20 MPa, gives an estimation of the boundary values for $\tau_{mob;max}$: 350, 250 and 150 kN/m^2.

These values are thus not based on the statistics of the maximum mobilized shear stress. They are more estimates based on the α_t values. When more data on this pile type is available, it is advised to re-elaborate these values.

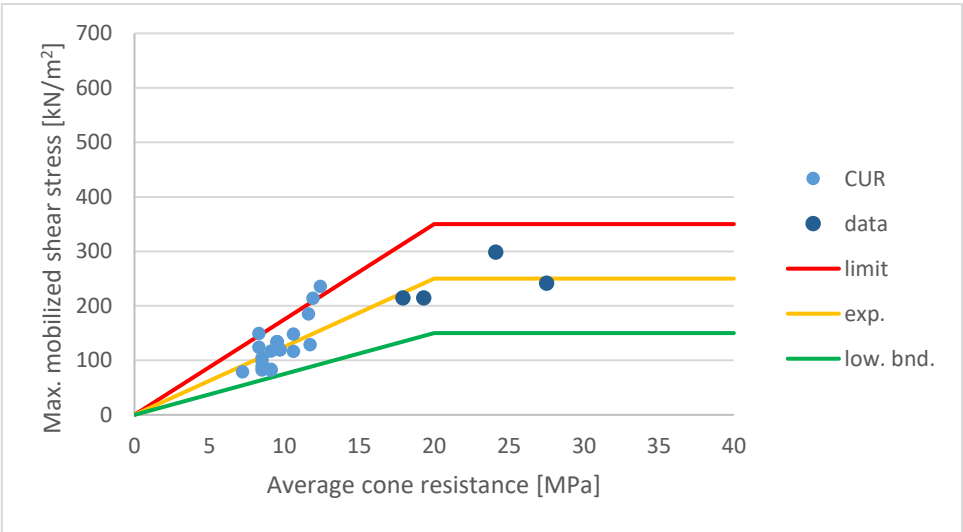

Figure C-15: Proposed limit values type D with respect to the data points

C.5.4 Summary proposed values

In the previous sections, new limit, average and lower bound values were proposed based on a statistical approach. The statistically determined values were not always equally convenient to use or remember in a design process, therefore they were slightly changed to more convenient ones as presented in Table C-7.

The proposal for new limit values is not just a proposal for types B, C and D, but also a sign that there is room for improvement for the limit values of all micropile types. Due to the availability of data however, this was not possible in this thesis.

Table C-8: Summary of the adapted statistical values

	Type B		**Type C**		**Type D**	
	$\tau_{mob;max}$	α_t	$\tau_{mob;max}$	α_t	$\tau_{mob;max}$	α_t
Limit	600	0.0300	350	0.0175	350	0.0175
Average	525	0.0210	300	0.0135	250	0.0125
Lower bound	300	0.0120	225	0.0100	150	0.0075

D Micropile design following CUR 236

In this appendix a flowchart with the possible options to get to the α_t parameter for a design is presented. The height of the α_t value that is allowed to use is mainly dependent on tests done before and after installation. Each block in the flowchart is explained below.

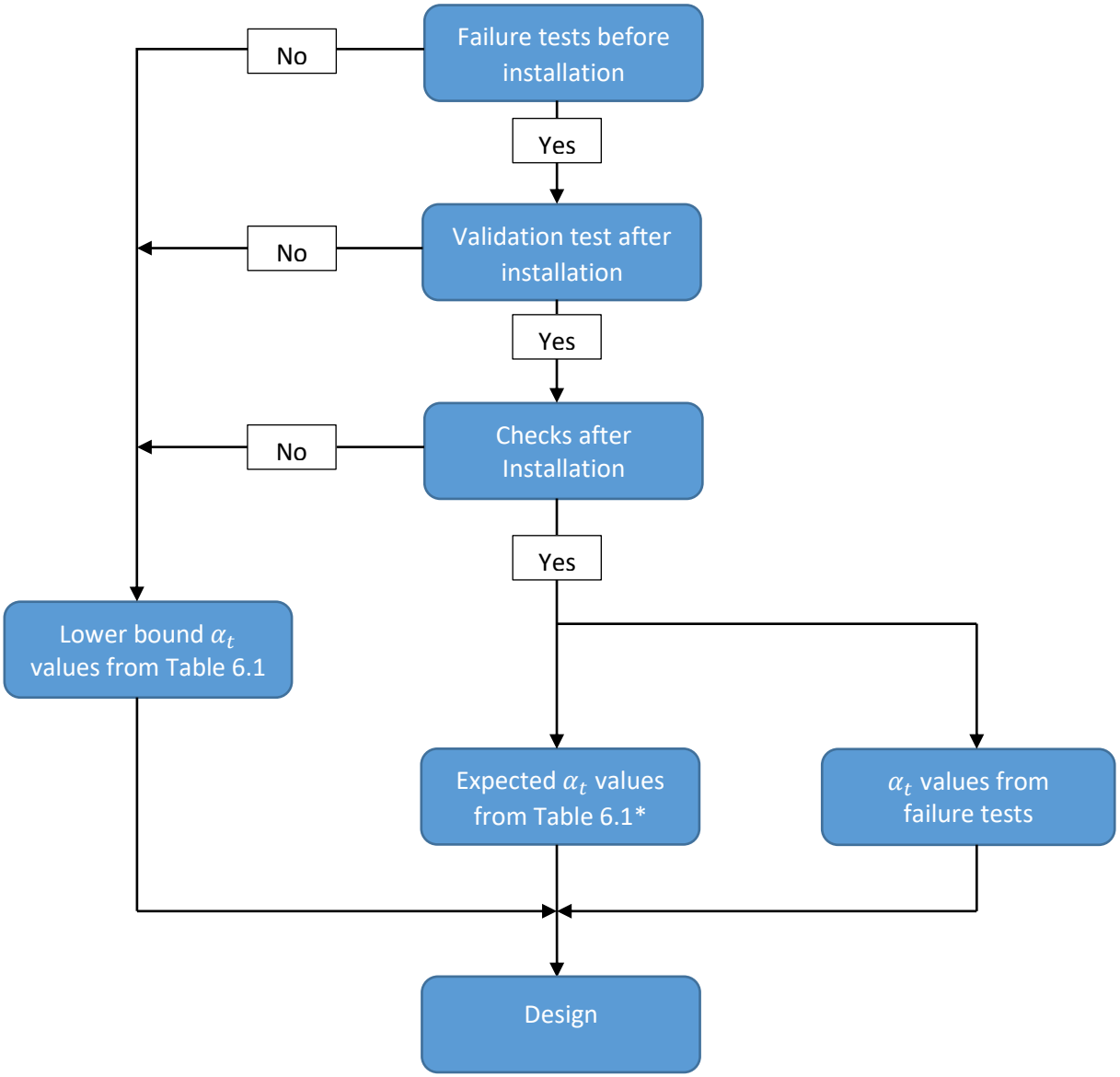

Figure D-1: Flowchart to α_t determination following CUR 236

* A design based on expected values is sometimes used when there is little time. Failure tests are then solely used to prove that the expected values are reached and the design is safe.

D.1 Testing

D.1.1.1 Failure tests

Failure tests are tests performed before installation. At least three piles are installed in de geological layer of which α_t has to be determined. After at least four weeks, the piles are loaded up to failure in a test. From the failure load, a layer specific α_t can be determined. It is not allowed to use this value for other geological layers at project location; or for other projects.

D.1.2 Validation tests

Validation tests are performed to verify the in situ capacity of installed piles. Because the test load, on the piles which have to be validated, can be higher than the net capacity (due to friction and compensation factors); these piles have to be picked beforehand and installed with thicker or more anchor steel.

At least 3% of the installed piles has to be tested, with a minimum of 3 piles. If, for some reason, validation tests cannot be performed, the lower bound values from CUR 236 Table 6.1 have to be used in the design. Even though failure tests were performed beforehand.

D.1.3 Checks

'Check' tests are used to check the axial spring-stiffness of the installed piles. Because only the net capacity of the pile has to be reached during the test, it is difficult to verify the soil mechanical capacity.

For checks also at least 3% of the piles have to be tested with a minimum of 3 piles.

D.2 α_t values

D.2.1 Lower bound α_t values from Table 6.1

Lower bound values for α_t have to be applied when no failure tests are performed beforehand, and no validation tests and checks afterwards. Lower bound α_t values are 0.011, 0.008 and 0.006 for respectively types A and B, C and D and E. When types A and B are not pressurized over the full length of the anchor body, 0.008 has to be used instead of 0.011.

Dependent on the amount of piles that have to be installed at a project, it might be more economic to design based on lower bound values, or based on failure tests. Turning point for this lies around 100 piles. Below this values it is more economic to use the lower bound values in the design, above 100, testing is a more economic option. Other options like time can also have effect in this decision.

D.2.2 Expected α_t values from Table 6.1

Expected values are allowed to be used when failure tests are performed beforehand, and validation tests and checks afterwards. The expected α_t values are 0.017 and 0.012 for respectively types A and B, and C and. No expected values for type E are present yet, due to its relative newness. When types A and B are not pressurized over the full length of the anchor body, 0.012 has to be used instead of 0.017.

When all tests are performed, it is allowed to use both the expected values and the optimized α_t values from the failure tests. However, using the expected values in a design while the optimized ones are higher, is illogical to do.

D.2.3 α_t values from failure tests

Optimized α_t values based on failure tests are allowed to be used when failure tests are performed beforehand, and validation tests and checks afterwards. Basically the same as for the expected values from CUR 236 Table 6.1 thus. If the tests result in a value lower than the expected value, this lower value has to be used in the design.

D.3 Design

With values for α_t known, a design can be made following equation D-1:

$$R_{t,d} = \int_0^{L_a} \frac{O_{p;gem} \cdot f_1 \cdot f_2 \cdot f_3 \cdot \alpha_t \cdot q_{c;z;exc}}{\xi \cdot \gamma_{s;t} \cdot \gamma_{m;var;qc}} dz \qquad \text{D-1}$$

With:

$R_{t,d}$	Design value for tensional resistance [kN]
$O_{p;gem}$	Average circumference of the pile [m]
L_a	Length over which shaft friction can develop [m]
z	Designation of depth [m]
α_t	Tensional shaft friction coefficient [$-$]
$q_{c;z;exc}$	Due to excavation reduced cone resistance [MPa] $q_{c;z;exc} = q_{c;z} \cdot \frac{\sigma_{v;z;exc}}{\sigma_{v;z;0}}$ for pile type E $q_{c;z;exc} = q_{c;z} \cdot \sqrt{\frac{\sigma_{v;z;exc}}{\sigma_{v;z;0}}}$ for pile types other than E $q_{c;z;NC} = q_{c;z;OC} \cdot \sqrt{\frac{1}{OCR}}$ for pile type E in a geologically overconsolidated situation
OCR	Overconsolidation ratio [$-$]
ξ	Correlation factor for the number of CPT's and the redistributive capacity of a construction [$-$]
$\gamma_{s;t}$	Partial resistance factor for piles in tension [$-$]
$\gamma_{m;var;qc}$	Partial load factor [$-$]
f_1	Factor for compaction effect ($f_1 = 1.0$ for micropiles) [$-$]
f_2	Factor for soil relaxation due to tensional loads on a pile group ($f_2 \leq 1.0$) [$-$]
f_3	Factor for pile length effect [$-$]

E Table of the t-distribution

Table B.2. Right critical values $t_{m,p}$ of the t-distribution with m degrees of freedom corresponding to right tail probability p: $P(T_m \geq t_{m,p}) = p$. The last row in the table contains right critical values of the $N(0,1)$ distribution: $t_{\infty,p} = z_p$.

	Right tail probability p							
m	0.1	0.05	0.025	0.01	0.005	0.0025	0.001	0.0005
1	3.078	6.314	12.706	31.821	63.657	127.321	318.309	636.619
2	1.886	2.920	4.303	6.965	9.925	14.089	22.327	31.599
3	1.638	2.353	3.182	4.541	5.841	7.453	10.215	12.924
4	1.533	2.132	2.776	3.747	4.604	5.598	7.173	8.610
5	1.476	2.015	2.571	3.365	4.032	4.773	5.893	6.869
6	1.440	1.943	2.447	3.143	3.707	4.317	5.208	5.959
7	1.415	1.895	2.365	2.998	3.499	4.029	4.785	5.408
8	1.397	1.860	2.306	2.896	3.355	3.833	4.501	5.041
9	1.383	1.833	2.262	2.821	3.250	3.690	4.297	4.781
10	1.372	1.812	2.228	2.764	3.169	3.581	4.144	4.587
11	1.363	1.796	2.201	2.718	3.106	3.497	4.025	4.437
12	1.356	1.782	2.179	2.681	3.055	3.428	3.930	4.318
13	1.350	1.771	2.160	2.650	3.012	3.372	3.852	4.221
14	1.345	1.761	2.145	2.624	2.977	3.326	3.787	4.140
15	1.341	1.753	2.131	2.602	2.947	3.286	3.733	4.073
16	1.337	1.746	2.120	2.583	2.921	3.252	3.686	4.015
17	1.333	1.740	2.110	2.567	2.898	3.222	3.646	3.965
18	1.330	1.734	2.101	2.552	2.878	3.197	3.610	3.922
19	1.328	1.729	2.093	2.539	2.861	3.174	3.579	3.883
20	1.325	1.725	2.086	2.528	2.845	3.153	3.552	3.850
21	1.323	1.721	2.080	2.518	2.831	3.135	3.527	3.819
22	1.321	1.717	2.074	2.508	2.819	3.119	3.505	3.792
23	1.319	1.714	2.069	2.500	2.807	3.104	3.485	3.768
24	1.318	1.711	2.064	2.492	2.797	3.091	3.467	3.745
25	1.316	1.708	2.060	2.485	2.787	3.078	3.450	3.725
26	1.315	1.706	2.056	2.479	2.779	3.067	3.435	3.707
27	1.314	1.703	2.052	2.473	2.771	3.057	3.421	3.690
28	1.313	1.701	2.048	2.467	2.763	3.047	3.408	3.674
29	1.311	1.699	2.045	2.462	2.756	3.038	3.396	3.659
30	1.310	1.697	2.042	2.457	2.750	3.030	3.385	3.646
40	1.303	1.684	2.021	2.423	2.704	2.971	3.307	3.551
50	1.299	1.676	2.009	2.403	2.678	2.937	3.261	3.496
∞	1.282	1.645	1.960	2.326	2.576	2.807	3.090	3.291

Figure E-1: Table of the t-distribution (Dekking, Kraaikamp, Lopuhaä, & Meester, 2005)